The Hallett Volcanic Province, Antarctica

GEOLOGICAL SURVEY PROFESSIONAL PAPER 456-C

Prepared on behalf of the National Science Foundation

The Hallett Volcanic Province, Antarctica

By WARREN HAMILTON

CONTRIBUTIONS TO THE GEOLOGY OF ANTARCTICA

GEOLOGICAL SURVEY PROFESSIONAL PAPER 456-C

Prepared on behalf of the National Science Foundation

UNITED STATES GOVERNMENT PRINTING OFFICE, WASHINGTON : 1972

UNITED STATES DEPARTMENT OF THE INTERIOR

ROGERS C. B. MORTON, *Secretary*

GEOLOGICAL SURVEY

V. E. McKelvey, *Director*

Library of Congress catalog-card No. 77-187573

For sale by the Superintendent of Documents, U.S. Government Printing Office
Washington, D.C. 20402 - Price 70 cents (paper cover)
Stock Number 2401-2054

CONTENTS

ILLUSTRATIONS

TABLES

CONTRIBUTIONS TO THE GEOLOGY OF ANTARCTICA

THE HALLETT VOLCANIC PROVINCE, ANTARCTICA

By WARREN HAMILTON

ABSTRACT

The Hallett volcanic province of upper Miocene to Holocene sodic basalt and trachyte lies along the Ross Sea coast of northeastern Victoria Land. The volcanic rocks occur primarily in four long offshore piles: one wholly an island (Coulman), the other three (Daniell, Hallett, and Adare Peninsulas) joined to the mainland by ice-filled troughs. Each pile is a broad elongate dome formed by eruptions mostly along a crestal fissure zone. The Daniell and Coulman domes remain symmetrical, but the Hallett and Adare piles were erupted mainly from vents east of the present peninsulas, the eastern half of each edifice having been since eroded away. The broad conical volcanoes rise gently above the general crests to altitudes of about 2,000 meters and are marked by large calderas.

Each volcanic dome consists mostly of subglacial palagonitic breccias and pillow-breccia complexes of spectacular character, erupted during late Miocene, Pliocene, and Quaternary times, when the Antarctic ice sheet was grounded on the Ross Sea shelf and was far more extensive that it is now. The breccias are capped by subaerial lavas and scoria.

Small masses of upper Cenozoic volcanic rocks occur on the pre-Tertiary rocks of the mainland, west of the offshore piles, and several large volcanoes also are present on the mainland.

The volcanic rocks belong to a sodic basalt-and-trachyte association. Mafic rocks, particularly alkaline olivine basalt and trachybasalt, are dominant; but more felsic rocks, including latite, trachyte, extremely sodic phonolite, and relatively potassic quartz trachyte, are abundant.

INTRODUCTION

The Hallett volcanic province consists of accumulations of upper Miocene, Pliocene, and Quaternary basalt and trachyte along the Ross Sea coast of northeastern Victoria Land. Most of the rocks apparently were erupted under ice which filled the present Ross Sea and which stood several kilometers above present glacier levels; the result was the formation of thick piles of breccias. The rocks are in general remarkably high in alkalis and include some of the most sodic igneous rocks known anywhere. This report describes the occurrence and petrology of these unusual volcanic rocks, with emphasis placed on physical volcanology.

ANTARCTICA

If its ice cap were melted, Antarctica would consist of one large landmass and many small ones (fig. 1). The large mass is about the size of Australia or the United States and is named East Antarctica because it is mostly restricted to east longitudes. The smaller masses collectively form West Antarctica, are limited to west longitudes, and comprise large and small islands rising from a continental platform which would be largely submerged even after isostatic rebound. These various large and small masses are now bridged by the continental ice cap.

East Antarctica consists of a Precambrian shield and, broadly coextensive with the high Transantarctic Mountains along the Ross and Weddell Seas, a late Precambrian and Paleozoic mobile belt (fig. 1). West Antarctica consists of Paleozoic and Mesozoic geosynclinal and plutonic rocks. For reviews of the geology of these provinces, the reader is referred to recent summary reports: Adie (1962), Anderson (1965), Ford (1964), Gunn (1963), Hamilton (1967a), Harrington (1965), Klimov, Ravich, and Solov'yev (1964), Ravich (1965), Ravich, Klimov, and Solov'yev (1965), Voronov (1964), and Warren (1965). The 76 reports on Antarctic geology in the compendium edited by Adie (1964) provide much information on detailed work, and the fine Soviet atlas of Antarctica (Bakayev, 1966) presents in cartographic form a wealth of topographic, geologic, glaciologic, climatic, and oceanographic data.

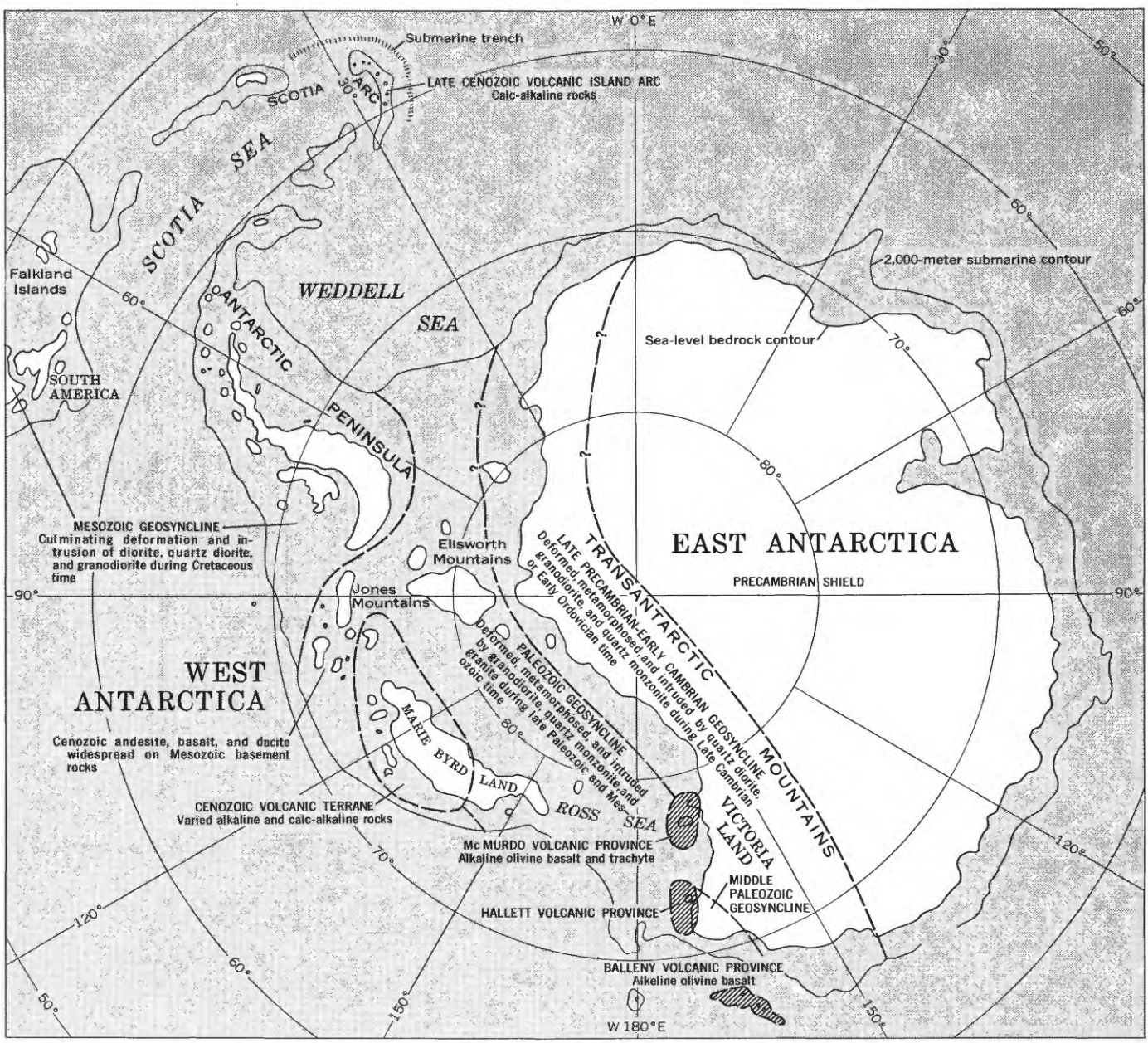

FIGURE 1.—Tectonic and volcanic provinces of Antarctica, showing location of Hallett Volcanic Province (lower center). Adapted from Hamilton (1967a, fig. 1). Line pattern, volcanic provinces.

The Hallett volcanic province of upper Miocene to Holocene basalt and trachyte lies in northeastern Victoria Land, along the Ross Sea coast of the Transantarctic Mountains south of New Zealand. The prevolcanic rocks of this corner of Victoria Land consist of very thick clastic sedimentary rocks, metamorphosed at low grade and intruded by numerous small plutons of granodiorite of Late Devonian or early Carboniferous age.

ROSS SEA PETROLOGIC PROVINCE

Upper Cenozoic basalt and trachyte form large volcanic piles scattered from the McMurdo Sound region to the Balleny Islands (fig. 2).

Harrington (1958) proposed that all the Cenozoic volcanic rocks of the Ross Sea sector of Antarctica be referred to a single formation, the "McMurdo Volcanics." The rocks share petrologic characteristics —most are alkaline olivine basalts and sodic trachytes

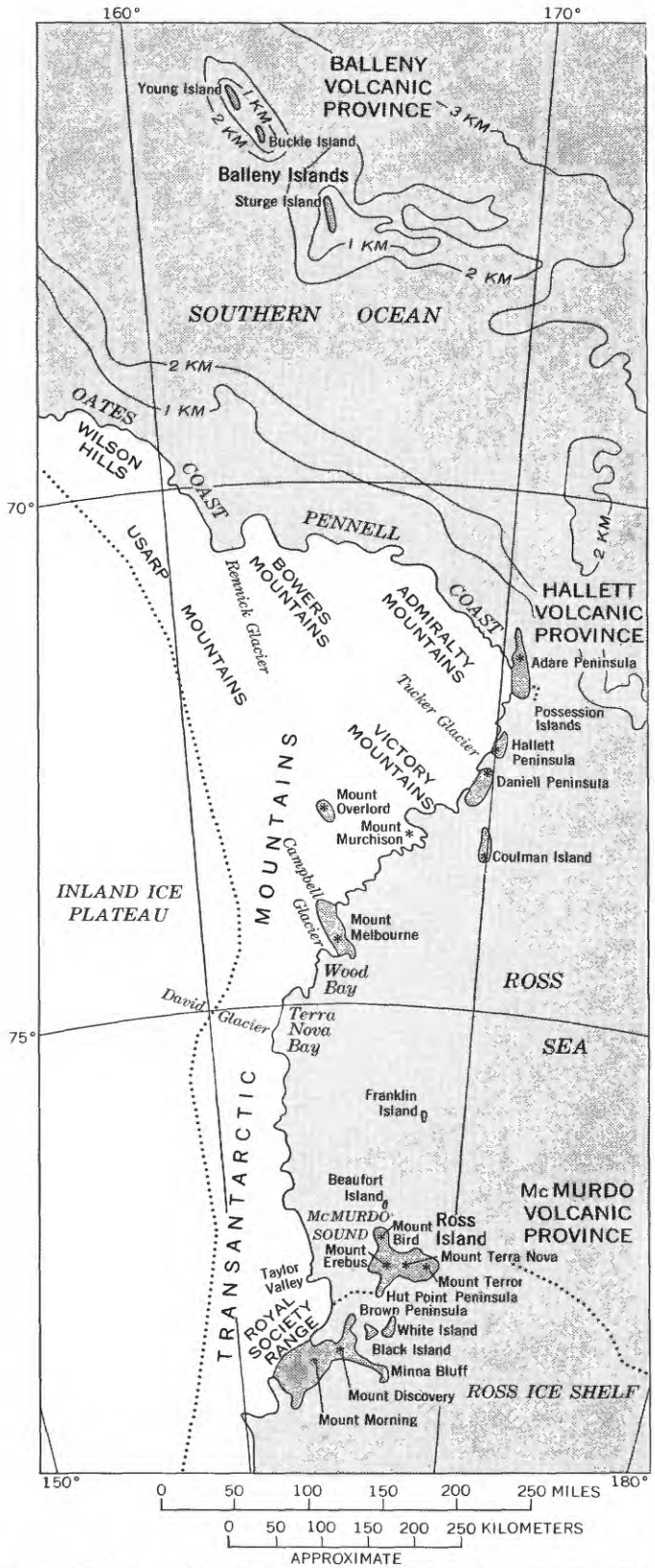

FIGURE 2.—Upper Cenozoic volcanic rocks (shaded) of the Ross Sea petrologic province. *, major young volcanic cone. Minor clusters of small cones and flows on the mainland are omitted. Base from 1 : 5,000,000 map of Antarctica by American Geographical Society, 1965.

—and they overlap in age at least in the Quaternary. The rocks certainly belong to a broad petrologic province, but referring them all to a single formation is of dubious utility, and the designation is not used here.

I will here instead refer to all the volcanic rocks shown in figure 2 as belonging to the Ross Sea petrologic province, and within this broad category will designate three major subprovinces—the McMurdo volcanic province (Mount Morning to Ross Island), the Hallett volcanic province (Coulman Island to Adare Peninsula), and the Balleny volcanic province. This leaves unattached the Beaufort, Franklin, Melbourne, and Overlord volcanic centers.

Each of the three major volcanic subprovinces so classified has a distinctively different occurrence. The McMurdo volcanic province is characterized by high subaerial volcanoes. The Hallett volcanic province consists of long coastal domes of subglacial breccias, surmounted by low subaerial volcanoes. The volcanoes of the Balleny province also form long domes, but these rise from the deep ocean.

Imposing volcanoes stand high above broader volcanic platforms in the McMurdo Sound region and form the high peaks of Ross Island and also of Mounts Discovery and Morning. A noteworthy volcanic form is that of the high rounded uncratered summit dome of Mount Discovery, which may be a large extrusive trachyte dome. Published information consists mostly of sample descriptions and is scattered widely through the Antarctic literature. During my own brief examinations of Hut Point Peninsula, the southeast slope of Mount Terror, White and Black Islands, Brown Peninsula, Minna Bluff, and Mount Discovery, I saw palagonite breccias, likely products of subglacial eruptions, only on Minna Bluff, and at Castle Rock on Hut Point Peninsula. The other exposed volcanic rocks that I have seen in the McMurdo volcanic province are products of subaerial eruptions—basalt flows and cinders, trachyte flows and domes.

Mounts Melbourne and Overlord are dominant volcanoes farther north in Victoria Land.

Each of the long volcanic piles—Coulman Island and Daniell, Hallett, and Adare Peninsulas—in the Hallett volcanic province consists of a thick foundation of spectacular subglacial breccias and a topping veneer of subaerial eruption products and low volcanoes. The breccia piles face the Ross Sea with straight, sheer cliffs whose heights reach nearly 2,000 m (meters).

The possibility that Ross Island and the other main McMurdo volcanic centers are connected to Coulman Island and the coastal peninsulas by extensive sub-

marine accumulations of volcanic rocks is eliminated by results of aeromagnetic surveys; submarine veneers of lava, however, could be present. The surveys show that high-amplitude, short-wavelength magnetic anomalies in the western Ross Sea are confined largely to the exposed volcanic piles and the neighboring areas (Robinson, 1964; Behrendt, 1964; Behrendt and Bentley, 1968, pl. 7).

The Balleny volcanic province consists of three elongate islands and a few islets rising from the ocean northwest of Cape Adare (fig. 2, this rept.; Dawson, 1969a, b, c; Mawson, 1950). Like the Coulman, Hallett, and Adare piles, the Ballenys are cliff sided and ice capped. Photographs (Hatherton and others, 1965, figs. 6, 7) show what appear to be breccias like those of the Hallett volcanic province: eruptions beneath ice caps may be indicated. Alkaline olivine basalts are present (Mawson, 1950).

OTHER WORK IN NORTHEASTERN VICTORIA LAND

In January 1841, a Royal Navy research expedition of the two ships *Erebus* and *Terror*, commanded by James Clark Ross, made the first penetration of the Antarctic pack ice and entered the Ross Sea. A landing was made at Possession Island, and the volcanic rocks collected were described by Prior (1899).

No one entered the region again until 1894, when whale-crewman C. E. Borchgrevink landed at Ridley Beach, Cape Adare, and collected volcanic-rock specimens subsequently described by David, Smeeth, and Schofield (1896). Borchgrevink later promoted an expedition of his own and returned in 1898. Two huts were built at Ridley Beach (fig. 3), and Borchgrevink and nine others remained there nearly a year. They were the first men to winter in Antarctica. Several published reports including that by Prior (1902) describe the rock specimens they collected, mostly upper Cenozoic volcanic rocks, about Robertson Bay and along the Ross Sea coast.

During Robert Falcon Scott's expedition of 1910–13, a six-man party, including geologist Raymond Priestley, built another hut at Ridley Beach and remained there from February 1911, until January 1912, conducting man-haul sledge excursions about Robertson Bay. They spent the following summer farther south in northern Victoria Land, where they were then marooned overwinter in an ice cave on a seal-and-penguin diet. Priestley (1923) described some of the geologic findings. The volcanic rocks collected from the Adare Peninsula and Terra Nova Bay regions were well described long afterward by Smith (1959; 1964a, b).

FIGURE 3.—Borchgrevink's huts at Ridley Beach, Cape Adare, as they appeared in November 1964. These structures, the first built in Antarctica, were occupied by the first party to winter on the continent, during 1898 and 1899. The living-quarters hut (foreground) is still in good condition, but the stores hut beyond has lost its roof and has partly collapsed.

The modern era of exploration began with the establishment by many nations of logistic and research stations in the Antarctic for the International Geophysical Year. Hallett Station was built in early 1957 and is operated jointly by the United States and New Zealand. A snow-cleared landing strip on the sea ice of Edisto Inlet handles wheeled aircraft each spring.

A geologic reconnaissance of the region was carried out from Hallett Station by an eight-man New Zealand party led by H. J. Harrington during the 1957–58 summer. The party traveled about Edisto Inlet and up the Tucker Glacier. Their geologic findings were reported by Harrington, Wood, McKellar, and Lensen (1967).

Three small New Zealand parties operated in northern Victoria Land during the 1962–63 summer. One explored the region from Mount Overlord to the upper Rennick Glacier (Gair, 1964, 1967), one the region south of Priestley Glacier (Skinner and Ricker 1968a, b), and the other the region southwest of upper Tucker Glacier (Le Couteur and Leitch, 1964). A six-man New Zealand party made a far-ranging sledge exploration in the summer of 1963–64 (Sturm and Carryer, 1970). Small New Zealand geologic parties operated in the southern part of northern Victoria Land during the 1965–66 and 1966–67 summers (Adamson and Cavaney, 1967; Nathan and Schulte, 1967, 1968; Riddolls and Hancox, 1968). The geologic map compiled by Gair, Sturm, Carryer, and Grindley (1969) incorporates most published mapping.

PRESENT WORK

The late Dwight F. Crowder and Donald A. Coates and I made a geologic reconnaissance study of 50,000 sq km (square kilometers) of northeastern Victoria Land during November 1964. The work was done by means of helicopters operating from Hallett Station. Crowder and Coates worked primarily with the metamorphic and granitic rocks of the mainland, whereas I concentrated on the Cenozoic volcanic rocks along the coast. Several brief summaries of the geologic results have been published (including those of Crowder and Hamilton, 1966, and Hamilton, 1965, 1967b), as has one longer report on the prevolcanic rocks (Crowder, 1968).

The work was supported by a grant to the U.S. Geological Survey from the Office of Antarctic Programs of the National Science Foundation. Air transportation to and from Hallett Station, by way of New Zealand and McMurdo Station, Antarctica, was provided by the U.S. Navy. The Navy also provided quarters and meals at Hallett.

Transportation in the field was provided by the three Bell UH–IB (Iroquois) helicopters of the U.S. Army Antarctica Support Aviation Detachment, commanded by Maj. W. C. Hampton. Pilots were Maj. J. B. Muck and CWO's J. J. Lockhart, J. S. Reid, and D. M. Shanklin. The cooperation of these men and the others in the detachment made possible the rapid study of a very large region, despite the difficult field conditions.

The high-performance turbine helicopters have high cruising speeds and rates of climb and are ideal for reconnaissance studies. A typical field day involved several hundred kilometers of flying plus perhaps five stops for sampling and study of rock outcrops. Geologic mapping was done mostly from the air: snow and ice cover is extensive, but rock exposures where present are generally superb.

My work on the volcanic rocks utilized 10 field days, and Crowder and Coates each worked with volcanic rocks on 2 days. Between us, we studied and sampled about 60 volcanic localities on the ground. The major volcanic piles (Coulman, Daniell, Hallett, and Adare) were each sampled in a number of places and were examined from the air throughout their extent. Most minor volcanic accumulations near the coast and north of latitude 73° S. were sampled also.

For field base maps, we used 1:250,000 enlargements of a prepublication edition of the 1:500,000 shaded-relief Northeastern Victoria Land sketch map, prepared from trimetrogon photographs controlled by ground tellurometer survey and triangulation (MacDonald, 1968) and later published by the U.S. Geological Survey. Topographic maps at a scale of 1:250,000 were subsequently prepared from the trimetrogon photographs but were published too late for incorporation in the maps of the present report. (The Hallett volcanic province lies within the area of three of the Survey's 1:250,000 Antarctica Reconnaissance Series maps: Cape Adare, SR 59–60/13, 1970; Cape Hallett, SS 58–60/2, 1970; and Coulman Island, SS 58–60/6, 1969.) We also used the trimetrogon aerial photographs, which had been taken by the U.S. Navy for the U.S. Geological Survey, for both field recording and photointerpretation. Of the altitudes noted in this report, some are geodetic determinations from the Northeastern Victoria Land sketch map, some are approximate altitudes from New Zealand and U.S. Navy maps, others are helicopter aneroid altimeter measurements, and some are estimates scaled on photographs with known dimensions. Attitudes of rocks on the maps were estimated from photographs.

Color slides taken freely yielded much information where careful field observation and recording were precluded by the pace of the fieldwork. Telephoto-lens pictures, providing closeups within large areas put in context with normal and wide-angle photographs, permitted office study of details with results comparable to field examination with binoculars. Lenses as long as 200 mm (millimeters) were used on hand-held 35-mm cameras. Photographs in this report not otherwise credited were taken by me.

Daily maximum and minimum air temperatures at sea-level Hallett Station during the month of fieldwork were typically about −4° and −12°C (10° and 25°F)—warm, by Antarctic standards, because of the coastal and northerly position of the station. Temperatures were far colder inland and at high altitude. Winds were generally from the south. Coastal fogs become a problem as open water progresses southward during early summer; during our November season, fog was common only in the Adare Peninsula region. Summaries of weather data from Hallett were presented by Rudolph (1966) and by Harrington, Wood, McKellar, and Lensen (1967, p. 82).

Four potassium-argon age determinations of basalts were generously made by Richard Lee Armstrong of Yale University in 1968, and are incorporated in this report.

This report was largely completed during 1969, although minor corrections and additions were made as late as 1971.

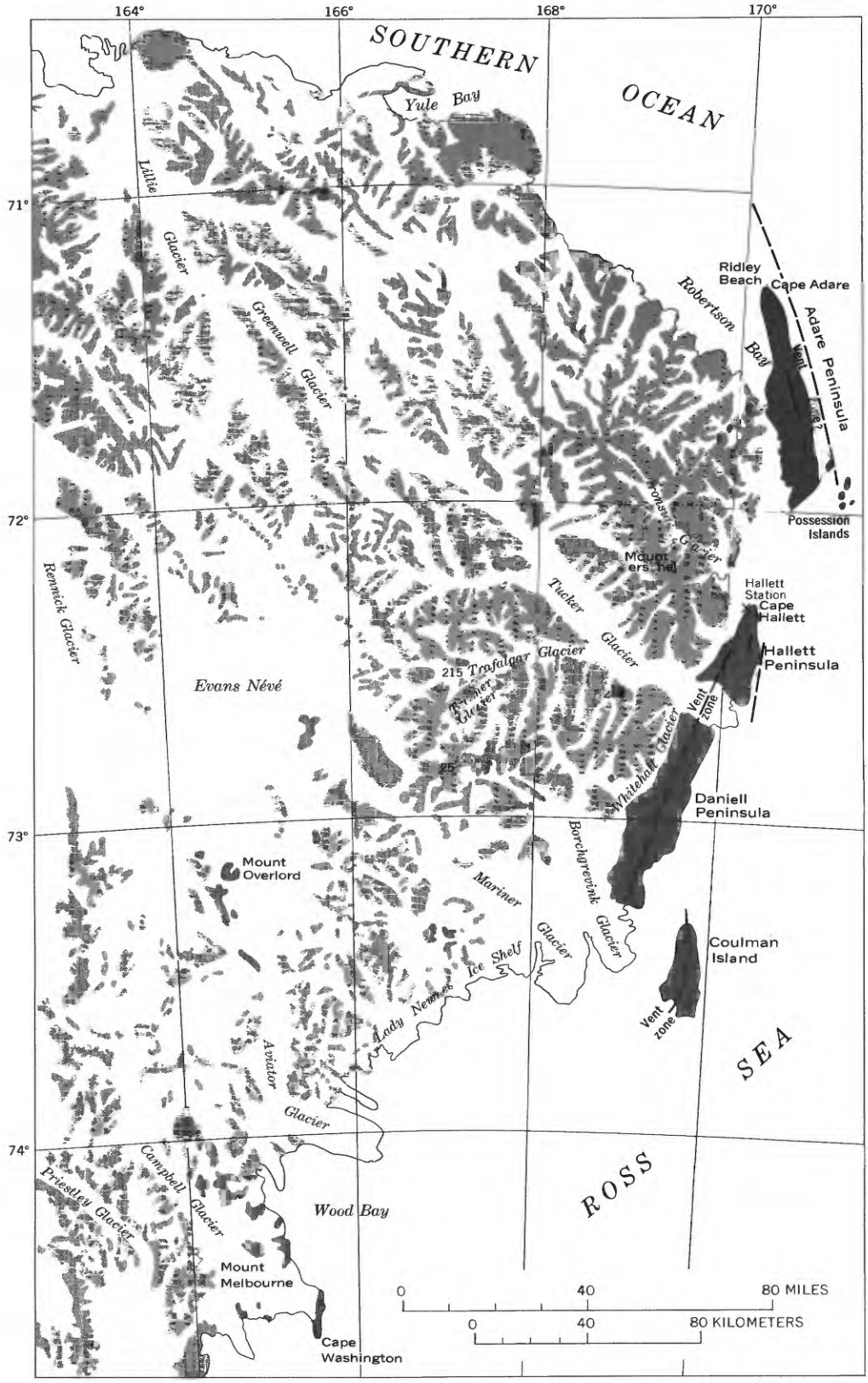

FIGURE 4.—Northeastern Victoria Land, showing distribution of pre-Tertiary rocks (light shaded) and of upper Cenozoic volcanic rocks (dark shaded). Base map adapted from an unpublished compilation by the American Geographical Society, 1967. The numbers are sample locality numbers used in the text.

OFFSHORE VOLCANOES

GENERAL

The volcanic rocks of the Hallett province occur primarily in four long piles along the west side of the northern Ross Sea (figs. 4, 5). One of these piles is wholly an island (Coulman), and the other three are peninsulas (Daniell, Hallett, and Adare) which are largely separated from the mainland by troughs filled with grounded and floating ice. The rocks are of late Miocene to Holocene age.

Each of these major volcanic piles is a broad elongate dome formed by the coalescing of basalt and trachyte erupted mostly from vents along a crestal fissure zone. The Daniell and Coulman domes remain symmetrical, the main vent zones trending along their midlines. The Hallett and Adare piles were erupted in considerable part from vents east of the present edges of the peninsulas, the eastern half of each dome having been since eroded away. The small Possession Islands, east of southern Adare Peninsula, may be remnants from the eastern part of the Adare dome.

Broad conical volcanoes rise gently above the general crestal levels to altitudes typically of about 2,000 m. Some of these volcanoes are marked by large calderas. Recent cinder cones along each crest attest to continuing activity. (Harrington and others, 1967, also recognized some of the volcanic features referred to in this report.)

Each volcanic pile consists mostly of subglacial palagonitic breccias and pillow-breccia complexes of spectacular character, erupted during late Miocene, Pliocene, and Quaternary times under the Antarctic ice sheet which was grounded on the Ross Sea shelf and which was far more extensive than it is now. The capping rocks of each pile are subaerial lavas and scoria, formed after the eruptions overtopped the ice.

Small masses of upper Cenozoic volcanic rocks occur on the pre-Tertiary rocks of the mainland, west of the large volcanic piles, and several large volcanic masses occur on the mainland farther west and southwest of the southern of the domes.

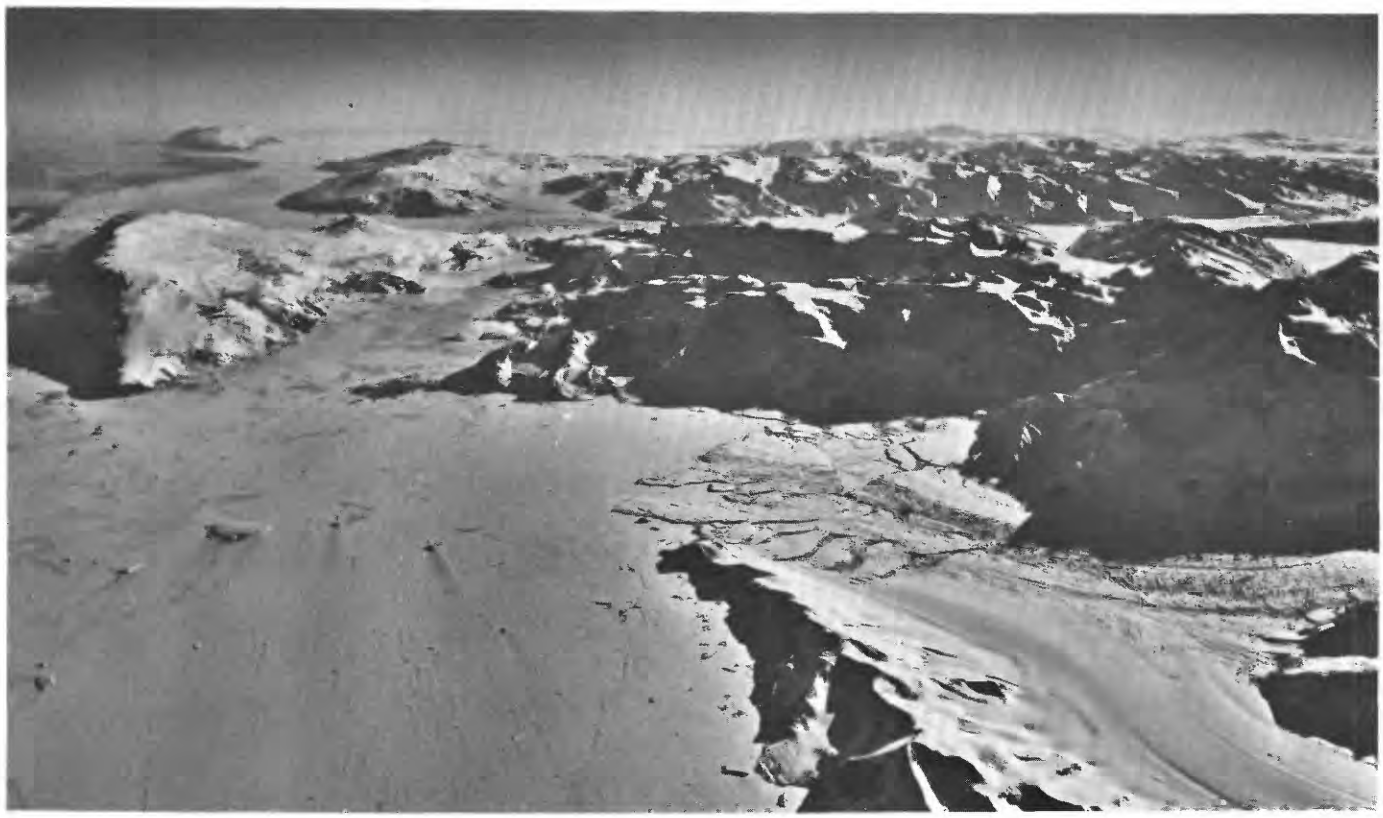

FIGURE 5.—Aerial view southward over Moubray Bay, showing relation of elongate volcanic piles to the mainland. Hallett Peninsula is at left center, Daniell Peninsula is beyond its right part, and Coulman Island is on the left skyline (130 km from the foreground ridge). Hallett and Daniell volcanic rocks are separated from the pre-Tertiary rocks of the mainland mountains by bays and glacier-filled troughs. Mount Herschel (right center) rises precipitously above floating Ironside Glacier, and stands 3,335 m (meters) above the wind-streaked sea ice. Photograph TMA 1036 F33, no. 180, by U.S. Navy for U.S. Geological Survey, altitude 7,600 m, 25 November 1962.

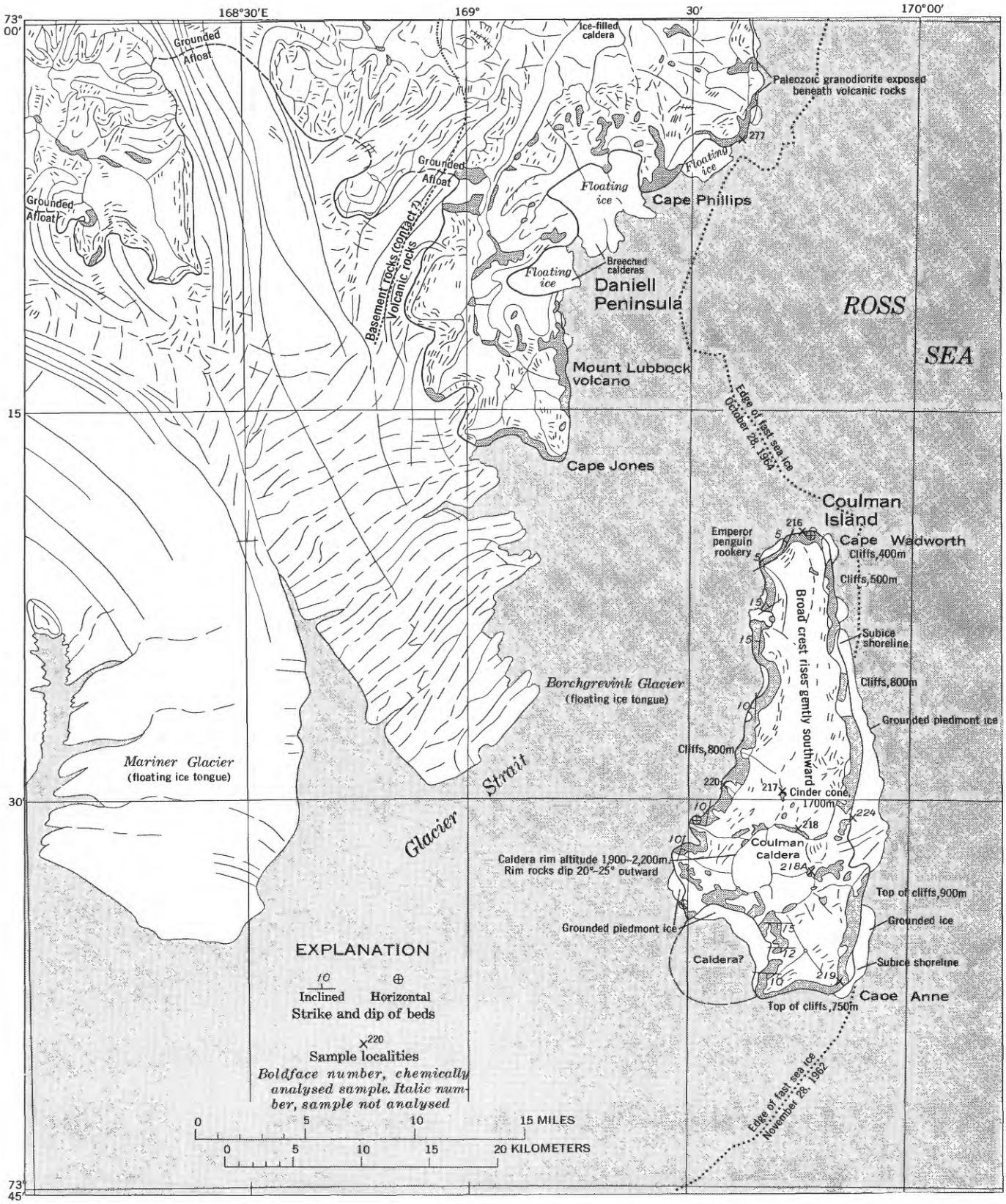

FIGURE 6.—Map of Coulman Island and the southern part of Daniell Peninsula, showing outcrops (shaded) of volcanic rocks. The cliffs rimming the island reveal subglacial breccias, whereas Coulman caldera is of subaerial trachyte. Lines indicate ridge crests, crevasses, and flow lines in glacial ice. Base map by U.S. Geological Survey.

CRUSTAL SETTING

The high mountains of pre-Cenozoic rocks slope steeply into the Ross Sea from altitudes of 2,000 to more than 3,000 m (fig. 24), and the offshore volcanic piles of the Hallett province rise from the continental shelf, which is typically about 500 m below sea level. Presumably normal faults and abrupt flexures bound the Ross Sea, although the actual structural features have yet to be mapped and can only be inferred from the topography. Rocks like those of the mainland continue beneath the volcanoes, as indicated by an island of granodiorite that projects into the basalts of the east side of Daniell Peninsula and by granitic xenoliths that occur in a cinder cone on McCormick Island, east of Adare Peninsula.

The scarps along the Ross Sea coast must reflect an abrupt westward thickening of the continental crust and deepening of the Mohorovicic discontinuity (Behrendt and Bentley, 1968). Intense volcanism has occurred in the narrow transitional zone between continental-shelf and mountain-region crustal structures.

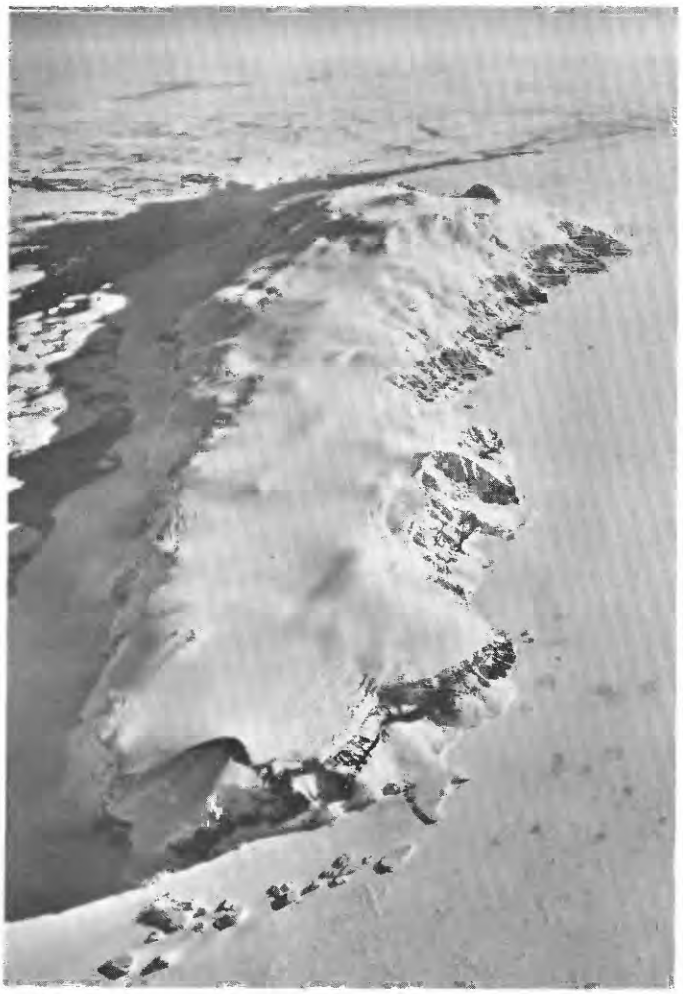

FIGURE 7.—Aerial view southward along Coulman Island. Coulman caldera at the far end is 6 km in diameter. The fast sea ice encloses tabular icebergs as seen at the bottom of the picture and is darkened by emperor penguin rookeries to the right of the near end of the island. Photograph by U.S. Navy for U.S. Geological Survey, TMA 1037, F 31, no. 191, altitude 7,600 m, 25 November 1962.

COULMAN ISLAND

The southernmost of the big breccia piles is Coulman Island (fig. 6). The island is 33 km long in the north-south direction, and widens southward from 5 km near the north end to 14 km near the south end. Cliffs ring the island, whose broad, ice-capped central crest rises gradually southward to the caldera-truncated cone which dominates the island (fig. 7). Most of the rocks probably were erupted from the zone, now marked by the axial crest and the caldera, along the center of the island.

The lower 200–500 m of the volcanic section exposed about most of the island consists of massive-outcropping palagonite breccias and pillow breccias. This lower section generally forms dark, unbroken cliffs that rise abruptly from the sea; this entire lower section stands as a vertical wall in many places (figs. 7, 26). The breccia section above these lower cliffs is commonly more thinly bedded and produces cliffs sloping typically between 50° and 60°. Much snow and thin ice cling to these upper cliffs, which rise to 700–1000 m around most of the island. The overall slope of the 750-m cliffs along the south coast, westward for 7 km from Cape Anne, reaches 80° in several places.

Dips in the breccias are low, generally less than 10° (fig. 6). The dips tend to be outward from the long axis of the island (figs. 7, 8). There are, however,

FIGURE 8.—Outward-dipping breccias of northwestern Coulman Island, 7 km south-southwest of Cape Wadworth. Dips flatten toward the observer. The grounded ice apron is fed by avalanches from the ice cap; a recent avalanche forms a large lobe. Relief shown in picture is about 1,100 m. The foreground sea ice is a rookery area for emperor penguins. 7 November 1964.

places, as in the cliffs west of Coulman caldera, where the section dips gently into the island.

COULMAN CALDERA

Coulman caldera, here named, truncates a high, broad cone which stands on the wide southern part of the island (figs. 6, 7). The circular caldera rim is about 6 km in diameter and has an altitude of 1,900–2,200 m. The rim forms a sharp ice divide, along which project narrow, discontinuous outcrops of subaerial trachyte lavas that dip 20°–25° radially outward. The broad ice dome in the center of the caldera, through which no rock projects, perhaps caps a postcollapse trachyte dome. The caldera rim is breached by outlet glaciers, which avalanche to the sea, on the northeast and south.

The caldera has a depth of at least 700 m. At the southern breach the inner rim of the caldera, covered by steep ice, has a height exposed above the caldera-filling ice of about 300 m. The scarp continues downward between the east wall of the southern breach and the outlet glacier for an additional exposed height of about 400 m and appears, in an oblique photograph, to have a general slope of about 60°.

The caldera cone is exposed in section in the inaccessible cliffs which extend southward for 6 km from the south-central breach in the caldera rim. At the north end of these cliffs—the east edge of the southern outlet glacier—the inner rim of the caldera as noted previously has a total exposed height of about 700 m, but the thinly layered lavas of the caldera cone are only about 300 m thick. Beneath them, much more massive rocks—palagonite breccias?—extend down to the ice apron. The thin-bedded lavas dip gently southward parallel to the top of the ice-capped ridge. The contact of lava over breccia is exposed for about 3 km southward along the cliffs, beyond which it is covered by ice cascading from the ice cap. The subaerial lavas do not reach the south end of the island, where the cliffs are entirely of the breccia series. The breccias display rough bedding subparallel to that of the overlying lavas in the cliffs that extend south from the caldera. The breccias may represent subglacial eruptions from the caldera center before the capping subaerial cone was formed. Or perhaps the breccias include downdip subglacial equivalents of the subaerial lavas.

The contact between lavas and breccias is hidden beneath ice around most of the caldera. The contact was however also observed at the west side of the southern outlet glacier, where lava is poorly exposed. The cliffs that extend westward from this locality are entirely of breccia. The lower cliffs along the west coast of the island also are everywhere of breccia; the upper cliffs west of the caldera appear from a distance to be similarly of breccia.

Several small cinder cones project through the Coulman Island ice cap. The best preserved and exposed of these cones lies two-thirds of the way down on the north slope of the cone of Coulman caldera, on the axis of the island (fig. 9). Cinders collected from this small cone are basaltic. The rim of another small cinder cone is exposed discontinuously through the ice cap, as seen in the lower left part of figure 7.

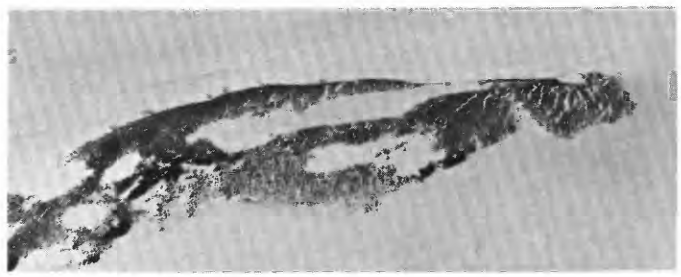

FIGURE 9.—Young basaltic cinder cone projecting through the Coulman Island ice cap. This cone is on the north slope of the broad cone of Coulman caldera, and lies on the inferred axial fissure zone of the island. 7 November 1964.

The southwestern coast of Coulman Island is indented by a semicircular bay, 7 km in diameter (fig. 6), which perhaps is another caldera, much modified by erosion.

DANIELL PENINSULA

The elongate volcanic pile of Daniell Peninsula trends south-southwestward along the coast, south from Tucker Glacier (figs. 4, 6, and 14). The peninsula is 70 km long and as much as 20 km wide. The northern two-thirds of Daniell Peninsula is a broad symmetrical dome (figs. 10, 11), whereas the southern third is embayed deeply by erosion. Ice-filled troughs separate the peninsula from the mainland mountains of Paleozoic rocks. Were the ice to melt, the peninsula would be almost an island, connected only by a short saddle between the heads of long fiords.

The volcanic pile is ringed by cliffs. Around the northern symmetrical part, the cliffs are 100–900 m high. On the west they are almost entirely covered by ice falls, and on the east they are discontinuously covered. Cliffs are higher in the deeply eroded southern part of the peninsula but are largely mantled by ice. The slopes and crest above the cliffs are almost everywhere ice covered.

The domical form of the northern two-thirds of the peninsula indicates formation from overlapping volcanoes concentrated along a crestal fissure zone. From the north end at Tucker Glacier, the crest rises southward to a prominent volcano, about 2,000 m high, thence drops to a level of about 1,500 m until the 2,000-m volcano of Mount Brewster is reached farther south. A broad upland just south of the southern high point perhaps marks an eroded, ice-filled caldera on the crest (fig. 11*B*). A crater indents the north end of the peninsula, and opens onto Tucker Glacier (fig. 12). The breccias and lavas exposed in the eastern cliffs of the peninsula dip outward, subparallel to the ice-covered surface above the cliffs.

The irregularly embayed southern part of the peninsula appears to be formed of overlapping volcanoes broken by two large deep breached calderas. The most obvious volcano is small Mount Lubbock, about 1,500 m high, which forms the south end of the peninsula. Between Mount Lubbock and the broad dome of the central part of the peninsula, two subcircular bays cut far into the east side of the peninsula (figs. 6, 10, 11*A*, 11*B*) and probably originated as calderas centered on the crestal fissure zone.

The eastern cliffs along the northern third of Daniell Peninsula are relatively well exposed. The lower half of the section is typically palagonite breccias and pillow breccias, whereas the upper half is mostly interlayered maroon and gray lavas which contain sparse palagonite lenses. The cliffs of the central third are mostly covered by icefalls, but the few avalanche-cleared sections seen from the air appear to mostly have a similar contrast between lower breccias and upper lavas. Well-exposed cliffs 550 m high at the headland 8 km northeast of Cape Phillips expose only assorted breccias and pillow complexes. No field examination was made of the peninsula south of this headland. The few exposures seen of the cliffs on the west side of the peninsula, along Whitehall Glacier, are breccias. Holocene cinder cones project through the ice that covers the high northern volcano.

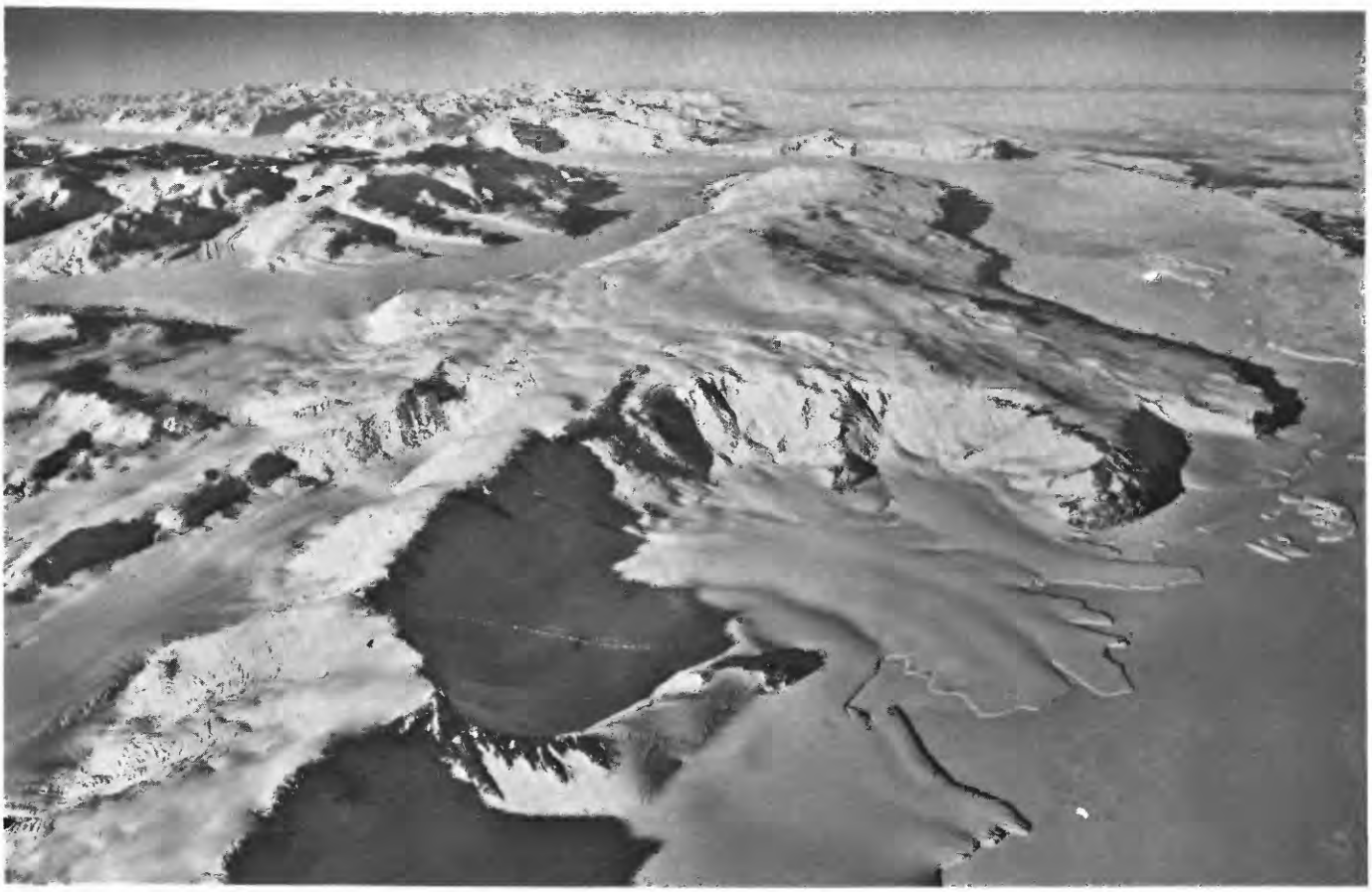

FIGURE 10.—Aerial view northward along Daniell Peninsula. Coalescing volcanoes along a crestal fissure zone have produced the broad dome. The large circular embayment below the center of the photograph probably marks a breached caldera. The floating ice shelf to the right of the embayment meets fast sea ice in the right foreground. In line with the peninsula to the north, across the trough of Tucker Glacier, is Mount Harcourt volcano of Hallett Peninsula. The higher peaks on the skyline reach altitudes of 4,000 m and are 170 km away. Photograph TMA 1037–F33, no. 197, by U.S. Navy for U.S. Geological Survey, altitude 7,600 m, 25 November 1962.

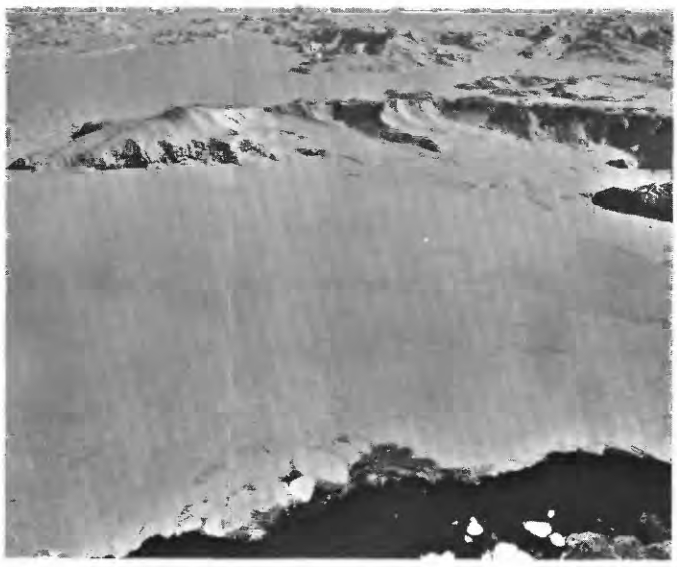

A

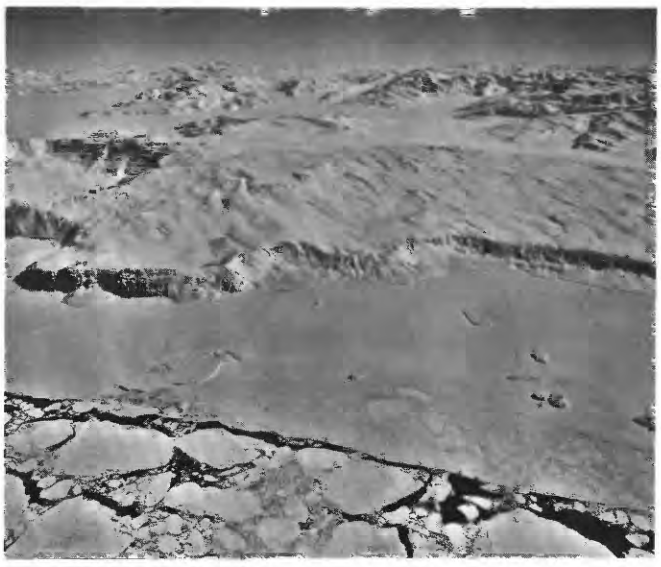

B

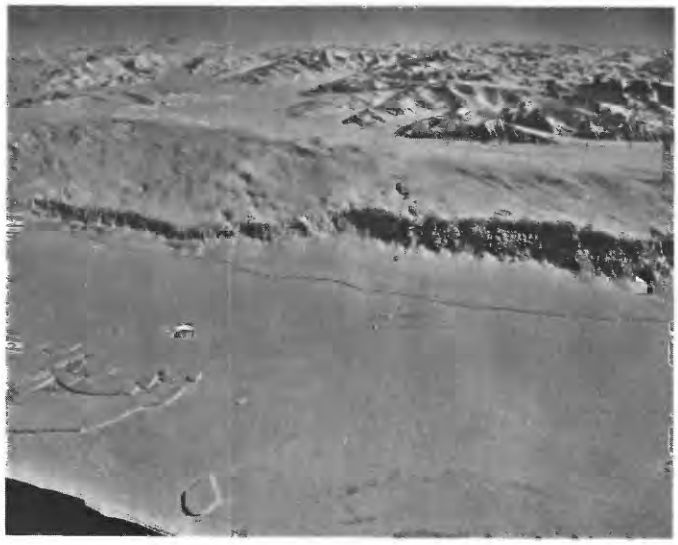

C

D

FIGURE 11.—Overlapping aerial views westward over Daniell Peninsula. Volcanic eruptions occurred mostly along the crest of the peninsula, which is 70 km long. The cliffs are formed largely of ice-contact palagonite breccias. Glacier-filled troughs separate the peninsula from the mainland mountains of pre-Tertiary rocks; the farthest skyline ranges are about 300 km distant. *A*, Most of the southern part of the peninsula is embayed deeply by erosion, probably by the breaching of two calderas. The young volcano of Mount Brewster (~2,000 m) forms the southern tip. *B*, The broad upland left of center stands about 2 km above sea level and may be an ice-filled caldera. Cape Phillips is in the left foreground. *C*, The palagonite cliffs on the right are about 1,000 m high. A floating ice shelf extends from the foot of the cliffs to the fast sea ice. *D*, Many outcrops mark the flanks of a volcanic dome right of center. A dark cinder cone stands on the far side of the ridge near the right end (Cape Daniell). Whitehall Glacier fills the trough separating the peninsula from Mount Northampton (2,500 m; the dominant peak right of center). Photographs TMA 712, F31, nos. 6, 12, 16, and 20, by U.S. Navy for U.S. Geological Survey, altitude 6,000 m, 3 November 1960.

FIGURE 12.—View southward across Tucker Glacier to the north end of Daniell Peninsula. The breached crater, and the broad volcano, 2,000 m high, of the skyline, are on the crestal fissure zone of the peninsula. 10 November 1964.

BASEMENT ROCKS

The only prevolcanic rocks exposed beneath any of the volcanic piles are present in cliffs 10 and 13 km northeast of Cape Phillips (figs. 6, 13), where an

FIGURE 13.—Basement rocks beneath basaltic breccias, east side of Daniell Peninsula 10 km northeast of Cape Phillips. The contact between light-colored Paleozoic granodiorite and dark Cenozoic basalt slopes down to the left through the center of the picture. The cliff on the right is about 200 m high. 26 November 1964.

island (or two small islands) of Paleozoic granitic rocks was buried by basaltic breccias. The granitic rocks rise from sea level to a maximum altitude of 250 m in the southern exposure and 350 m in the northern one. The rock is light-gray biotite granodiorite, resembling that of the batholith of Mount Northampton on the mainland to the west; it is perhaps part of the same pluton. The northern exposure displays a fair flow structure, sparse flat dark inclusions, and a few pegmatite dikes. The southern and larger exposure contains many large, irregular inclusions of contact-metamorphosed gneiss and is cut by many very irregular and discontinuous dikes of fine-grained dark rock.

HALLETT PENINSULA

Hallett Peninsula forms an isosceles triangle, whose baseline, 22 km long, trends west-northwestward along Tucker Glacier and whose 33-km sides intersect at Cape Hallett in the north (fig. 14). This is the best known of the peninsulas because of its easy accessibility from Hallett Station and because of the quality of its exposures. Most of the surface of the peninsula is hidden by an ice cap, but rock exposures are spectacular along the eastern cliffs, good along the southern cliffs, and fair along the northwest side.

The peninsula is a wholly volcanic composite pile of breccias and lavas erupted partly from an eastern zone of centers near the east edge of the present peninsula and partly from a southwestern zone. The constructional upper surfaces of the two accumulations meet at a swale that trends northward from Tucker Glacier to the Arneb Glacier (figs. 14, 16).

EASTERN BELT

The crest of the peninsula lies along the top of the imposing cliff which forms the straight east side. The cliff rises directly from the sea at an average slope of 60° to a height of 1,500–1,700 m along most of its length. (The map exaggerates the horizontal width of the cliff.) From the top of the cliffs, the constructional surface of the volcanic pile slopes gently northwestward to Edisto Inlet at the north and gently westward to the dividing swale at the south (fig. 14).

The rocks of the northern part of the eastern belt were erupted largely from a center within the present peninsula, but the rocks of the rest of the belt were erupted mainly from centers east of the present crest.

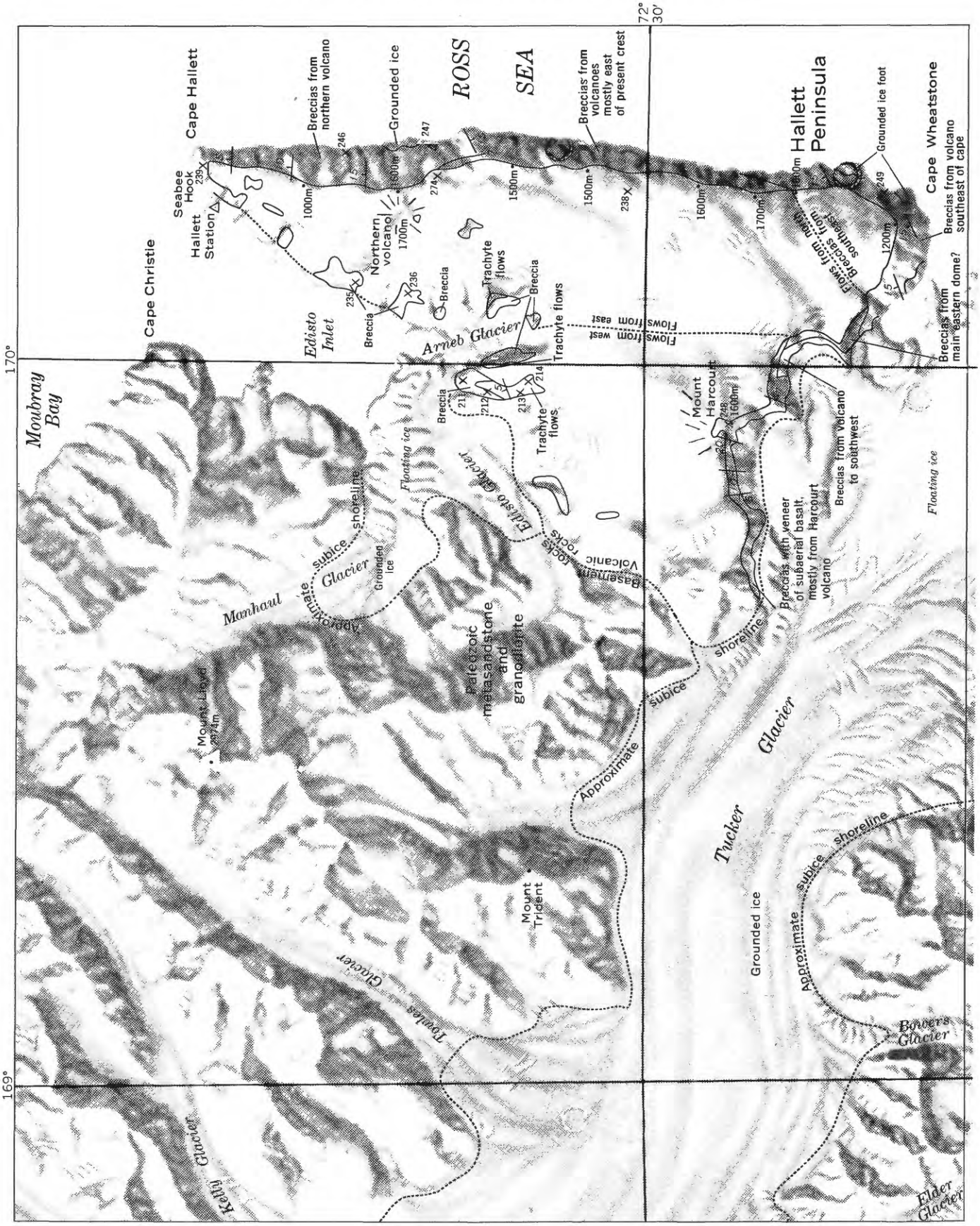
170°
169°
72° 30'
Cape Christie
Cape Hallett
Seabee Hook
Hallett Station
Moubray Bay
Edisto Inlet
Arneb Glacier
ROSS SEA
Breccias from northern volcano
Grounded ice
Breccias from volcanoes mostly east of present crest
Northern volcano
1700m
1500m
1000m
Breccia
Trachyte flows
Flows from west
Flows from east
Hallett Peninsula
Grounded ice foot
Cape Wheatstone
Breccias from volcano southeast of cape
Flows from volcano southeast
Breccias from main eastern dome?
1600m
1200m
Mount Harcourt
Breccias from volcano to southwest
Breccias with veneer of subaerial basalt, mostly from Harcourt volcano
Floating ice
shoreline
subice
Approximate
Grounded ice
Manhaul Glacier
Mount Lloyd
2574m
Mount Trident
Paleozoic metasandstone and granodiorite
Volcanic rocks
Basement rocks
Flatstad Glacier
Tucker Glacier
Bowers Glacier
Elder Glacier
Kelly Glacier
Tenaya Glacier

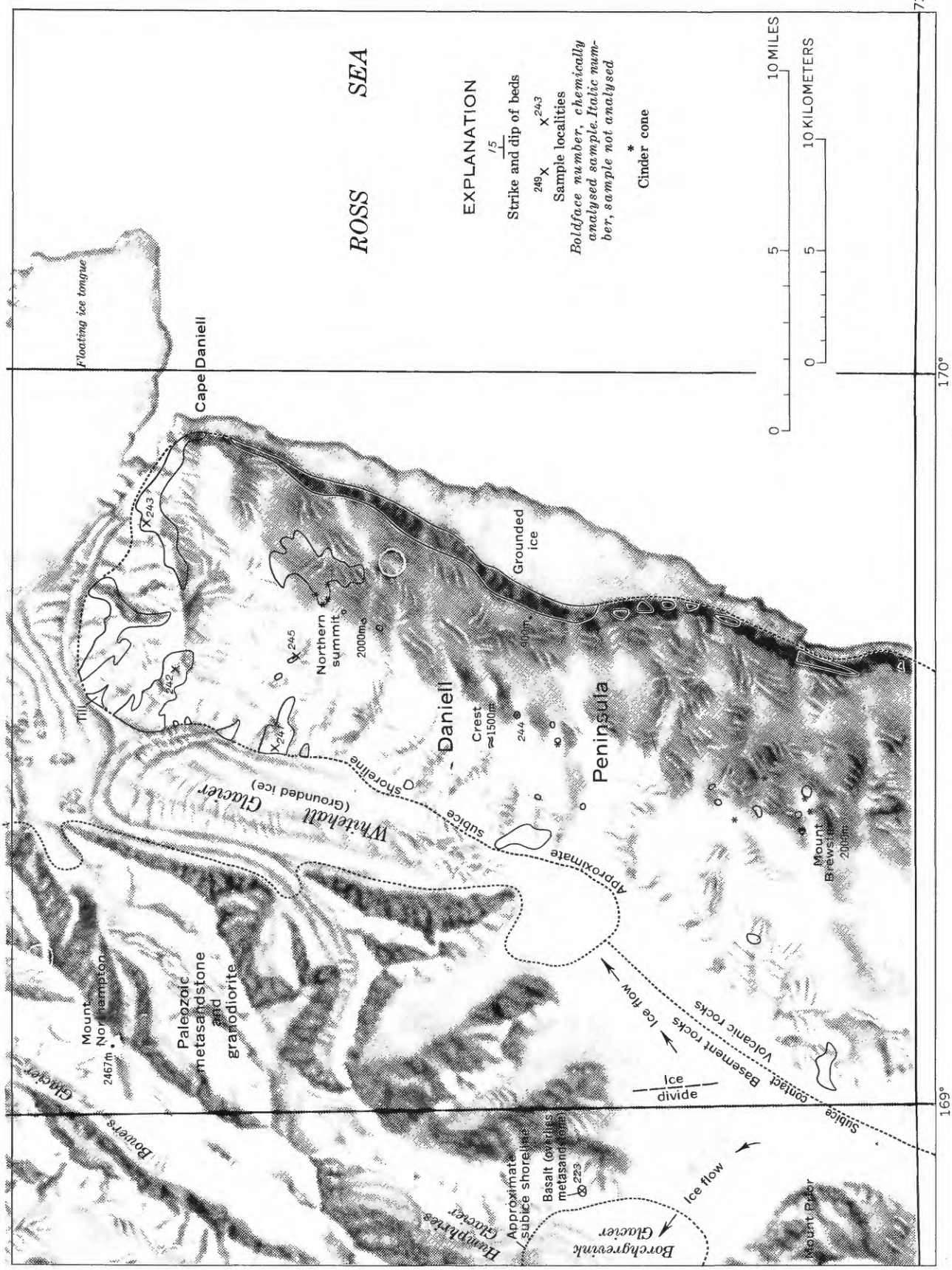

FIGURE 14.—Shaded-relief map of Hallett Peninsula and northern Daniell Peninsula, showing outcrops of volcanic rocks. Outcrops are not distinguished from ice on the mainland, which is of Paleozoic metasedimentary and granitic rocks except where noted. Base map by U.S. Geological Survey.

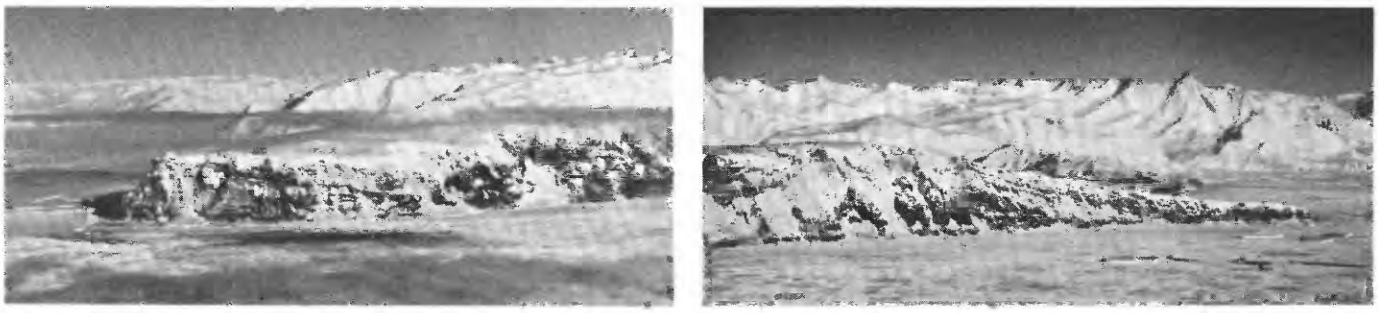

A *B*

FIGURE 15.—Aerial views westward over south and north ends of Hallett Peninsula. Late October, 1963. *A*, Cape Wheatstone. The breccias dipping northwestward into the peninsula were erupted from a vent since removed by erosion. The cliff at the cape is 1,200 m high. Tucker Glacier is on the left. *B*, Cape Hallett. Breccias and lavas erupted from the 1,700-m crest, left of center, dip northward to the cape.

Along most of the length of the peninsula, more than half of the eastern belt has been eroded away from the east. The eastern belt before this erosion must have resembled present Daniell Peninsula, an elongate volcanic dome.

NORTHERN VOLCANO

The only major volcano of the eastern belt that has an apex within the present peninsula forms a large dome 10 km south of Cape Hallett and 1 km west of the clifftop (fig. 14). The breccias and subordinate lavas of this volcano form the entire 1,600-m cliff directly to the east. The dip of the volcanic rocks decreases northward, from 15° near the volcano to 5° near Cape Hallett, and the crest of the peninsula drops correspondingly to a height of only about 200 m at the cape (fig. 15*B*). Rock units tend to thicken down the dip, so that the dip decreases upward in the section. The ice-covered slope northwestward from the volcano to Edisto Inlet presumably also is the surface of the volcano.

The rocks of the volcano also dip away from it to the south. The dip is marked—15°—low in the section; but the units thicken downdip, so that the dip decreases upward in the section, and within a few kilometers south of the volcano the dip of the upper units is subhorizontal. The general trace along the cliff of the layering in the breccias from here southward for 15 km is also subhorizontal, and in these chaotic materials it was not possible to distinguish the products of the different volcanoes.

The cliffs on the west side of the northern volcano are much lower than those on the east side, are mostly covered by ice, and expose varied palagonitic and pillow breccias, lavas, and pillow lavas. The best of the western exposures are those around Cape Hallett, north from Seabee Hook and Hallett Station (fig. 19). The cliffs here, a few hundred meters high, are of palagonite breccias and pillow complexes, which are capped by several tens of meters of interlayered scoria and subaerial lavas.

EASTERN VOLCANOES

South of the northern volcano, the surface of the eastern belt rises gently to its abrupt truncation by the eastern cliff, so that only a part of the west slope of the volcanoes is preserved. All major centers which contributed to the present surface lay east of the clifftop. There were no dominant circular volcanoes: no radiation of flows and breccias can be inferred from the uniform gentle westward slope of the surface, from the evenness of the 1,500- to 1,700-m crest, or from the subhorizontal trace of bedding in the breccias exposed in the eastern cliff. Perhaps the major eruptions were from long fissures; or perhaps they were from many centers scattered along a rift zone.

The eastern cliffs expose to their crest palagonitic breccias and pillow breccias. Of the rare exposures through the ice cap on the summit surface of the eastern volcanic pile, however, the several visited are of subaerial scoria.

SOUTHEASTERN VOLCANO

The breccias of the southeastern corner of Hallett Peninsula dip northwestward, even at Cape Wheatstone (figs. 15*A*, 16), and hence were erupted from a volcano southeast of the present peninsula. These breccias dip beneath those of the main eastern rift belt, indicating that this southeastern volcano is somewhat older. A minor swale separates the surface of the northwest-dipping corner breccias from the rest of eastern belt.

FIGURE 16.—Aerial view northward over Hallett Peninsula. From the conical volcano of Mount Harcourt (center), lavas slope westward to the rugged spurs of the mainland mountains. Most of the peninsula is formed of breccias erupted from a rift zone offshore from the eastern crest. Cape Wheatstone, far right, is formed of breccias dipping northwestward from an offshore source. Ice-capped Adare Peninsula (center skyline) is 100 km beyond Mount Harcourt, which stands 1,600 m above floating Tucker Glacier. Photograph TMA 720, F 31, no. 278, by U.S. Navy for U.S. Geological Survey, altitude 6,100 m, 4 November 1960.

SOUTHWESTERN VOLCANOES

The eastern belt of Hallett Peninsula is joined in the southwest to the mainland by a triangular mass of volcanic rocks, 15 km on a side (figs. 14, 16). From the highest, southeastern part of this mass rises the conspicuous conical volcano of Mount Harcourt (fig. 18). Mount Harcourt is directly in line with the crest of Daniell Peninsula (fig. 10), and the southwestern volcanic rocks of Hallett Peninsula apparently were erupted mostly from the north end of the Daniell rift zone. The rift zone is crossed at right angles by Tucker Glacier, which has removed any volcanoes that erupted in its path.

Young Mount Harcourt volcano dominates the southwestern mass (figs. 16, 18). The cone has been glacially eroded (presumably after breaching of a crater) back to its 1,600-m apex so that its structure is exposed in cross section. Eruptions from the volcano produced subaerial rocks at high levels but subglacial ones downdip.

Subaerial basalt lavas and cinders form the apex and veneer the slopes, and on the lower flanks lie unconformably upon older flows and breccias. The rocks of the volcano are otherwise entirely subglacial breccias. Between the all-subaerial and all-breccia sections is a zone of intertonguing, wherein subaerial rocks give way downdip to breccias (fig. 18). The transition-zone contact between subaerial and subglacial rocks occurs as high as 1,300 m, and as low as about 700 m, thus probably defining fluctuating levels of Tucker Glacier, against which the rocks were erupted. The youngest subaerial rocks were not seen to give way to breccias at any altitude, hence they represent eruption at a time of low ice levels more like those of the present.

The breccias within the erosional embayment dip outward from the center of Harcourt volcano and hence clearly were erupted from it. To the west, dipping breccias give way to interbedded subhorizontal breccias and lavas, across whose eroded surface lap subaerial flows and cinders. Whether these western breccias and subaerial rocks were erupted from Harcourt or from some unidentified center is not known. The breccias dipping outward from the center of Harcourt volcano are exposed southeastward for about 4 km from the volcano, at which distance the top of the breccias disappears beneath ice.

Breccias from a volcano centered either south or southeast of Mount Harcourt are exposed in cliffs east of Mount Harcourt (fig. 14). These remnants of a vanished volcano dip eastward beneath a westward-thinning wedge of other breccias, which presumably were erupted from a center along the eastern crest of the peninsula. The wedge is in turn overlain near its west edge by subaerial flows and cinders whose source was not established.

Cliffs and bare slopes west of Arneb Glacier expose well the north end of the southwestern volcanic mass of the Hallett Peninsula. Only palagonite and pillow breccias are exposed below an altitude of 300 m. Above this breccia complex, thin subaerial lavas and scoria

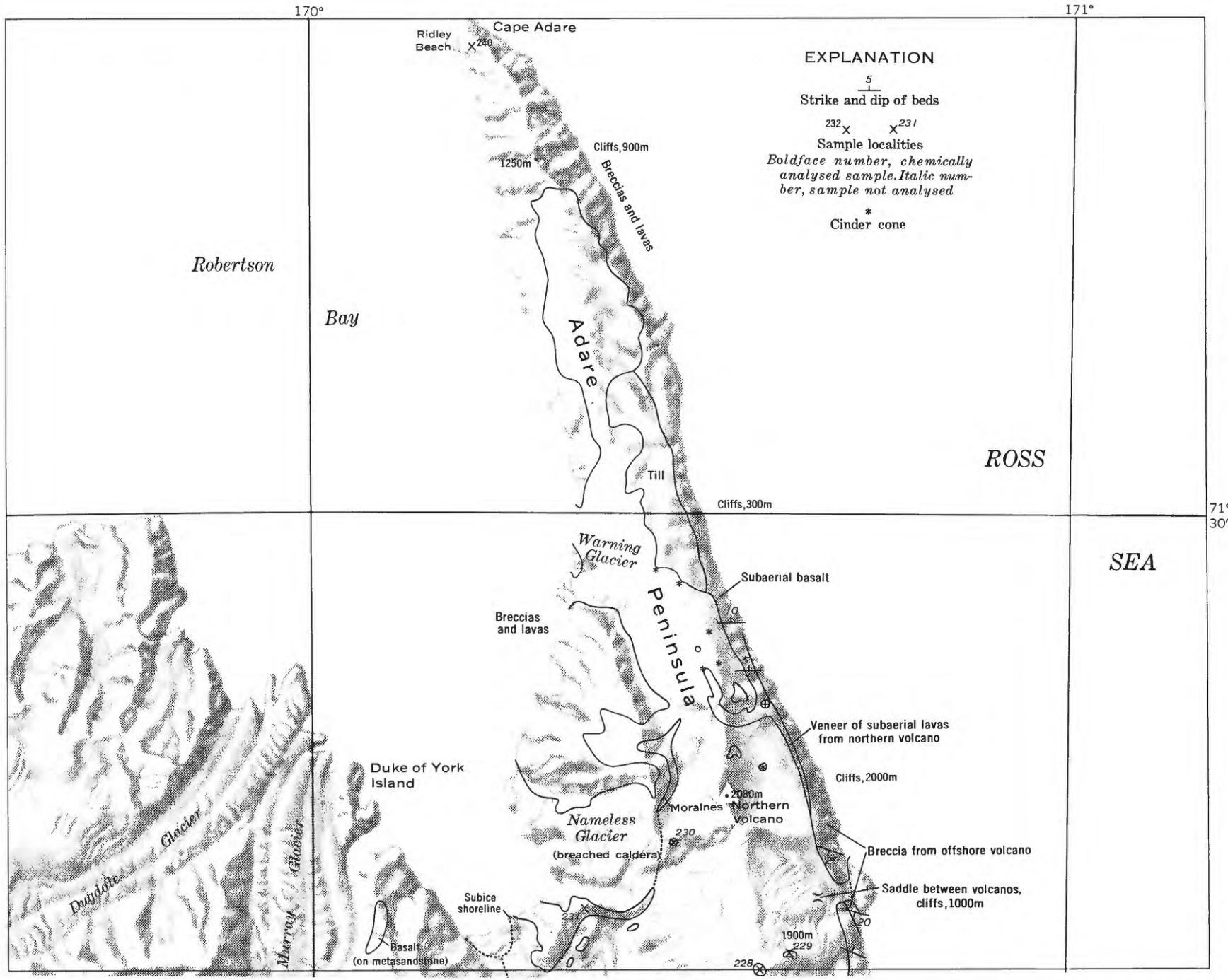

FIGURE 17.—Shaded-relief map of Adare Peninsula region, showing outcrops of Cenozoic volcanic rocks. Outcrops are not distinguished from ice on the mainland, which is of Paleozoic metasedimentary and granitic rocks except where noted. Base map by U.S. Geological Survey.

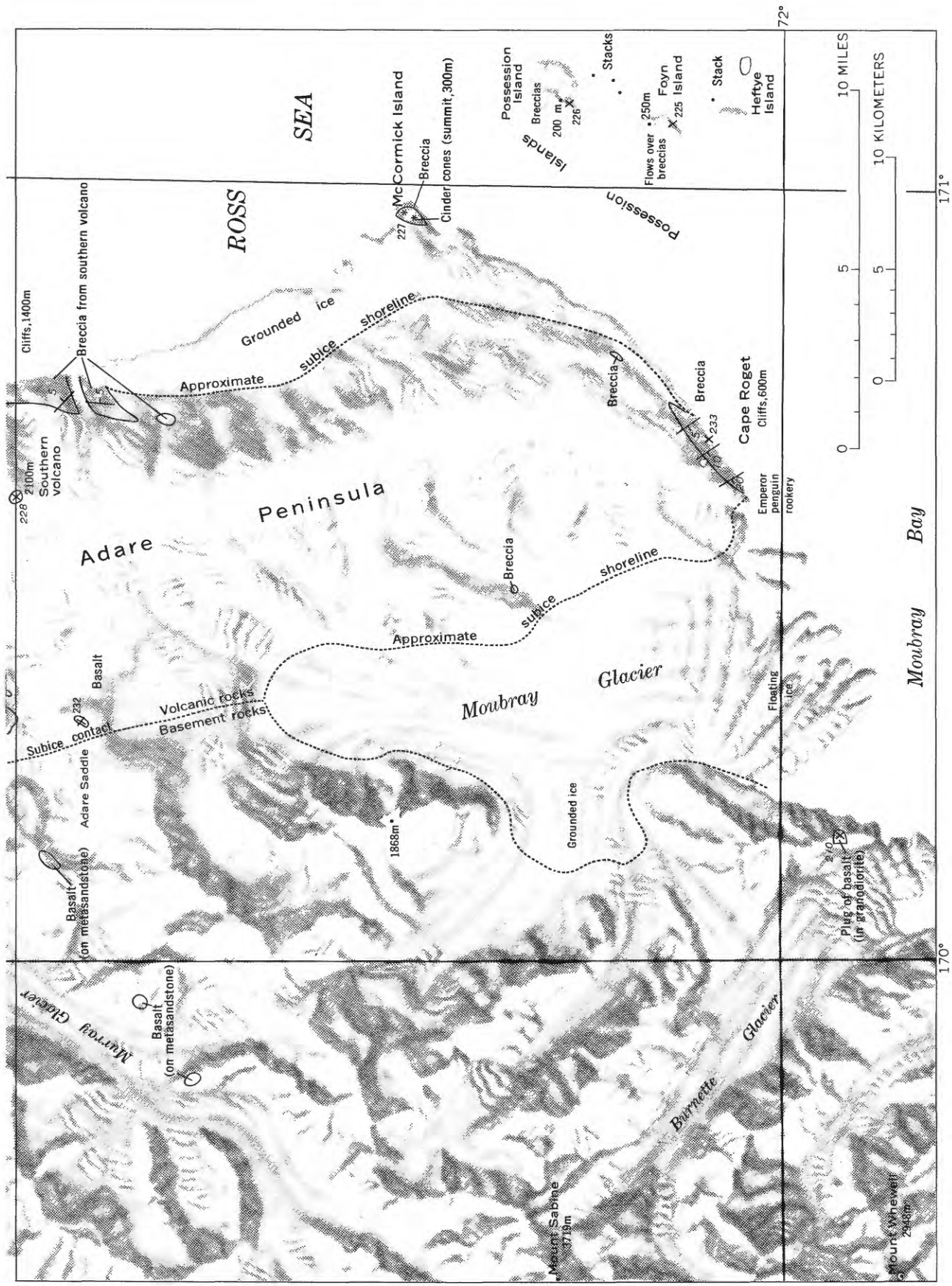
ROSS SEA
McCormick Island
Breccia
Cinder cones (summit, 300m)
Possession Islands
Possession Island
Breccias
200 m
226
Stacks
Flows over breccias
250m
Fayn Island
225
Stack
Heftye Island
72°
10 MILES
10 KILOMETERS
0
5
5
0
171°
170°
Cliffs, 1400m
Breccia from southern volcano
Grounded ice
Approximate subice shoreline
Southern volcano
2100m
228
Adare Peninsula
Breccia
Cape Roget
Cliffs, 600m
233
Emperor penguin rookery
Moubray Bay
Moubray Glacier
Floating ice
Volcanic rocks
Basement rocks
Subice contact
Basalt
232
Adare Saddle
Basalt (on metasandstone)
1868m
Grounded ice
Plug of basalt (in granodiorite)
210
Murray Glacier
Basalt (on metasandstone)
Burnette Glacier
Mount Sabine
2719m
Mount Whewell
2940m

FIGURE 18.—Mount Harcourt (1,600 m), looking northward from floating Tucker Glacier. Subaerial lavas and cinders form the apex of this young volcano and veneer its slopes, but give way downdip to ice-contact breccias. The dashed line on the right marks the approximate intertonguing contact between subaerial and subglacial rocks. 15 November 1964.

sheets cap the cliffs and cover the upper slopes. Both the lower breccia complex and the upper lava series dip gently northward, parallel to the constructional upper surface of the pile. The topographically highest and southermost exposures are at an altitude of 450 m.

FIGURE 19.—Aerial view, steeply downward to the east, of Cape Hallett (far left) and Seabee Hook. The hook is formed of beach-worked till. Fast sea ice surrounds hook and cape. Hallett Station is at the near (northwest) end of the hook, and the Adélie penguin rookery occupies most of the remainder. The hook consists of volcanic-rock till from a glacier which came down the steep slope from the crest of the peninsula and was grounded in this part of the inlet, as now is the glacier farther right in the photograph. The till of the southeastern part of the hook—the dark apron at the foot of the cliffs—preserves its primary angular blocks and hummocky topography. The till of the remainder of the hook has been variably modified by marine erosion and deposition and by ice push, during a stand of sea level higher than the present one. The broadly arcuate north edge of the hook has been most modified and now consists of a beach-gravel ridge, in which the larger boulders commonly have a diameter of half a meter. Low ridges and swales extending southward from the beach ridge in the narrow part of the hook may be modified from recessional-moraine lines. The broad west end of the hook is marked by west-trending beach features at the north side, and by irregular low ridges and swales roughly concentric to the southern shore. Photograph TMA 713–F31, no. 110, taken 3 November 1960 by U.S. Navy for U.S. Geological Survey.

SEABEE HOOK

Seabee Hook projects 1 km westward into Edisto Inlet from the west side of Cape Hallett (fig. 19, this rept.; Harrington and others, 1967, fig. 3 and folded map) and is formed of beach-worked till. The hook rises a maximum of about 5 m above sea level.

ADARE PENINSULA

The longest (77 km) exposed volcanic pile is that of Adare Peninsula. From the saddle by which it is attached to the northeastern corner of the mainland, the peninsula projects far to the north-northwest and a shorter distance to the south-southeast (fig. 17). The southern half of the peninsula is about 15 km wide; but northward from the middle, the peninsula narrows to Cape Adare.

Adare Saddle marks the contact between volcanic rocks of the peninsula and the basement rocks of the mainland. The sea-level length of the saddle is only about 12 km. Moubray Glacier fills the trough extending south from the saddle and is grounded almost to Cape Roget at the south end of the peninsula, beyond which it projects as a floating ice tongue. Very little ice is grounded north of the saddle; from the saddle the mainland coast extends northwestward, large Robertson Bay being enclosed between mainland and peninsula.

SOUTHERN DOME

The southern two-thirds of the peninsula is a broad, elongate, ice-capped asymmetrical dome (fig. 20*B*).

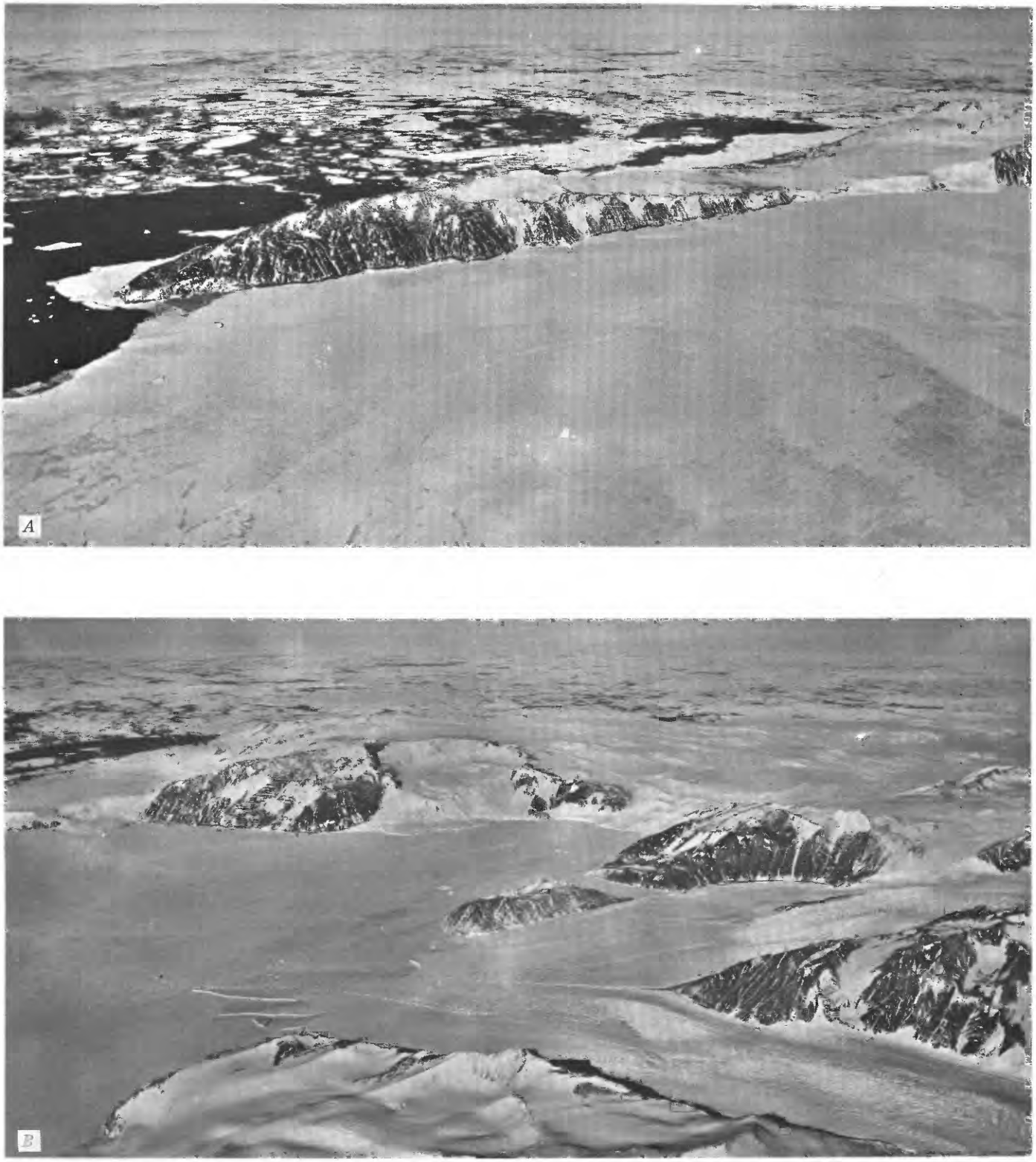

FIGURE 20.—Overlapping aerial views eastward to Adare Peninsula. *A*, The high, narrow northern part of the peninsula is separated from the broad shield volcano (right) by a broad saddle. Triangular Ridley Beach (beach and moraine) projects into Robertson Bay from Cape Adare (left). Length of peninsula at shoreline within picture is 30 km. The crest in the center of the picture is 1,400 m high. *B*, The broad shield volcano (center distance) rises 2,100 m above the sea ice of Robertson Bay. Nameless Glacier spills from a breached caldera on this shield. The volcanic pile is separated from the folded metagraywacke mountains of the foreground and right center by ice-filled Adare Saddle. (Photographs TMA 715, F31, Nos. 228 and 238, by U.S. Navy for U.S. Geological Survey, altitude 6,000 m, 3 November 1960.)

The 2,000-m crest of the dome lies east of the midline of the peninsula. The long, smooth, gentle south slope of the dome is almost entirely ice covered. The north slope is much steeper and, facing the midday sun, is mantled only thinly by ice, through which project many outcrops and cinder cones.

The high part of the dome is a composite of at least four major volcanoes. The most obvious of these has a caldera, 6 km in diameter, breached and filled by Nameless Glacier (fig. 20*B*). The flanks of the caldera volcano are relatively steep, and rocks apparently erupted from it extend only about 8 km north from the rim and an even shorter distance to the south. Subaerial basalts were sampled on the high east rim, and trachyte of uncertain occurrence on the lower southwest rim. The volcano was not examined elsewhere.

Two major volcanoes form the crest east of Nameless Glacier caldera, and their products cover those of a third volcano, whose original apex probably was offshore. The relations among the volcanic rocks from the three centers are seen in the cliffs on the east side of the peninsula. Breccias and pillow complexes from the offshore center extend almost to the 2,000-m top of the cliffs, where they are capped by a northward-thickening veneer of subaerial rocks from the northern volcano (fig. 21). Navy air photographs indicate that the breccias dip more gently northward than the overlying subaerial rocks and are bevelled against them; the subaerial rocks appear to reach sea level and are so indicated in figure 19. At least five cinder cones are exposed along the north slope of the northern volcano (figs. 17, 21) and indicate continuing activity along a crestal vent zone. All preserve circular rims and closed craters but show varying degrees of ice erosion. Breccias from the offshore volcano, dipping about 20° southward, are overlapped by breccias dipping gently outward from the southern volcano. Subaerial basalt and trachyte were collected from near the summit of the southern volcano, but no veneer of these rocks is apparent in photographs of the cliffs to the east. The surfaces of the southern, northern, and offshore volcanoes meet in a swale, from which an outlet glacier tumbles to the sea and supplies a grounded ice foot.

FIGURE 21.—Aerial view westward over the northern part of the main shield volcano of Adare Peninsula to Robertson Bay and the mainland. The cliffs rise 2,000 m above the sea ice; the lower 1,800 m is of palagonitic and pillow breccias, whereas the capping darker 200 m is of thin-bedded subaerial lavas. One cinder cone on the left, and two on the right, project through the capping ice; exposures between them are partly of moraines. Nameless Glacier caldera indents the far side of the summit plateau on the left. Photograph TMA 712, F 31, no. 61, by U.S. Navy for U.S. Geological Survey, altitude 6,000 m, 3 November 1960.

The south end of the peninsula is ice capped except near Cape Roget, where 600-m cliffs expose breccias and pillow complexes. The uppermost 50 m in some of these cliffs is of thinly layered dark rocks, which could be subaerial. The breccias dip southwesterly, hence the rocks probably were erupted from a source near the east side of the peninsula.

The smooth southwesterly slope of the southern half of the peninsula, little modified by erosion, is the constructional top of the volcanic pile. There is no comparable constructional slope to the east, for, from the divide near the east side of the peninsula, ice falls much more steeply to the sea. The original vent zone and constructional crest must have lain east of the present topographic divide, the eastern half or more of the volcanic edifice having been eroded away. The breccia platforms of McCormick Island and the Possession Islands presumably are remnants of the missing edifice. As is discussed subsequently, the Possessions may have formed near major vents, so they may mark the vent zone of an enormous volcanic structure, of which the southern part of Adare Peninsula preserves only the lower half or third of the western flank.

NORTHERN PENINSULA

A broad, low saddle marks the beginning of the northern peninsula. Warning Glacier tumbles into Robertson Bay from the west side of the saddle (fig. 20*A*), but sea cliffs several hundred meters high bound the east side. As the crest climbs northward from this saddle, the peninsula narrows and the bounding sides rise and converge at a 1,400-meter apex. The crest is close to the seaward east side, where sheer cliffs rise several hundred meters above the water, and broken cliffs extend to the crest. On the bay side, the basal cliff is lower and the upper slopes are moderate. The original volcanic crest lay east of the present topographic crest.

Gently sloping parts of the crest near the north end of the peninsula are veneered by till, which is formed largely of local volcanic rocks. Up to an altitude of 520 meters, however, numerous erratics of mainland metasandstone and metasiltstone, and a few of granitic rocks, were seen during an air-and-ground inspection. Thus, an ice sheet filling Robertson Bay and moving northward and eastward away from the mainland at one time extended to at least this altitude and may well have covered the entire peninsula. Till mantles most of the exposed surface of the broad saddle between the high central volcanic dome and the narrow northern peninsula, but this till was not examined and it is not known whether it contains mainland erratics.

The sea cliff on the west side of Cape Adare consists of basalt flows and a massive basalt unit of undetermined character. The northern peninsula was sampled only at outcrops through till at the top of the bluffs east of Ridley Beach. The lower of these outcrops consists of a subaerial breccia of ropy basalt fragments (bombs?), the upper of basalt of undetermined occurrence. Priestley (1923, p. 8–11) reported that the northern part of the peninsula is composed of interbedded basalt lava and subordinate breccia, dipping gently northward. His photographs (1923, pls. 7, 8) show breccias, megapillows, and agglomerate.

Priestley (1923, p. 11 and pl. 11) described a remarkable agglomerate at Cape Adare, which contains in a matrix of tuff abundant "foreign boulders . . . which both from their heterogeneity and the shape of individual boulders are undoubtedly glacierborne erratics." The dominant erratic type is "green quartzite," but schist, granitic rocks, and varied volcanic and porphyritic rocks are present also. I infer subglacial eruption through morainal debris at the base of an ice sheet extending from the mainland.

RIDLEY BEACH

Triangular Ridley Beach projects westward into Robertson Bay from Cape Adare (figs. 20, 22, this rept.; see also map by Priestley, 1923, pl. 2). It consists of two sets of ridges standing a few meters above sea level and separated by swales. One set forms concentric arcs parallel to the southwestern shore, curving northwestward from initial trends almost tangential to the peninsula. These ridges are truncated at high angles by the second set, which consists of less regular ridges along the northwest edge in a belt 150 or 200 m wide. The beach is composed of gravels dominated by volcanic rocks but containing numerous erratics from the mainland. Sounding and bottom sampling by Priestley (1923, p. 2 and pl. 2) showed that similar gravels extend at least 700 m to the northwest and 500 m to the west of the exposed beach.

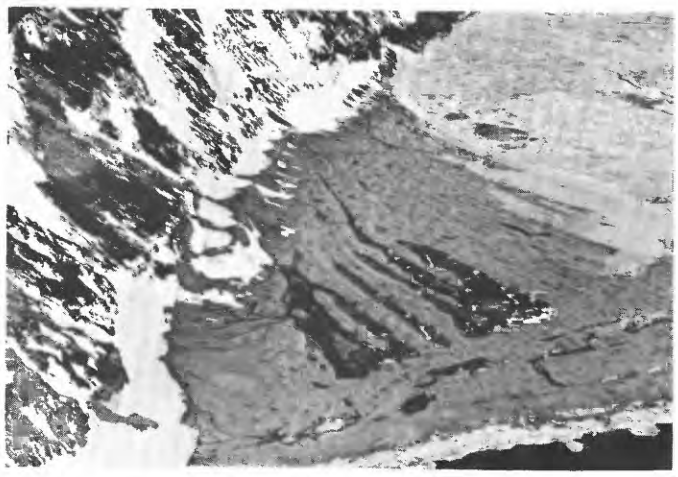

FIGURE 22.—Aerial view southward over Ridley Beach, which projects 1 km westward into Robertson Bay from Cape Adare. The ridges along the near shore have been produced by beach processes, but the arcuate ridges subparallel to the far shore, and forming most of the area, may be recessional moraines. The low terrace along the foot of the cliffs is of protalus ramparts and of till from past hillside glaciers. 14 November 1964.

The concentric arcuate ridges which form most of the beach may be recessional moraines from an ice sheet that once filled Robertson Bay. All the arcuate ridges have been modified uniformly by beach processes and ice push along the north edge of the triangle (fig. 22); the arcuate ridges are older than the northern beach ridges and did not form concurrently with them.

McCORMICK ISLAND

McCormick Island (Cape McCormick on older maps) is joined to southern Adare Peninsula by grounded ice. The island consists of a platform of breccia, ringed by a sea cliff and surmounted by two

A

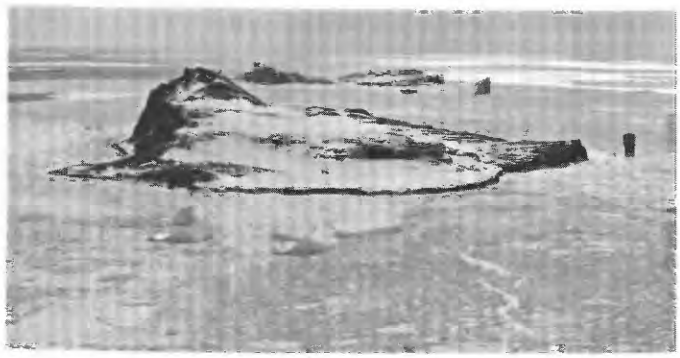

B

FIGURE 23.—Aerial views of the islands east of southern Adare Peninsula, 8 November 1964. *A*, Northward across McCormick Island. Two Holocene cinder cones lie upon a sea cliff-ringed platform of breccia. The unbreached crater contains a lake. Summit altitude is about 300 m. *B*, North-northeastward over Foyn Island (center) and stacks to Possession Island (distant). The high point of Possession Island, 200 m high, is held up by a basalt dike that dips toward the swale in the center of the island.

very young basalt cinder cones, one breached and the other not (fig. 23*A*). The breccia platform could have been beveled by either sea or ice erosion, but the cinder cones have not been eroded by ice, and hence they are younger than all prior periods of glaciation appreciably more extensive than the glaciation of the present time. The northern cone was sampled and found to contain abundant xenoliths of white granitic rock.

POSSESSION ISLANDS

Volcanic remnants form the small Possession Islands, east of southern Adare Peninsula (figs. 17, 23*B*). Four islands and four stacks form a group 10 km long in a northerly direction and 3 km wide. All the islands are ringed by sea cliffs. The two main islands, Possession and Foyn (fig. 23*B*), bear permanent snowfields, but none of the islands has an ice cap. The rocks that were seen are entirely basaltic. Names of the individual islands have been used inconsistently; the convention followed here is that of the Northeastern Victoria Land Sketch Map of the U.S. Geological Survey.

Possession Island is the northernmost of the group and, with a diameter of about 2.5 km, is also the largest. A prominent rib trends along the west side of the island to form its 200-m crest, from which cliffs fall directly to the sea. The rib is formed by a dike of basalt, about 50 m thick, that dips 35° eastward and is well exposed in the sea cliffs; the east slope of the rib is the stripped upper surface of the dike. Beneath the dike (or perhaps part of it) is a megapillow complex (fig. 30*B*). A sharp low swale separates the rugged western third of the island from a rolling platform, formed of nearly horizontal basalts, that rises gently eastward to the top of sea cliffs 60–100 m high.

Foyn Island (fig. 23*B*) is an uneven platform 2 km in diameter that rises to a 250-m peak at the north end. The high northern sea cliffs expose basaltic breccias, pillow complexes, and a megapillow (fig. 30*C*). The surface of the island where examined in its southern part is formed of apparently subaerial basalt —mostly dense lava and partly scoriaceous lava. Small cinders are abundant, and a large pile of them may represent an ice-eroded cinder cone, but other than this possible cone no vents for either flows or cinders were recognized.

No landings were made on Heftye Island (fig. 30*A*) or on the small unnamed southern island of the Possession group, but telephotographs taken from Foyn Island show their structure clearly. Both islands consist of breccias and megapillow complexes. Heftye has a rolling surface from which vertical cliffs fall 60–80 m to the sea, whereas its unnamed neighbor has a rugged summit of about 250 m.

Possession, Foyn, and Heftye Islands have rolling surfaces, and the basaltic rubble that covers most of the surfaces of at least Possession and Foyn has been much redistributed by ice. No mainland erratics were noted. Whether the ice consisted of local caps or was part of a large Ross Sea ice sheet is unknown. As no elevated beaches or raised sea cliffs were recognized, marine planation is not called upon to explain the rolling erosion surfaces.

The Possession Islands expose in general much more massive rocks than do any of the large coastal volcanic piles. Palagonite breccias and thin flow units, which dominate all the coastal complexes, are a minor component of the islands, whereas massive megapillows, at least 50 m in diameter, are conspicuous on the islands (fig. 30). The islands presumably owe their preservation to the resistance of these massive rocks

to erosion, any surrounding palagonitic and thinly layered complexes having been eroded away.

The Possession Islands may mark the vent region of an old pile of breccias like those of the large coastal accumulations. The massive megapillows perhaps formed near the source, and the breccias away from it. The northerly alinement of the islands is the general direction to be expected for a vent zone in this region.

AGE OF VOLCANIC ROCKS

The volcanic rocks of the Hallett province are of very late Miocene, Pliocene, and Quaternary age, and all major volcanic piles are still active. Table 1 presents potassium-argon whole-rock determinations of the age of basalt samples as analyzed by Richard Lee Armstrong (written commun., 1968) of Yale University. The general reliability of such whole-rock determinations of age of unaltered basalts is demonstrated by the concordance between determinations from separated minerals and those from whole rocks (Burke and others, 1969).

Three of the dated samples are from topographically and structurally low positions in the volcanic piles of Coulman Island and Hallett Peninsula and are of latest Miocene and early Pliocene[1] ages—7.3, 6.6, and 5.4 m.y. (million years). The volcanoes rise from a continental shelf 300–600 m deep; this depth is small relative to the 1,500- to 2,000-m altitudes of the crests, so presumably volcanism began within very late Miocene time.

The fourth sample is from the south end of Adare Peninsula and has an age of 2.6 m.y.—late Pliocene, if we accept the age of 1.8 m.y. favored by Bandy and Wilcoxon (1970), Kennett, Watkins, and Vella (1971), and others for the Pliocene-Pleistocene boundary. The sample is from the base of the 600-m cliffs at Cape Roget. This represents middle rather than basal levels in the exposed volcanic structure: older rocks are exposed in the much higher cliffs farther north. The lower part of the Adare volcanic pile must be of Miocene or early Pliocene age.

The volcanic structures of Coulman Island and Hallett and Adare Peninsulas thus have been built during the same late Miocene to Holocene time span insofar as their ages can be defined.

TABLE 1.—*Potassium-argon dates from whole-rock samples of basalt low in the volcanic piles of the Hallett province*

[Analyses by Richard Lee Armstrong, Yale University, 1968. Constants used for calculations of dates: $K_{\lambda\beta}$, 4.72×10^{-10} year; $K_{\lambda\epsilon}$, 0.584×10^{-10} year; K^{40}/K, 0.0119 atom percent. Sample localities are shown on figures 6, 14, and 19. Radiogenic argon calculated at standard temperature and pressure]

Field No.	Type of volcanic rock	Radiogenic $Ar^{40}\times10^{-6}$ cm^3g^{-1}	Air correction (percent)	Potassium (percent)	Age (10^6 years)
220C	Pillow in palagonite breccia, west side Coulman Island	0.609	85	2.09, 2.10	7.3±0.48
247G	Massive basalt, grades into palagonite breccia, east side Hallett Peninsula	.277	82	1.04, 1.06	6.6±0.37
249B	Pillow in palagonite breccia, Cape Wheatstone, Hallett Peninsula	.448	55	2.07, 2.08	5.40±0.15
233D	Pillow in palagonite breccia, Cape Roget, Adare Peninsula.	.072, .078	95 96	0.732, 0.717, 0.726	2.60±0.4

BATHYMETRY

The volcanic peninsulas and Coulman Island rise from a continental shelf which has a depth of mostly between 300 and 600 m (fig. 24). At the north end of the Ross Sea, the shelf break is at about 500 m, the continental slope trends northwestward, and the ocean floor at its foot has a general depth of about 2,200 m. The relatively deep shelf break is characteristic of Antarctica and is generally attributed to isostatic depression of the continent under the load of its ice cap.

The Adare Peninsula volcanic field appears from the submarine topography to extend far to the southeast, east, and north from the exposed peninsula: volcanism has extended the continental slope northeastward by building upon it. The northward underwater projection of the peninsula continues to the edge of the continental slope. East of the peninsula, the continental slope trends northward, perhaps there also expanded by volcanism. The 400-m isobath may roughly outline the volcanic pile and if so the volcanic axis trends north-northwestward, passing through the Possession Islands and near the east side of the exposed peninsula.

The 400-m isobath lies close to the southern ends of both Daniell and Hallett Peninsulas, but swings far

[1] In these designations, I am following the time scale of Berggren (1969), which places the Miocene-Pliocene boundary at about 6 m.y.; see also Charlot and others (1967). This age is thought to be that of the boundary between the Epochs as defined by marine invertebrates in the Mediterranean region, although ambiguities permit a boundary within the range 5.5–7 m.y. The 12 m.y. age of the boundary established in North America between the Barstovian and Clarendonian vertebrate stages, long assumed to be late Miocene and early Pliocene, respectively, apparently is much older than the type European Miocene-Pliocene boundary.

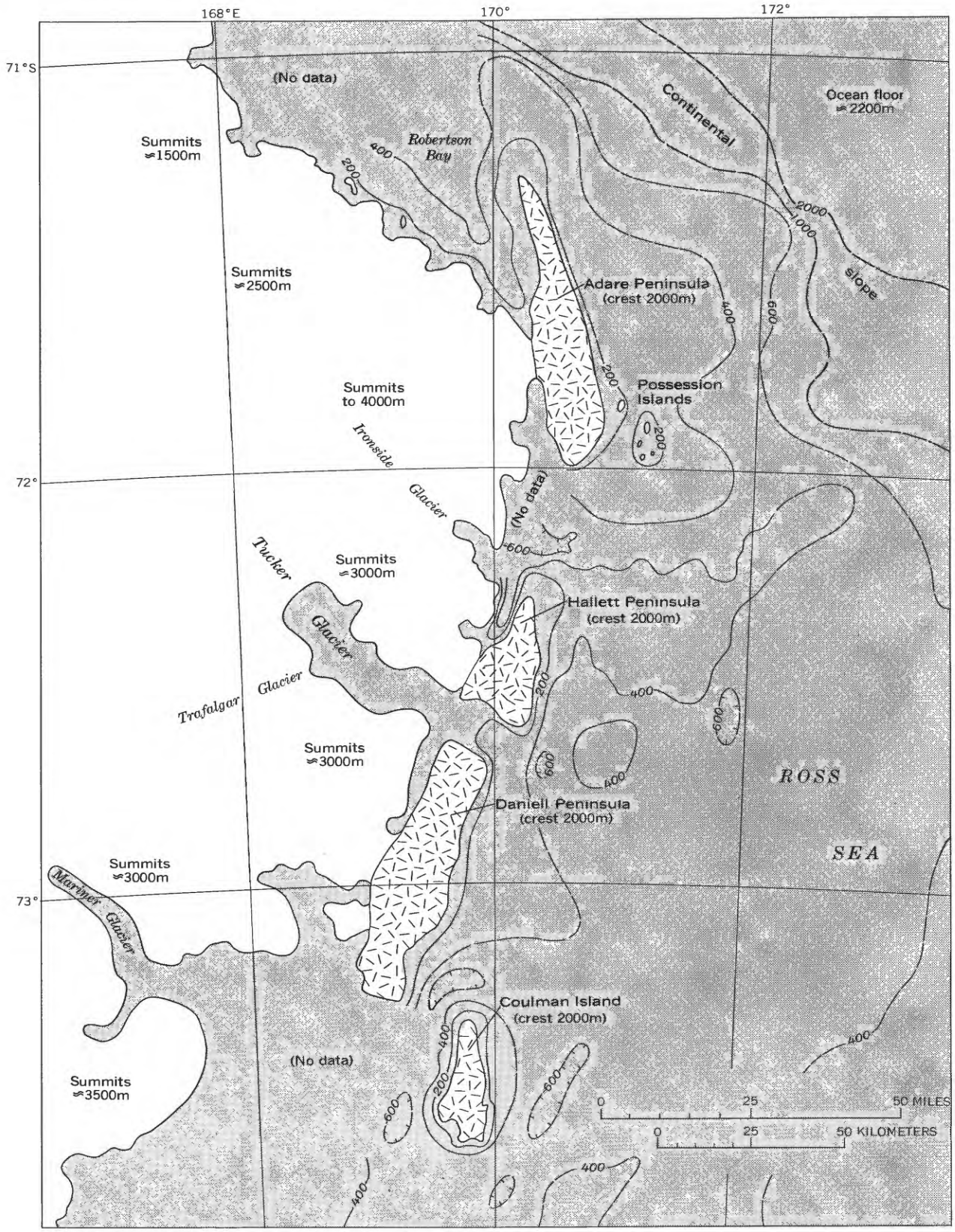

FIGURE 24.—Bathymetric map of the northwestern Ross Sea. Contours in meters; dashed where control poor. The major exposed volcanic piles are marked by a pattern. The coastline shown is the subice shoreline as interpreted beneath grounded ice where present. Contoured from soundings reported on U.S. Navy Hydrographic Office Charts 6626 (1962), 6627 (1966), 6628 (1966), 6636 (1966), 6663 (1959), and 6665 (1963).

eastward from central Daniell and from northern Hallett without obvious relation to known and inferred vent zones. Coulman Island is closely surrounded by deep water, and depths between it and the mainland exceed 600 m. There is no suggestion in the bathymetry that any underwater volcanic pile connects the island with Daniell or Hallett Peninsulas. Nor does a submarine ridge connect Adare and Hallett Peninsulas to suggest continuity of volcanism between them; on the contrary, the peninsulas are separated by a west-trending submarine low, which has a depth of more than 600 m. Erosion by an enlarged Ironside Glacier is inferred.

THE BRECCIAS

Each of the offshore volcanic piles largely consists of breccias and lavas apparently formed by eruptions beneath ice sheets and melt-water lakes. The chaotic varicolored volcanic complexes are exposed spectacularly in cliffs that reach heights of 2,000 m. Many of the rock characteristics are shown in the photographs (figs. 25–30) and are described by the photograph captions.

The complexes consist mostly of irregularly anastomosing layers and lenses, or marble-cake chaoses, of nodular basalt in palagonite breccia, and include minor amounts of bedded palagonite tuff. Dikes, sills, and megapillows intrude these complexes, which are interpreted to have formed in contact with ice and melt water. More evenly layered units of lava flows and reddish scoria and breccias also occur.

The paucity of throughgoing bedding markers and the complicated lateral and vertical gradations and mixing of contrasted rock types apparently indicate that thick sections formed during single episodes of continuous volcanism. Figure 26*B* illustrates a 400-m section formed mostly of two volcanic-episode units. The upper 200 m of figure 26*A* represents one unit. The only obvious break in the section of figure 26*C* occurs at a height of about 250 m in the 600-m section. Still thicker units can be inferred in much higher cliffs such as those of figure 25. The clear definition of volcanic-episode units of Daniell Peninsula illustrated by figure 29*A* is exceptional.

PALAGONITE BRECCIA

Palagonite breccia consists of clasts, nodules, and granules of basalt in a palagonitic matrix. The light-colored breccia occurs primarily as lenses intercalated, interfingered, and anastomosed with dark nodular flows and pods of basalt to form thick composite units. This section describes the breccia component of these units. The amount of breccia in the composite units is generally between 20 and 70 percent, but the content drops to 5–10 percent in some units, in which it adds an irregularly striped or marble-cake appearance to the otherwise relatively massive basalt, or discontinuously separates thin pods or lenses of lava (figs. 26, 27, 28, 29).

The breccia lenses are mostly yellowish or brownish gray and range in thickness from less than 1 m to more than 50 m. Throughgoing bedding planes, separating composite units, are commonly hundreds of meters apart. The units separated by such discontinuities consist of breccia and lava intertongued at all levels; each unit consists of two rock types that formed simultaneously and accumulated without major break in volcanism.

Basalt clasts vary greatly in size within single lenses, typically from 1 cm (centimeter) to 1 m in maximum dimension, but reaching 10 m. Varying concentrations and sizes of clasts define obscure, discontinuous bedding within breccia lenses (fig. 27*A*).

Clasts vary widely in texture and appearance. They are dense to richly vesicular, the vesicles being either empty or lined with secondary minerals but not commonly filled (figs. 27*B*, *C*). Concentric rims of vesicular basalt on blocks of more dense basalt (figs. 27*B*, *C*) demonstrate that fragmentation and fluid eruption overlapped in time. Clasts, like the rock of the lenticular flows intercalated with the breccias, are of gray—not reddish and oxidized—basalt.

Fragmentation of the lenses and pods of nodular basalt to produce clasts like those in the breccia is apparent along most contacts between breccia and lava (figs. 27*D*, *E*). The nodular lavas are closely jointed, and many parts of them are fractured to granule size; the lavas grade into breccias as their marginal fracture-bounded chunks become separated and the interstices are filled by granules of palagonite and of varied basalt. The breccias are the most fragmented parts of the lava flows.

Clastic dikes of palagonite breccia and palagonite tuff cut through the breccia sequences and have exposed heights of hundreds of meters in many places. Some, like those of the east side of Coulman Island (fig. 26*C*), are as thick as several tens of meters. The abundance of these clastic dikes emphasizes the mobile character (due to water lubrication and "slippery" mineralogy?) of the tuffs and breccias during the volcanic episodes.

PALAGONITE TUFF

The brightest colors of the volcanic piles, the yellows and subordinate reds and oranges, are provided by the palagonite tuffs. The tuffs are bedded to massive and occur as large masses of relatively pure tuff,

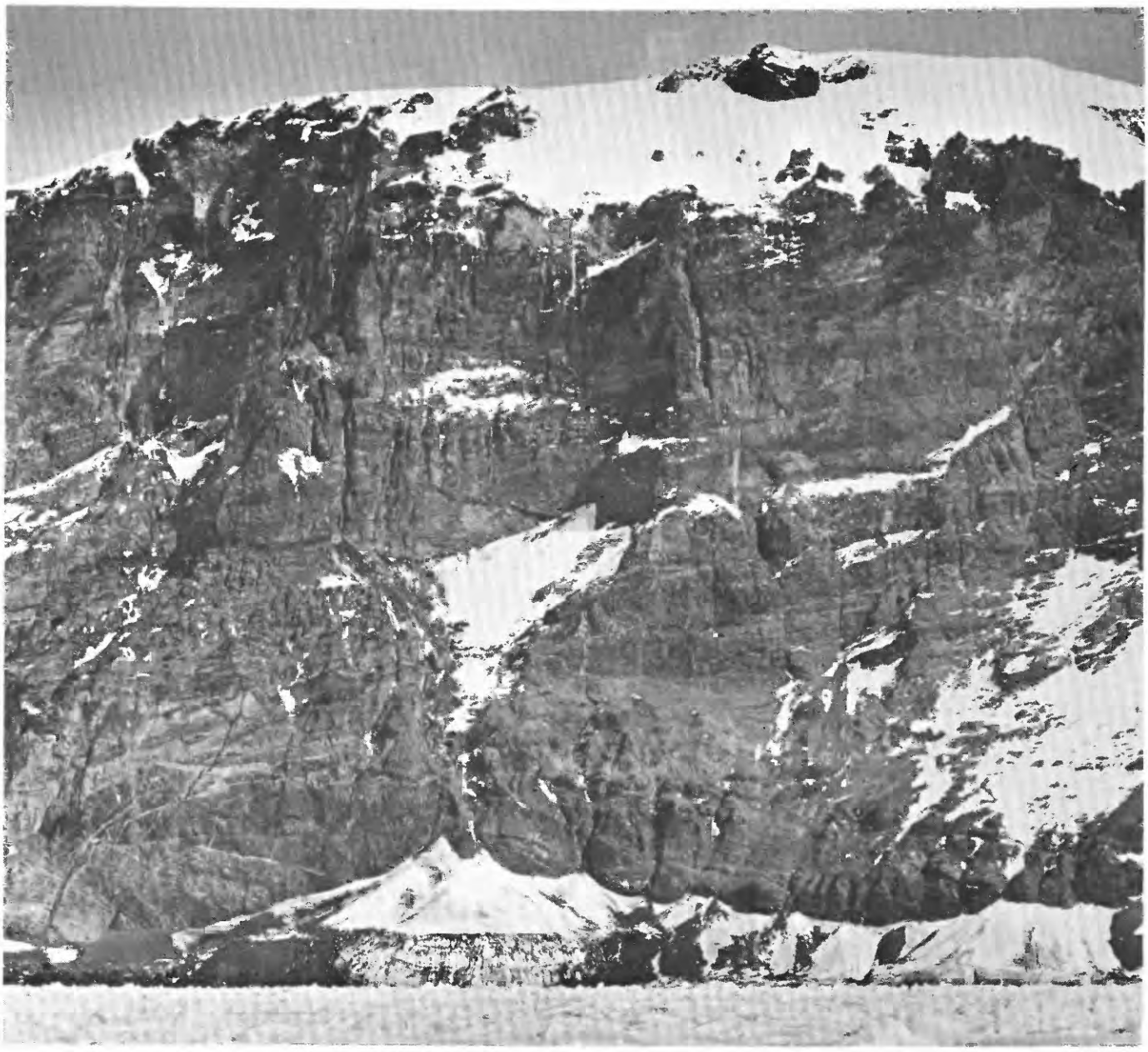

A

FIGURE 25.—Breccias of east side of Hallett

A, Palagonite breccia, nodular lavas, and subordinate amounts of palagonite tuff, with varying dips due to superposition of products from several vent areas. Note the paucity of throughgoing bedding planes. Center of peninsula.

B

Peninsula, exposed in cliffs 1,400–1,500 m high.

B, Palagonite breccia, nodular lavas, and palagonite tuff. No bedding plane can be traced with confidence across the picture. The well-bedded lavas of the lower left, for example, merge right of center with marble-cake breccia and lava which grades upward into interlayered breccia and lava. Twelve km north of Cape Wheatstone.

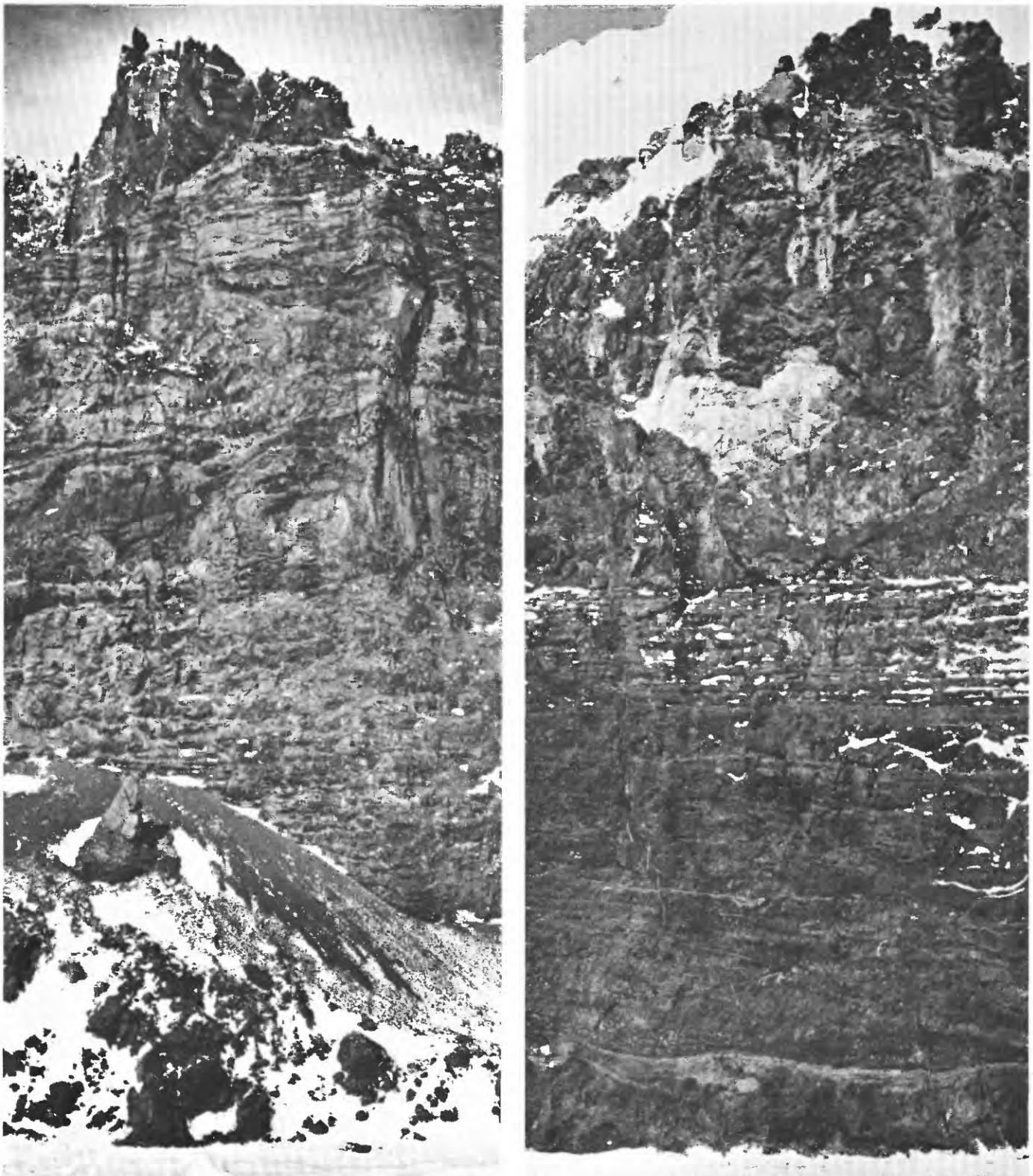

A *B*

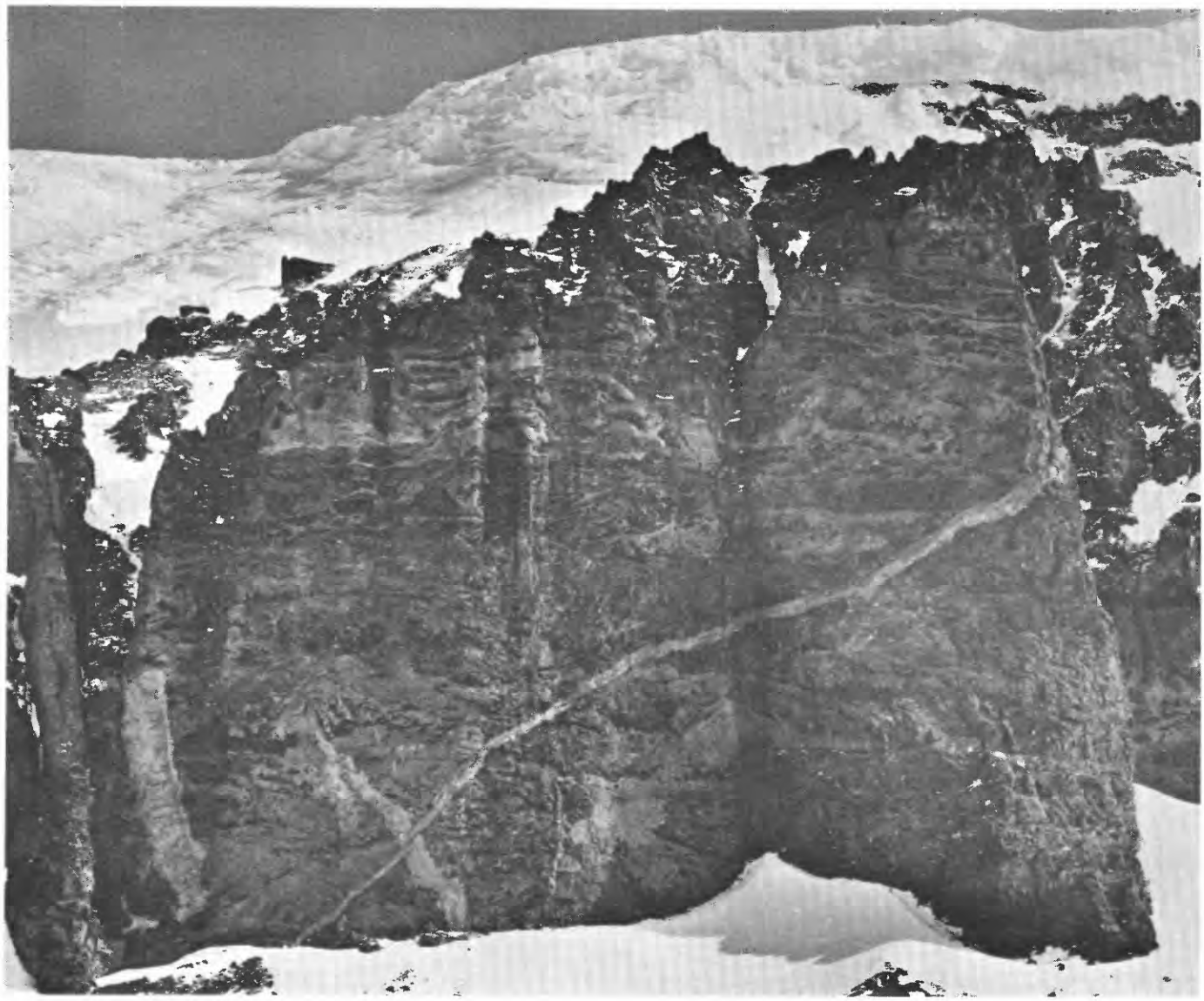

C

FIGURE 26.—Breccias of Coulman Island. *A*, Palagonite breccia (light) and nodular lava (dark). West side of Coulman Island; locality 220 is just to the right of the illustrated area. The foreground cliff is 350 m high, the background peak 800. See figs. 29*C* and 29*D* for closer views of parts of the section. *B*, Palagonite breccia (light) and nodular lava (dark). The upper half of the section consists of chaotically jumbled palagonite breccia and pods and irregular masses of lava, and encloses large autoliths of light-colored palagonite tuff. Below this is a thin section of well-bedded breccia and nodular lava. These intertongue downward in a thin zone (mostly out of the picture area to the left) with lenticularly bedded breccias and lavas which extend to the base of the exposure, and are striped by palagonite tuff. Within this lower sequence, only the thickest and lowest bed of light tuff can be traced across the exposure well beyond the photographed area, all other units anastomosing or lensing out. The section is interpreted to have formed during three eruptive episodes, the conspicuous light tuff and the top of the thinly layered rocks marking the contacts between the eruptive units. North end of Coulman Island, locality 216; the cliff is 400 m high. *C*, Marble-cake palagonite breccias and irregular lavas, cut by clastic dikes of palagonite tuff. Note the lack of continuity of bedding in most of the exposure. Cliff 600 m high, near center of east side of island.

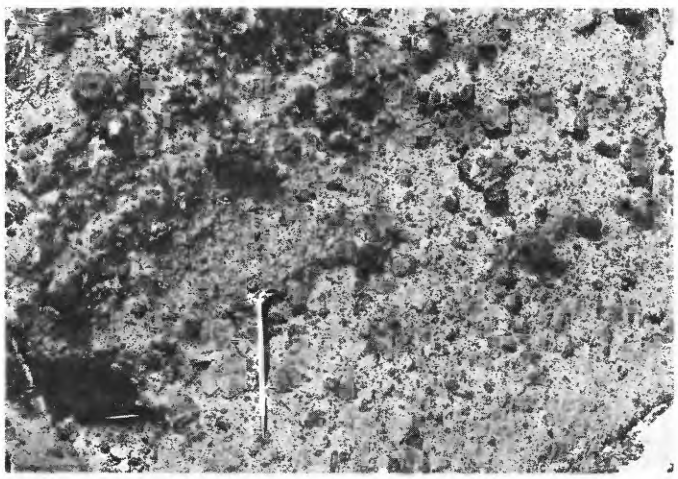

A

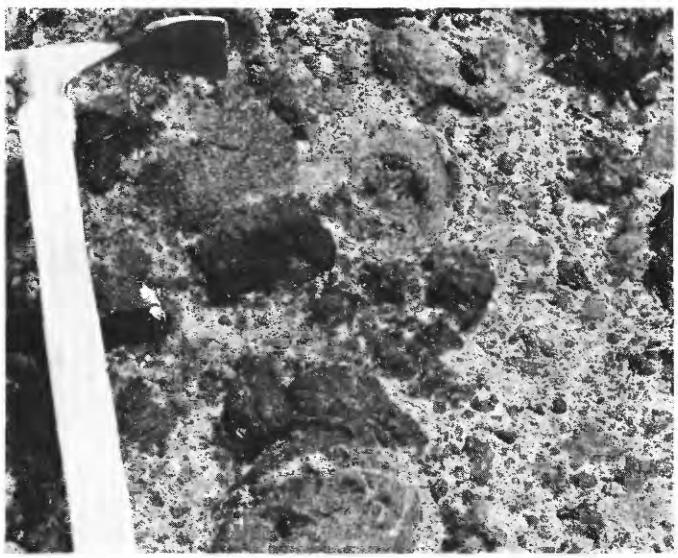

B

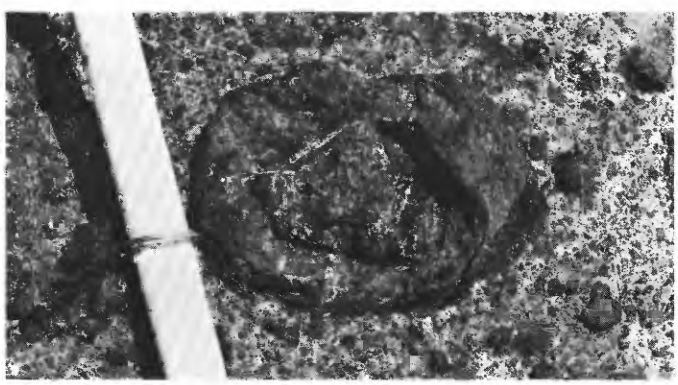

C

D

E

FIGURE 27.—Palagonite breccia, base of cliffs at west side of central part of Coulman Island, locality 220. 7 November 1964. *A*, Rudely bedded breccia containing fragments and spheroids of basalt in a soft palagonitic matrix. *B*, Closer view of part of same outcrop, showing basalt clasts which are variously dense, vesicular, and scoriaceous. Two spheroids, one above the center and one at bottom center, have concentric structure. *C*, Close view of another spheroid in outcrop shown in *A*. A block of vesicular basalt is rimmed by a shell of more dense basalt containing small partly filled vesicles. *D*, Breccia containing a large block (left) of much-fractured dense basalt, fragmentation of which provided clasts for the breccia. *E*, Closer view of the same outcrop, showing gradation (across center of picture) from fractured basalt to separated clasts.

as the finer grained parts or beds in palagonite breccias, and as inclusions in basalt flows.

The tuffs consist of sand- and granule-sized fragments of glassy basalt and palagonite in a soft, porous, earthy palagonitic matrix. The small clasts show varying palagonitization, being mostly fresh in some tuffs, wholly palagonitized in some, and marginally altered in others. Adjacent clasts can vary widely in degree of palagonitization. Crystal fragments form minor clasts. Color boundaries cross bedding layers (figs. 28*A*, *B*, *C*), indicating that postdepositional processes have caused variations in the oxidation, hydration, and concentration of iron.

Much of the palagonite tuff is bedded and forms water-laid horizontal and inclined sheets, cones, and fragments of cones, deposited on and covered by breccias and lavas. Relatively even and subhorizontal units of bedded tuff (fig. 28*H*) are uncommon.

The bedded palagonite tuff occurs primarily as abundant lenses and cones intercalated in, and intertonguing with, complexes of palagonite breccia and nodular basalt. Irregular lenses of palagonite tuff are visible as the light-colored rocks in breccia complexes in figures 26*B* and 28*F*. The largest masses of bedded palagonite tuff occur as cones, 100–300 m high (figs. 28*A*, *B*, *C*, *D*). The cones are truncated at the top and cut away by erosion, presumably by subaqueous slumping, bulldozing by lavas and intrusions, and cutting by water currents set up by nearby hot lava. Internal erosional unconformities are common.

The tuff cones are all buried by, and interfingered downward with, palagonite breccias and nodular lavas (figs. 28*A*, *D*, *E*), showing that magmatism was synchronous with subaqueous deposition of the tuff beds. The beds in the cones dip at angles up to 35° away from masses of breccia and lava, demonstrating that these masses had steep sides and were at least as high as the 300-m height of the taller cones. Eruptions built steep-sided masses, down which cascaded lavas and palagonitic tuffs and breccias. It is inferred that the steep-sided masses were table mountains which filled cylindrical caverns melted upward into the ice sheet by volcanic heat, and that the tuff cones were formed in the surrounding melt water when melting widened the hole about the table mountain.

Masses of palagonite tuff form contorted inclusions from a few centimeters to a hundred meters or more in diameter in thick lava flows. At least some of the inclusions were formed by the incorporation of masses of tuff from the cones into the lavas. Tuffs and lavas obviously were mobile simultaneously. Figures 28*E*, *F*, and *G* illustrate stages in the formation of tuff autoliths.

PALAGONITE

The term "palagonite" has two meanings, one specific and mineralogic, the other general and lithologic. The mineralogic meaning is that of a nearly isotropic mineraloid formed by the hydration of basaltic glass (sideromelane). The lithologic meaning, which is that primarily employed in this paper, is that of a soft, brown or yellow material derived largely by the hydration and alteration of basaltic glass but including clay, zeolite, carbonate, and other secondary minerals in addition to the mineraloid palagonite. A detailed study by X-ray and other laboratory methods of these secondary minerals in the Hallett volcanics would shed light on the important problems regarding the temperature and time of alteration, but no such study is attempted here.

The mineraloid palagonite can form by wet-tropical weathering of basaltic glass (Hay and Iijima, 1968) and by slow hydration of sea-floor lava at a rate of something like 1 mm per million years (Moore, 1966). Bonatti (1965) argued that such low-temperature hydration is subordinate to rapid hydration at high temperature during subaqueous eruption, but his conclusion is disputed by others.

An explanation by high temperature seems more likely to apply to the Hallett rocks than does one by low temperature. Permafrost must severely retard hydration in the Antarctic. In the Hallett province, there is no apparent increase in degree of hydration with increasing age. Thus, tuffs from the north tip of Cape Hallett, stratigraphically high in the Hallett Peninsula section, and from Cape Roget, high in the Adare Peninsula section and dated as about 2.6 m.y. old, are as palagonitic as the tuffs from the oldest parts of the various volcanic piles. And on the other hand, some of the oldest tuffs examined contain basalt-glass sand and granules showing almost no palagonitization. The alteration in the Hallett province involves the formation of various secondary minerals, but detailed information regarding them is lacking.

NODULAR LAVAS

Pods, lenses, and sheets of nodular lava form most of the nonbreccia component of the breccia complexes. These nodular lavas are illustrated by figure 29 and by many of the preceding photographs in this report. The nodular lavas occur primarily as anastomosing lenses a few meters thick. Many are evenly interlayered with breccia, whereas many others are in chaotic complexes of contorted, broken lava masses in breccia.

The pods of lava approach pillow shapes, but well-developed small pillows in piles of nested spheroids

A

B

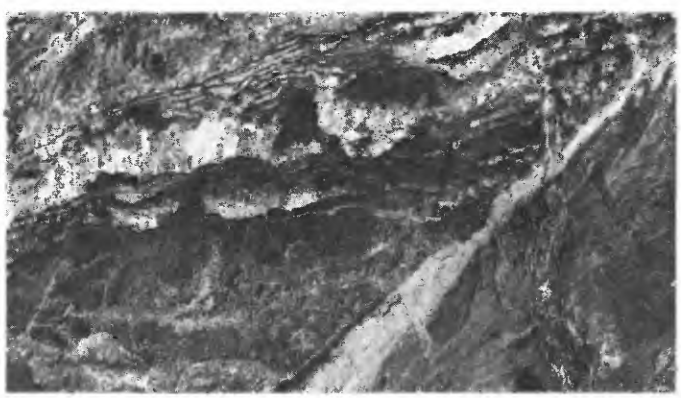

C

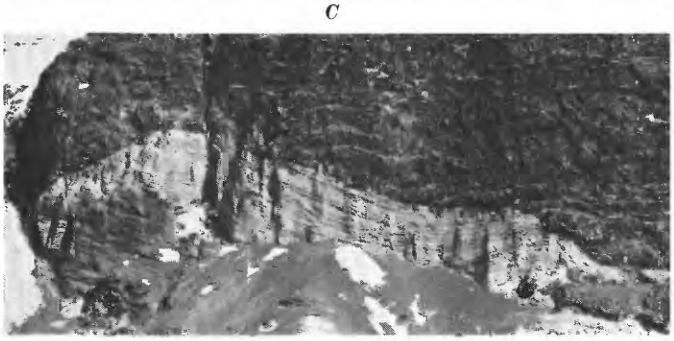

D

E

F

G

H

FIGURE 28.—Occurrences of palagonite tuff. *A–D*, cones of bedded tuff; *E–F*, intermediate stages in formation of large autoliths of tuff; *G*, autolith; *H*, subhorizontal bedded tuff. *A*, Two cones of tuff, with apexes in center and at right edge of picture, overlain by, and intertonguing downward to the left with, nodular basalt and palagonite breccia. The exposure is about 400 meters high; sea level is at the base. Hallett Peninsula, 11 km north of Cape Wheatstone. *B*, Closer view of the right-hand cone in *A*. A basalt dike cuts into, but not through, this cone from the right. *C*, Gently dipping nodular basalt and palagonite breccia (lower left) and nodular basalt and scoria (upper left) lap onto bedded palagonite tuff, which dips moderately left in the lower-right third of the picture. The tuff is partly yellow (photographs light) and partly moderate red (photographs dark), the color boundary cutting across bedding. An irregular basalt dike cuts steeply through the section on the right. The exposure is about 200 m high, the base being near sea level. Daniell Peninsula, 9 km northeast of Cape Phillips. *D*, Eroded right limb of a cone interfingering downdip with nodular basalt, which laps onto the depositional right side and eroded left side of the tuff mass. The exposure is 200 m high, and the altitude of its base is 300 m. Hallett Peninsula, 8 km north of Cape Wheatstone. *E*, Light-colored palagonite tuff in very irregular contact with dark basalt on the right, and interfingered with nodular basalt on the left. Nodular basalt lava underlies and overlies the tuff. The extremely irregular contact on the right is interpreted to indicate that the tuff accumulated simultaneously with the swelling of basalt pods. The exposure is several hundred meters high, and its base is several hundred meters above sea level. East side of central part of Coulman Island. *F*, Bedded tuff (light colored) has an upward protrusion (center) that contains basalt masses. The accumulation of tuff and the formation of basalt apparently were contemporaneous. Height of exposure, 200 m, base near sea level. Hallett Peninsula, 8 km north of Cape Wheatstone. *G*, Irregular mass of light-colored tuff enclosed in basalt, and in turn enclosing contorted masses of basalt with chilled margins. It is inferred that tuff from a bedded cone was engulfed in and carried along by a very thick lava flow, some of the lava from which was mixed into the churning tuff while still molten. Height of exposure 50 m, base near sea level. Hallett Peninsula, 11 km south of Cape Hallett. *H*, A thick bed of palagonite tuff, high in a section of breccias and nodular lavas, contains lava lenses. The cliff rises about 400 m above the sea ice. Daniell Peninsula, 8 km northeast of Cape Phillips.

were nowhere seen. Many clasts in the breccias display concentric structures (figs. 27*B*, *C*) and hence must have hardened slowly in a hot environment after detachment from larger masses of partly molten lava. Breccias that contain such detached pillow clasts are referred to as pillow breccias.

There is no clear distinction between lava pods and breccia clasts where irregular pods and lenses of lava occur in breccia. Pods are intricately fractured, and their margins display arrested stages in the breaking away of clasts into the breccia (fig. 27*D*). Contorted lava lenses within the palagonite breccia tend to be thoroughly fragmented (fig. 29*D*). Apparently the breccias were mobile, and a churning produced many of the clasts by breaking up lava masses.

The nodular lavas of layers and pods in many places display chilled margins (fig. 29*B*), but more commonly do not. Presumably the lack of chilled margins indicates that the breccias generally were hot at the time the lavas formed. This accords with the conclusion that palagonitization was the result of high-temperature hydration, not of low-temperature weathering.

Many cliff sections in all the volcanic piles display breccia-and-lava units that appear to be products of single eruptions. Each unit consists of a lower chaotic breccia which grades or intertongues upward into intercalated nodular lavas and reddish breccias and scoria. A series of five such units is exposed in the east-central part of Daniell Peninsula (figs. 29*A*, 28*C*). The lower part of each unit consists of massive or marble-cake lava and dark breccia, marked by irregular seams of yellowish-gray palagonite tuff. The upper part consists of lenses (either thin and regular or thick and contorted) of light-colored nodular lava, interlayered with palagonite tuff low in this part of the unit but interlayered with red breccia and scoria high in it. The iron-oxide coloring of the red scoria is generally superficial rather than pervasive. Nearby to the south, these five rhythmic units give way, by way of intertonguing, variable dips, and gradational and abrupt transitions, to the common chaotic assemblage of breccias, lavas, and tuffs (fig. 28*H*).

Similar units consisting of lower chaotic breccias and upper nodular lavas and reddish breccias and scoria were seen in many other exposures (figs. 26*B*, 29*E*). Only at the Daniell Peninsula locality, however, was there found a series of clearly defined rhythmic units; many cliff sections display no such units at all, but only the more chaotic breccias.

The reddish scoria and relatively even layering of the upper parts of these units cannot be taken as evidence that this part formed subaerially, above the level of surrounding water or ice. The levels of transition from lower to upper parts are stratigraphic, not horizontal, and dip with the units. The cyclic units give way laterally to the usual breccia chaoses: the upper well-layered parts do not continue far laterally. Each unit shows an upward progression similar to that of the adjacent units, and an explanation based on water level would have to postulate that water depth changed between eruptions by just the amount needed to place the surface halfway up the potential thickness of the products of the next eruption to come.

The reddish breccia and scoria have hardened under oxidizing conditions. Such oxidation can be accomplished in air or steam but probably not in liquid water. Oxidation by air is improbable for the reasons just noted; oxidation by steam of lava erupted beneath ice is inferred. (That ice several kilometers thick was present in this region during much of late Miocene, Pliocene, and Quaternary time is indicated by the character of the breccias, by the occurrence of mainland erratics on northern Adare Peninsula, and by the

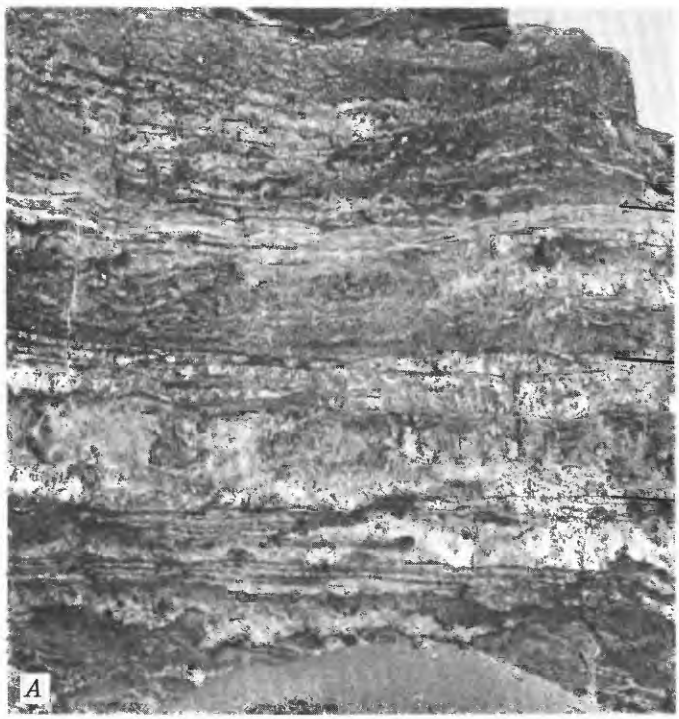

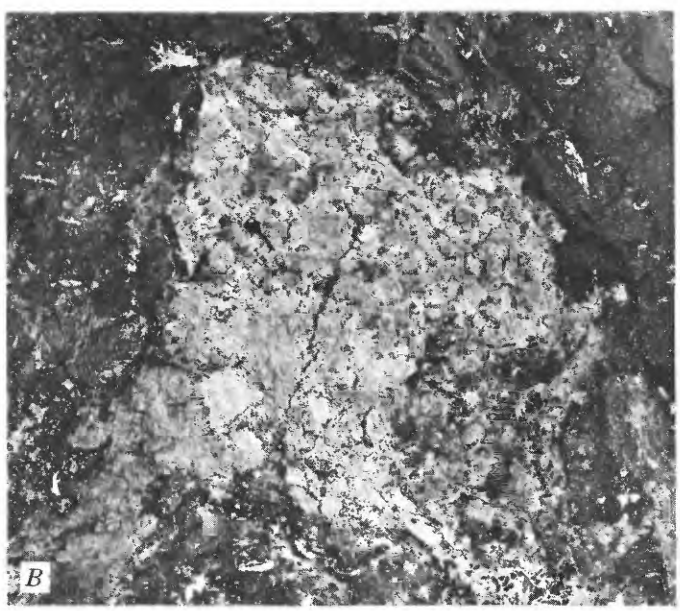

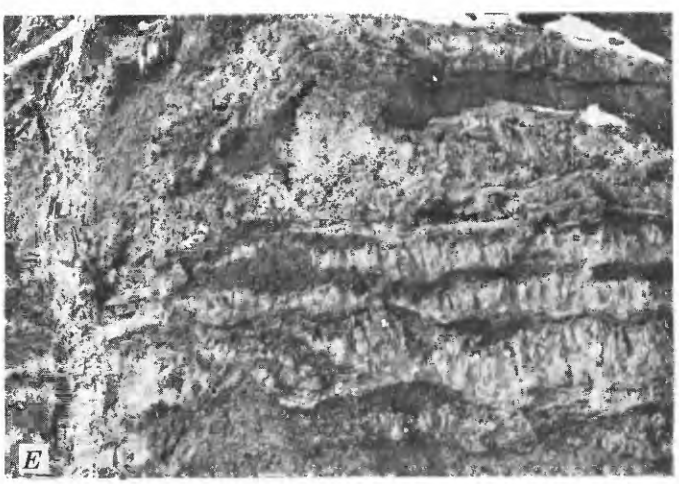

FIGURE 29.—Nodular lavas in the breccia piles. *A*, Rhythmic breccia-and-lava units. Units (separated by lines at right edge of picture) each about 100 m thick consist of lower zones of contorted lenses of breccia and lava and upper zones of long, thin lenses of reddish (dark on the photograph) breccia and scoria and light-colored lava. Each composite unit presumably represents an episode of continuous volcanism. Figure 28*C* shows a closer view of the lowest of these units in a nearby section. Daniell Peninsula near locality 277. *B*, Block of breccia (light) surrounded by pods of vesicular basalt. Selvages of black basaltic glass about 1.5 cm thick mark contacts between pods and breccia, and between adjacent pods. The exposure is about 1 m wide. East side of Hallett Peninsula, locality 247. *C*, Intertonguing, relatively well bedded palagonite breccia (light) and nodular lava (dark). This is a 50-m section in the top-center part of the Coulman Island cliff of figure 26*A*. *D*, Marble-cake contorted lenses of lava and palagonite breccia. The contortions appear to be primarily flow folds rather than irregular intrusions. This is a 50-m section in the central part of the Coulman Island cliff of figure 26*A*. *E*, Vertical dike and horizontal lenses of light-colored nodular lava in dark palagonite breccia. The exposure is about 30 m high and is midway up the cliff at the north end of Hallett Peninsula, and it represents the upper part of a lava-and-breccia unit.

glacial topography of the mainland—matters discussed elsewhere in this report.) It is postulated that eruptions beneath the ice melted a vault that did not, within the time span represented by the rhythmic breccia-and-lava units, extend to the surface. Einarsson (1966) argued on physical grounds that such limitation of melting to a basal vault should characterize many subice eruptions. Early eruption products were in contact with ice and with liquid water, and they formed the breccias of the lower part of each unit. Later in each cycle, a void over the lake in the vault was filled with steam, which oxidized the fragmental eruption products and allowed the fluid lava to spread out into thin flows instead of quenching it in pods and breccia.

MEGAPILLOWS

Large, ellipsoidal, concentrically structured masses of basalt occur in the breccia piles and are referred to here as megapillows. Particularly well developed megapillows were noted at the north end of Coulman Island and on Possession, Foyn, and Heftye Islands of the Possession group (fig. 30). Megapillows less well exposed were seen elsewhere about Coulman Island and at several places along the cliffs bounding Daniell and Hallett Peninsulas.

The megapillows are irregular ellipsoids of concentrically structured basalt. They typically show an inward progression from irregularly jointed basalt through small radial columns to large radial columns (fig. 30*C*), with or without a core of concentrically jointed basalt (fig. 30*B*). Shapes vary from subspherical (fig. 30*B*) to flat ellipsoidal (fig. 30*C*) and may be highly irregular. Thicknesses (or diameters) reach at least 150 m (figs. 30*B*, *C*). The megapillows form parts of thick units of breccias and nodular lavas, and appear to be intrusive into these units where well-exposed contacts were seen.

The concentration of megapillows in the exposures of the small Possession Islands is interpreted, as discussed previously, to be due partly to the resistance to erosion of these masses. The islands are interpreted to be near the vent region of an initially very large volcanic pile: the greater fluidity of lava near the vents, and the smaller proportion of breccia within it, may have facilitated the formation of megapillows. It will be recalled that the Possession Islands lie near the center of a broad submarine high of which Adare Peninsula is the exposed western one-quarter. Only a few megapillows were seen away from the Possession Islands.

The megapillows appear similar to those illustrated by Snyder and Fraser (1963, fig. 5) in a sill that intruded semiconsolidated volcanic mud in the submarine complex of Unalaska Island in the Aleutian arc.

The Antarctic megapillows apparently formed, simultaneously with the breccias they intrude, from large masses of lava that swelled within the unconsolidated and mobile breccias. The megapillows are parts of the breccia complexes, not unrelated younger intrusions.

THE BRECCIAS AND GLACIATION

The breccias are inferred to have formed largely by eruption of lava beneath a continental ice sheet that lay on the Ross Sea continental shelf during most of late Miocene, Pliocene, and Quaternary time. Grounded ice on the shelf far beyond present limits can be demonstrated by geologic data independent of arguments regarding the origin of the breccias.

PRIOR ICE LEVELS

The mainland valley glaciers of northeastern Victoria Land now all reach the sea, but the valleys display hanging tributary valleys, glacially overridden topography, and upper limits of valley-side planation and oversteepening far above present ice levels. The upper limit of altitude of these features decreases toward the coast, but the relative altitude above present ice increases: the inland level of the continental ice sheet was little higher than the present level. Near the coast, main-valley ice levels 1,100–1,200 m above present ice levels are shown clearly by well-preserved features of glacial erosion; older, subdued, and more ambiguous features suggest levels at least an additional few hundred meters higher. Projection of standard Antarctic ice profiles (see fig. 31 and following discussion) to the 1,200-m level requires grounded ice to have extended at least 50 km into the Ross Sea beyond the present coastline.

Past glaciations high above present levels characterize the valleys of Victoria Land along the rest of the Ross Sea to the south of this region also (fig. 2). In Taylor Valley in the McMurdo Sound region, for example, till is widespread up to 1,000 m above the floor, now ice free, of the valley (Péwé, 1960), and valley-glacier sculpture extends to at least 1,500 m above the floor (Armstrong and others, 1968). Mainland erratics have been found as high as altitudes of 600 m on Ross Island and on the 200-meter crest of Beaufort Island (Harrington, 1963).

Cape Adare lies 30 km northeast of the present limit of grounded ice along the mainland coast of Robertson

A

B

C

FIGURE 30.—Megapillows of the Possession Islands. *A*, North face of Heftye Island. Irregularly interswirled scoria, breccia, and lava on the left give way to irregular megapillows on the right. The summit is about 80 m high. *B*, Basalt megapillow at the southwest end of Possession Island. Concentric zones define a semicircle on the left that is part of a megapillow whose left half has been eroded away. The outer zone is massive and dark, the intermediate one is radial-jointed and dark, and the large core is irregularly jointed and light colored. The top part of a smaller megapillow, not obvious on the photograph, forms the lower half of the central part of the picture area; dark breccia lies above and to the right of the two megapillows. Locality 226; the cliff is about 150 m high. *C*, Megapillow at the northwest end of Foyn Island. Concentric zones of varying types of radial-jointed basalt define a long pod that thickens gradually to the left across the entire picture area. The megapillow is intrusive into palagonite breccia around the corner to the left. The cliff is about 150 m high.

Bay (fig. 17) and, as noted previously, mainland erratics occur as high as 520 m above sea level on the Cape. As also noted previously, an older glaciation beyond Cape Adare is indicated by Priestley's finding of glacial erratics within volcanic breccia in the Cape section. Figure 31 illustrates maximum and minimum ice profiles which can account for the high erratics.

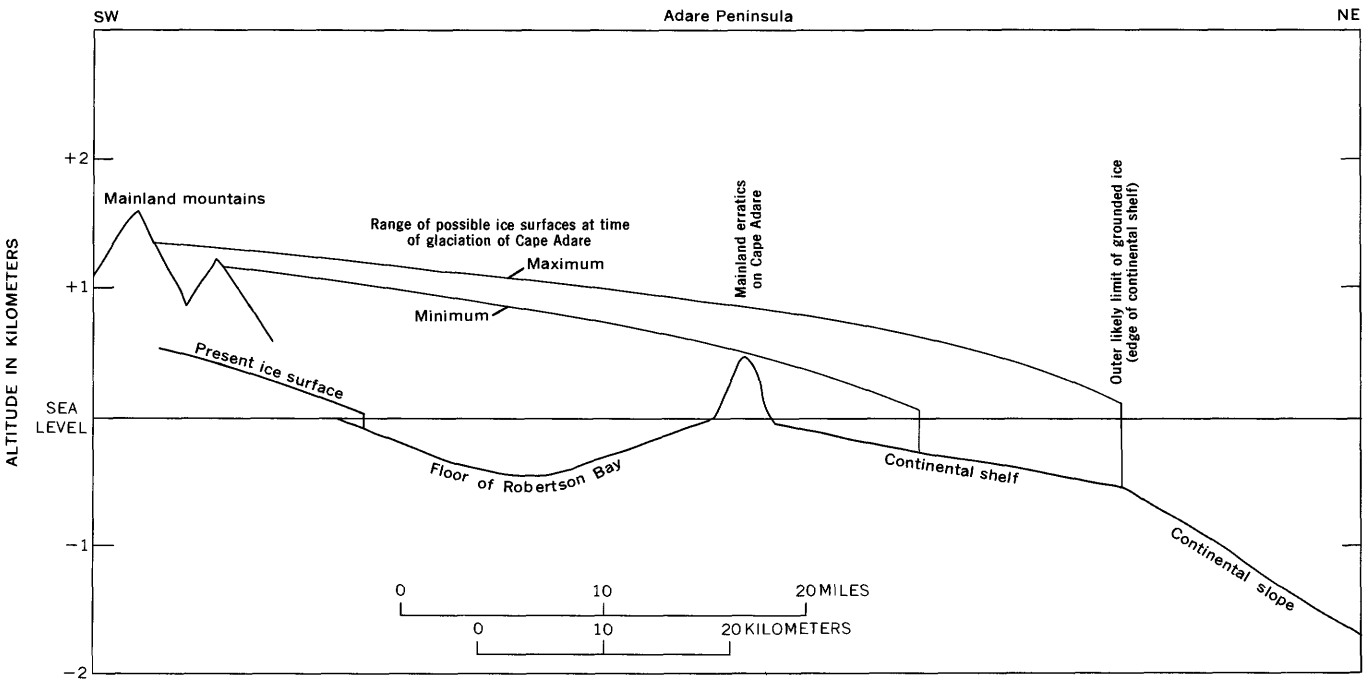

FIGURE 31.—Schematic profile across Robertson Bay, Cape Adare, and the continental shelf, showing ice levels at the time the continental ice sheet overrode Cape Adare. The ice-cap profile (shown in maximum and minimum positions) is that now typical of the Antarctic ice sheet (Bakayev, 1966, pls. 21, 22). Isostatic depression due to more extensive glaciation is not included but would increase maximum ice thickness above Cape Adare by several hundred meters. Vertical exaggeration × 10.

If the erratics were carried on the top of the ice sheet from which they were melted, then projection of standard ice-sheet profiles, disregarding isostatic altitude changes, indicates that the ice sheet extended about 15 km north of Cape Adare and that it stood about 800–1,000 m above present ice levels at the mainland margin of Robertson Bay. It is of course unlikely that the erratics were at the top of the ice sheet. The outer limit for grounded ice is provided by the shelf break, which is only about 15 km beyond the minimum limit of the ice. Projection of a standard profile from the shelf break provides about 300–400 m more ice at Cape Adare and perhaps 200 m more at the mainland coast (fig. 31). Adding the allowance for isostatic depression of Robertson Bay and the continental shelf by the load of the expanded ice sheet into these calculations increases the thickness of ice that is permitted at Cape Adare by the shelf-break limitation by something like 300 m, or to a height of about 1,200 m above present sea level.

The central Adare Peninsula breccias inferred to be of ice-contact origin to the present altitude of 1,800 m are 40–50 km from the shelf break (fig. 24). Projection of a standard ice profile (fig. 31) from the shelf break would put ice to 1,000–1,200 m above sea level at east-central Adare Peninsula, and to this height should be added approximately 500 m for isostatic depression of the continental shelf. This gives a total of about 1,600 meters of ice above present sea level. This calculation, using uncertain variables, thus yields an ice thickness about the same as that inferred from the upper limit of the breccias.

ICE-CONTACT BRECCIAS OF ICELAND

Palagonite breccia complexes strikingly like those of the Hallett province were produced in Iceland by eruptions beneath Quaternary ice caps. These basaltic complexes form about an eighth of the surface of Iceland and have been described and interpreted by various geologists, including Einarsson (1966), Jones (1969a, b, 1970), Kjartansson (1967), Noe-Nygaard (1940), Peacock (1926), van Bemmelen and Rutten (1955), and Walker and Blake (1966).

The most distinctive occurrences are in steep-sided table mountains, which consist largely of piles of massive to thinly interbedded palagonite breccia and tuff. The breccias contain abundant but disconnected pillowlike nodules of basalt, and fragments derived from them, in a matrix far richer in glass and palagonite than that of subaerial Icelandic tuffs. Breadcrust

bombs, scoria, airborne ash, and lapilli are lacking in the palagonitic complexes. Masses of pillow lavas, with primary dips to 30°, are abundant. Overlying many of these piles of palagonite breccia are irregular nodular flows, which in turn are overlain by normal subaerial basalt flows. Published descriptions of the various tuff, breccia, and nodular occurrences could largely be applied to the analogous complexes in the Hallett region, but the proportion of palagonitic breccias and tuffs low in the section is much greater in the Antarctic volcanic piles than in the Icelandic ones, and the Antarctic piles lack good pillow lavas.

The steep sides of the table mountains are regarded as constructional, not erosional, by most Icelandic geologists (but not by Einarsson, 1966), and as generally interpreted by them require accumulation against ice walls: the mountains were built by volcanism in cylindrical chambers that were melted in the ice from beneath by volcanic heat. The first eruptions must have occurred in vaults at the base of the ice, and the final subaerial lavas must have formed after the structures were built above the ice level or after the ice had receded. The nodular lavas just beneath the capping subaerial lavas presumably hardened at shallow depths beneath the lake surfaces. The many geologists studying the palagonite complexes agree that they were deposited wholly under water that was in contact with ice but disagree on details, such as which of the breccias were erupted under water and which were erupted explosively above the melt-water lakes from lava that was quenched by its rise through the saturated pile.

ORIGIN OF THE ANTARCTIC BRECCIAS

Like the Icelandic breccias, the breccias of the Hallett region formed in contact with water and were hydrated when hot. The palagonite tuffs were water laid. Fragmentation and hydration of lava produced palagonite breccias. Some of these were hot and mobile and moved as thick masses that contained molten or solid lava lenses which were deformed and fragmented by the motion of the whole. Concentrically structured spheroids of lava, now clasts in the breccias, crystallized from detached globs of magma in hot, moving breccias. Other breccias were less mobile and grew upward and outward primarily by the outflow of new material on their surfaces rather than by motion of the body as a whole. Lava within the hot breccias intruded them complexly as dikes, sills, and megapillows; small intrusions may have had little relation to vent areas, representing instead only migrations of magma within mobile breccias. The mobility of the breccia is further demonstrated by the abundant clastic dikes of palagonite breccia. Many eruptive units display an upward succession from chaotic breccias to thinly interlayered lava and breccia, showing that fluidity of extrusions in such units increased during the eruptive episodes. Units hundreds of meters thick formed during single episodes of eruption. The cones of moderately dipping palagonite tuff demonstrate that some of the breccia units had steep sides at least several hundred meters high, down which the tuff cascaded.

The steep temporary sides of the breccia units recorded by the cones perhaps occur where extrusions were dammed against the ice walls of the melt-water vaults, the cones having formed after the ice wall melted back. Violent convective currents in the water around the hot breccias may have winnowed out the fine clasts and carried them to the sides of the masses to what became the apexes of the cones. Continuing growth of the breccias buried the cones. Breccias may also have been extruded upon ice and may have then been jumbled when the ice was melted.

Basalt magma, chilling from its liquidus to 0° C, could melt ice to about ten times its own volume (Goranson, 1942). Actual melting would be less, for much heat would be lost to the atmosphere through steam escaping to the surface and through evaporation of hot water after melting had produced a lake reaching the ice surface. Presumably the melting would tend to form an upward-widening conical chamber within the ice. The thinner the ice cap above the vent and the more voluminous the eruption, the greater the likelihood that melting would proceed to the surface and produce a lake rather than a melt-water vault at the base of the ice.

A melt-water vault, pressurized and partly sealed by the overlying ice, might contain very hot water with or without steam, or even supercritical water, in contact with the eruptive mass. Rapid loss of heat from magma should produce a violently convecting water mass varying greatly in temperature. (This situation is not to be compared with eruption into a lake or the ocean, for the water volume would be small proportional to the lava volume, and a large allowance must be made for melting inertia of the ice and loss of heat to the atmosphere.) On the other hand, insulation of the igneous mass by a thick chilled crust would retard the release of heat, and the vault or lake could then be filled with cool water.

An origin of the breccias by submarine eruptions is not indicated. Breccias of this type are not known elsewhere in submarine complexes; and compact pillow lavas are lacking here. Were the breccias submarine, they would have had to be erupted in water 2,000 m

deep—fully oceanic depths—yet continental basement rocks lie beneath them; and all of the uplift to present altitudes would have to have occurred in late Quaternary time.

The contrast between the Antarctic breccias and the products of submarine eruptions is perhaps due in considerable part to the presence of very hot water in contact with the lavas. The breccias were saturated with water—liquid, steam, or supercritical—from the times of their initial fragmentation, which presumably was at a temperature near their solidus, throughout their cooling histories. The slower the cooling, the more thorough would have been the palagonitization of small clasts. Water fluidized the breccias and permitted them to flow. Chilled margins were produced on masses of lava mixed into cold breccias, but not where breccias were hot.

The altitudes of the breccias provide minimum thickness for the past ice sheet of the Ross Sea. The upper limit of exposed ice-contact breccias is at an altitude of about 1,500 m at the southwest end of Hallett Peninsula (fig. 18), 1,500 m on Coulman Island, 1,700 m on the seaward side of Hallett Peninsula, 1,800 m on the seaward side of central Adare Peninsula (fig. 21), and higher than 600 m on the outer coast of Daniell Peninsula. Ice grounded on the continental shelf of the Ross Sea, about 500 m below present sea level, reached to at least these altitudes above sea level. It was shown previously that even the Adare Peninsula limit is compatible with formation against an ice sheet grounded across the continental shelf.

There are few volcanic rocks which could be interpreted as subaerial—I recognized none that are certainly subaerial—below the capping veneers of the various volcanic piles. Throughout most of the period of volcanism in the region, then, the Antarctic ice sheet was much more extensive than it is at present, and grounded ice thickly filled the Ross Sea region.

LATE CENOZOIC GLACIATION OF ANTARCTICA

The late Miocene and Pliocene age determinations for basalts in subglacial breccias low in the Hallett and Coulman volcanic piles indicate that ice grounded on the continental shelf of the Ross Sea, far beyond present ice limits, existed throughout late Cenozoic time. This conclusion is in accord with much information obtained in the last few years from Antarctica and the Southern Ocean.

In the McMurdo Sound region of South Victoria Land, most of the glacial sculpturing of valleys now largely free of ice occurred before the eruption of basalts 2.7–3.7 m.y. ago (Armstrong and others, 1968; Denton and others, 1970), and hence within Tertiary time. In Marie Byrd Land, ice-contact breccias of several early (the oldest date is given as 42±9 m.y.), middle, and late Cenozoic ages have been found by Le Masurier (1970), indicating at least intermittent glaciation beyond present ice levels during much of the Tertiary.

Antarctic and Arctic waters are now characterized by sinistrally coiled *Globigerina pachyderma* (a planktonic foraminifer). This foram had major expansions toward the equator in the middle Pliocene and very late Miocene, indicating that the Greenland and Antarctic ice sheets were probably then much more extensive than they are now (Bandy, 1968). No period markedly warmer than the present is recorded in the sediments representing the last 5 m.y. in the Southern Ocean (Goodell and others, 1968).

The Antarctic Convergence is marked by its high biological productivity and correspondingly high rate of pelagic sedimentation. The thickest pelagic sediments of the Southern Ocean lie between 50° and 55° S., considerably north of the present convergence, and indicate that during most of the past 10 m.y. or so the convergence has been well north of its present position (Ewing and others, 1969). This accords with the concept that Antarctica was ice covered well beyond present ice limits during most of late Miocene and Pliocene time.

Margolis and Kennett (1971) studied subantarctic deep-sea cores and identified early Eocene, late-middle Eocene, and Oligocene episodes of Antarctic glaciation on the basis of the presence of ice-rafted sand (recognized by electron microscopy) and of low-diversity foraminiferal faunas in the sediments. They found a general warming recorded through the early and middle Miocene by increasing species diversity and by lack of rafted sand. A sharp cooling is recorded in the late Miocene sediments, and continued cold since.

A worldwide drop in sea level during late Miocene time is suggested by many data from some relatively stable coastlines, and the drop presumably accompanied the onset of major glaciation in Antarctica (Alt, 1968; Kennett, 1967). Shorelines in the southeastern United States record a marked eustatic drop of sea level following late Miocene time, from a level of about 70 m above present sea level; Pliocene levels were at their highest about 30 m above present sea level, and Quaternary ones fluctuated from 15 m above to far below the present level (Alt, 1968). The late Miocene withdrawal of water needed to cover Antarctica with an ice sheet would account quantitatively for the Miocene and Pliocene sea levels.

The extensive and prolonged late Miocene and Pliocene glaciation of Antarctica renders untenable the speculation by Hollin (1962) and Grindley (1967) that Antarctic glaciation markedly more extensive than that of the present could occur only when sea level was lowered by widespread glaciation in the Northern Hemisphere. The Antarctic data give no support to the more general assumption by some geologists (for example, Péwé, 1966) that Antarctic glacial advances have been synchronous with the glaciations of middle northern latitudes.

Ice-contact breccias such as characterize the volcanic piles of the Hallett province are, as noted in the introduction, uncommon in the McMurdo volcanic province at the south end of the Ross Sea. I infer from this that the exposed McMurdo volcanic rocks are largely of Quaternary age and that they postdate the great late Miocene and Pliocene ice sheet of the Ross Sea.

EROSION

The offshore volcanic piles have constructional upper surfaces formed of upper Quaternary lavas and tuffs but largely covered by ice caps. These surfaces where exposed show evidence of only minor glacial erosion.

The sides of the volcanic piles by contrast are mostly erosional cliffs which fall sheer from the summit surfaces to sea level. The volcanic structures are formed mostly of poorly consolidated tuffs and breccias which are subject to rapid erosion. Marine and glacial erosion have both obviously contributed to the formation of the cliffs, although the proportion of each is uncertain. These cliffs are highest on the seaward (east) sides of the piles and reach a height of 2,000 m on the east face of central Adare Peninsula. The height of the cliffs is largely a measure of the amount of lateral erosion into the volcanic structures, although steep sides of primary "table mountains" may have contributed. Each pile, if complete, would be a symmetrical elongate dome with a maximum crestal altitude of about 2,000 m. Coulman Island and the northern two-thirds of Daniell Peninsula preserve this symmetry and have been cut back only moderately from the sides. Hallett and Adare Peninsulas by contrast have been eroded from the east to or beyond their crestlines: more than half of each volcanic pile has been removed by erosion.

Erosion by the Ross Sea ice sheet may have caused much of the erosion of the seaward sides of the peninsulas and of both sides of Coulman Island. The highest cliffs that are clearly attributable to glacial erosion, however, are those on the south side of Hallett Peninsula, where Tucker Glacier has cut cliffs as high as 1,200 m (fig. 16). The lower cliffs on the west sides of Daniell and Hallett Peninsulas must also have been cut largely by ice.

Marine erosion must have contributed to all the seaward cliffs and may have been the dominant factor in their formation. Antarctic storms are the most violent on earth and wave attack must be correspondingly severe during open-water periods. Strong currents flow northward along the west side of the Ross Sea and may serve to carry away and redistribute debris eroded from the volcanic piles. The cliffs bounding the islands and stacks of the Possession group (fig. 23) are obviously sea cliffs and reach altitudes of 200 m, limited only by the elevations of the island summits.

Calderas have been breached by erosion, chiefly glacial, on Adare Peninsula (fig. 20*B*), Daniell Peninsula (figs. 10, 11*A*, 12), and Coulman Island (fig. 7). The floors of the southern Daniell calderas are near sea level, so the breaching of these calderas gives their sector of the peninsula a very irregular map configuration. The walls of the calderas stand as cliffs where not buried by ice and reach heights of 2,000 m.

VOLCANIC ROCKS OF THE MAINLAND

Small masses of upper Cenozoic volcanic rocks lie on the Paleozoic rocks of the mainland west of the large offshore volcanic piles (figs. 4, 14, 17; the size of some of the exposures is exaggerated in fig. 4 to permit their depiction). All exposures shown north of 73° S. and east of 166° E. were seen during the present work; three of the localities were sampled on the ground, but the others were only mapped from the air. Larger masses of volcanic rocks are present in the coastal region south of 73° S. These were not visited in this work, but published information on them is summarized briefly.

VOLCANIC ROCKS NORTH OF 73° S. LATITUDE

The small mainland exposures of volcanic rocks north of 73° S. and east of 166° E. are of basalts and subordinate trachyte, which have been much eroded by ice.

The small mass between Whitehall and Borchgrevink Glaciers, west of central Daniell Peninsula (fig. 14), consists of basaltic aa breccia, which fills a small saddle on a ridge in Paleozoic metasandstone. The source of this remnant has been removed by erosion.

A minor vent area for olivine basalt eruptions is exposed near upper Trafalgar Glacier (loc. 215, fig. 4). A bench eroded in metasandstone is partly covered

by the glaciated remnant of a red scoria cinder cone, from which flowed an aa breccia flow. The metasandstone ridge crest above the bench is capped by a flow remnant of massive basalt and by an agglomerate of spatter, cinders, and bombs; the agglomerate remnant dips northwestward across the ridge, and the proportion of spatter increases updip, demonstrating that the vent from which it came and which has been removed by erosion lay to the southeast.

Vent-filling basalt in Paleozoic granodiorite is exposed at the northwest edge of Moubray Bay (loc. 210, fig. 17). The vent is exposed in the eastern cliffs of the ridge from an altitude of 50 meters to the crest at 200 meters, and it widens upward to a diameter of 150 meters. Harrington, Wood, McKellar, and Lensen (1967, p. 60–61) described the basalt and palagonite tuff and breccia of this vent.

The other small mainland masses of volcanic rocks shown on the maps were seen only from the air. They consist mostly of dark basalts capping minor ridges or benches and lacking obvious relationship to the present topography.

MOUNT OVERLORD AND MOUNT MELBOURNE

Two high, young volcanoes—Overlord and Melbourne—stand above low volcanic piles west and southwest of Coulman Island (fig. 4). Mount Overlord (fig. 32*A*) has been described briefly by Gair (1964, 1967) and by Nathan and Schulte (1968). They found varied highly alkaline rocks: trachybasalt, trachyandesite, phonolite, syenite, and alkaline gabbro. The symmetrical cone of Mount Melbourne (fig. 32*B*) also has been visited by New Zealand geologists who collected trachyandesite in the summit area and found active fumaroles and alkaline basalt, trachyandesite, and trachyte in other parts of the volcano (Nathan and Schulte, 1967, 1968). Smith (1964a, b) described erratics of basalt and trachyte collected by Priestley from Campbell Glacier.

Mount Overlord and Mount Melbourne resemble the main young volcanoes of the McMurdo Sound region in rising high and steep sided above their surroundings. They contrast correspondingly with the low central volcanoes that stand on the long coastal volcanic piles of the Hallett province. Harrington, Wood, McKellar, and Lensen (1967) suggested that such differences are due to a greater volcanic maturity of the dominant-cone terranes and that high, steep volcanoes may ultimately be built on the Hallett piles.

A

B

FIGURE 32.—Aerial views eastward over stratovolcanoes toward Wood Bay. *A*, Mount Overlord. The caldera rim of this highly alkaline volcano has an altitude of about 3,400 m. Mount Murchison stands on the center skyline and Coulman Island on the left. Photograph by U.S. Navy for U.S. Geological Survey, TMA 710, F 31, no. 342, altitude 6,000 m, 31 October 1960. *B*, Mount Melbourne. Summit altitude is about 2,500 m. Photograph by U.S. Navy for U.S. Geological Survey, TMA 325, F 31, no. 48, altitude 5,000 m, 3 December 1956.

PETROLOGY

The volcanic rocks of the Hallett province constitute a very sodic assemblage containing approximately 70 percent of alkaline olivine basalt and subordinate olivine trachybasalt, 15 percent of trachyte, and no more than a few percent each of basanite, andesine basalt, latite, phonolite, and quartz trachyte. Included are some of the most sodic igneous rocks yet reported anywhere. The assemblage is strongly bimodal: only a small amount of rock is intermediate between basalt and trachyte.

Of the 250 hand specimens collected of the volcanic rocks, about 65 were selected for petrographic study, and 34 of those were used for whole-rock chemical analysis. A little X-ray work was done also. This reconnaissance study permits characterization of the broad features of the petrologic province.

ROCK CLASSIFICATION

Alkaline volcanic rocks vary greatly in mineralogic and chemical compositions. The following rock-name classification, used in this report, is based primarily on mineralogy, but available chemical analyses are integrated particularly for their information regarding the relative amounts of occult alkali feldspars and feldspathoids. Numbers refer to those reported in the tables of chemical analyses (tables 2, 3).

Felsic rocks

Trachyte—leucocratic rock composed largely of alkali feldspar, which may be sodic oligoclase, albite, anorthoclase, or sanidine, alone or in combination. (Analyses 8, 12, 23.)

Quartz trachyte—trachyte containing quartz. (Analyses 13, 14, 19.)

Phonolite—leucocratic rock composed mostly of alkali feldspar and feldspathoids. (Analyses 6, 7.)

Hydrated trachyte glass. (Analysis 9.)

Intermediate rocks

Latite—contains moderate to large amounts of both alkali feldspar and andesine or calcic oligoclase and a small or moderate amount of mafic minerals; may contain a minor amount of feldspathoids. (Analyses 22, 30.)

Mafic rocks

Basalt—contains abundant plagioclase more calcic than andesine, and clinopyroxene. (No analyzed specimens.)

Andesine basalt—mafic rock containing abundant clinopyroxene and little alkali feldspar, and in which the plagioclase is andesine rather than a more calcic variety. (No analyzed specimens.)

Trachybasalt—contains plagioclase more calcic than andesine, abundant clinopyroxene, and a moderate amount of alkali feldspar. (Analyses 1–5, 11.)

Any of the above mafic rock types can contain small amounts of olivine, feldspathoids, or alkali feldspars. All carry substantial quantities of opaque minerals.

Olivine basalt—contains abundant clinopyroxene and plagioclase more calcic than andesine, and more than 5 percent of olivine. Most is alkaline. (Analyses 10, 15–18, 20, 21, 24–28, 32–34.)

Palagonite—hydrated basalt glass. (Analysis 29.)

Ultramafic rocks

Basanite—pyroxene-rich rock, containing olivine, minor feldspathoids, and little or no plagioclase. (Analysis 31.)

DISTRIBUTION OF ROCK TYPES

Field designations of rock type generally were attempted only as to "trachyte" and "basalt," which correspond approximately to the "felsic" and "mafic" groups of rock types. Many of the trachytes are light-gray rocks, with or without an olive or yellowish cast; they display a bright sheen reflected from flow-oriented feldspars and can be identified at a glance. Many of the basalts are dark gray and contain conspicuous phenocrysts of pyroxene and olivine; hence they also are easily recognized. Between these two populations of readily distinguished rocks is a large family of medium-gray rocks, which include both mafic and felsic types and which where aphanitic and nonporphyritic were, in many instances, incorrectly designated in the field. The light-colored rocks were purposely collected in more than their true proportion to the dark-colored ones. These factors and the small number of samples studied petrographically preclude the making of quantitatively accurate statements regarding frequency distribution of the rocks.

The occurrences of the trachytes and the other felsic rocks are in general the same as those of the mafic rocks. Trachyte forms hydrated breccias and tuffs, nodular lavas, megapillows, dikes, and plugs, just as does basalt in the breccia sections. The large calderas however may be produced only by trachytic eruptions: the rim of Coulman caldera is formed exclusively of trachyte where sampled, and in the rim of the similarly large caldera of southern Adare Peninsula trachyte and basalt occur together. Abundant trachyte was found both low and high in the Hallett pile, and a minor amount of trachyte was found low in each of the other piles.

The proportion of mafic to felsic rocks may be higher in the small mainland accumulations than in the large offshore volcanoes.

PETROGRAPHY

The dominant rock types, alkaline olivine basalt and olivine trachybasalt, vary greatly in thin-section appearance. Many samples are holocrystalline, but even most of these are exceedingly fine grained, are clouded by opaque dust or tiny granules, and contain much material that cannot be fully identified by petrographic methods. Interstitial alkali minerals, glass and

hydrated glass, and brownish secondary materials vary greatly in abundance. Many specimens are mostly vitric, the glass being either fresh or hydrated.

Olivine is present in most specimens of basalt and trachybasalt, but in these occurs mainly in amounts of only a trace to 5 percent; it was not seen to constitute much more than 10 percent of a specimen. Olivine is greenish yellow to nearly colorless where fresh and occurs entirely as small phenocrysts in some specimens and as phenocrysts and groundmass granules in others. The phenocrysts are variously euhedral, fragmental, and resorbed, only one of these types being abundant in any one specimen. The phenocrysts are altered in various degrees to iddingsite(?) in some specimens, and the groundmass granules in some samples are completely altered.

The pyroxene in the basaltic rocks is exclusively monoclinic and pale colored. Most of the phenocrysts are yellowish gray or dusky yellow in thin section. Phenocrysts in some specimens have narrow yellowish-brown rims. Groundmass granules and microprisms are faintly green or pale yellowish brown. Pleochroism is weak, and extinction angles mostly moderate. Some of the basalts and trachybasalts contain abundant phenocrysts of augite that is black and of almost vitreous appearance in hand specimen.

Plagioclase in the basaltic rocks occurs primarily as groundmass laths but also forms sparse phenocrystic tablets or fragments in many specimens. The composition is typically labradorite, but andesine is common and some bytownite was found. Interstitial anhedra of alkali feldspar are present in amounts up to about 15 percent in many specimens; the grains are too small to be satisfactorily identified optically, but X-ray examination of specimens by George M. Fairer (written commun., 1967) revealed the common presence of high-temperature anorthoclase. Anhedral nepheline was recognized in only a few sections. Analcite is common both as a filling or lining of vesicles and as an anhedral groundmass mineral.

Much of the basalt and trachybasalt occurs as palagonite tuff and breccia. The tuff and breccia consist of clasts of all sizes, from less than a millimeter to many meters, of widely varied basalts, in porous frameworks whose interstices are partly filled by clays, calcite, and analcite and other zeolites. The smaller clasts typically have groundmasses of yellowish-orange nearly isotropic hydrated glass—palagonite. Most of the larger clasts are much less altered, even though they too contain considerable clay, carbonate, and zeolite. Most of the clasts display rapid chilling in their fabrics.

Most of the trachytes are porphyritic with well-shaped or resorbed phenocrysts of oligoclase (uncommonly andesine) or anorthoclase, or both. Groundmasses are mostly dominated by flow-alined laths of alkali feldspar that is variously oligoclase, albite, sanidine, and anorthoclase. Interstitial material consists of anhedra of alkali feldspar, analcite, and nepheline(?), glass, and unidentified secondary minerals. The dominant mafic silicate is clinopyroxene, generally greenish, limited to the groundmass, and variously acicular, granular, and anhedral. Some specimens contain long prisms of brown hornblende, which are more or less replaced by opaque granules. A little olivine, or reddish iddingsite(?) after it, is present in some of the trachytes, and a little brown biotite occurs in others. Opaque dust and granules are generally abundant, and they render the groundmasses of some trachytes nearly opaque, as seen in thin section.

The trachytes also form hydrated tuffs which occur in the same manner as the basaltic palagonites. Clasts of trachyte varying widely in texture and mineralogy are much altered to clay, analcite, and other secondary minerals.

Latites are common but subordinate in amount to trachytes. The latites contain phenocrysts of andesine and either augite or brown hornblende, or both. Groundmasses display laths of andesine or oligoclase, abundant microprisms of clinopyroxene and granules of opaque minerals, generally some olivine or iddingsite, and much alkali feldspar, glass, analcite, and secondary minerals.

The three specimens of quartz trachyte that were examined all contain phenocrysts of anorthoclase, which shows at most poorly developed grid twinning. Groundmasses are dominated by flow-alined laths of alkali feldspar, mostly sanidine in one specimen, but mostly albite in two others which contain also abundant anhedral interstitial anorthoclase. Quartz occurs as veinlets, tiny pods, and interstitial anhedra in two of the specimens, and the chemical analysis of the third indicates the occult presence of quartz in glass. One of the quartz trachytes contains sparse microphenocrysts of green clinopyroxene, one contains a fibrous secondary amphibole, and the third has a barkevikitic(?) amphibole. Opaque minerals, as dust, granules, and interstitial or replacement anhedra, are abundant in all three specimens.

Phonolite was recognized in only one occurrence—an intrusive megapillow on the east side of Hallett Peninsula—but it presumably is present elsewhere. The holocrystalline specimen that was examined consists of about one-third nepheline, one-third sanidine, and one-third total clinopyroxene, opaque minerals, oligoclase, hornblende, natrolite, and analcite.

Only one specimen that was identified certainly as basanite was studied in thin section. This is a pyroxene-rich olivine-bearing ultramafic volcanic rock which contains no visible feldspar or feldspathoid, although its chemical analysis indicates that a little calcic plagioclase and considerable feldspathoid are occult in the brown glass that forms about a quarter of the specimen.

A single specimen of a possibly ultramafic volcanic rock type was examined in thin section but was not analyzed chemically. This rock contains about 10 percent of tiny grains of augite, 25 percent of yellowish-brown hornblende, and 5 percent of fresh olivine, in glassy matrix clouded by opaque material. No feldspar is visible.

ULTRAMAFIC INCLUSIONS

The only ultramafic inclusions found are sparse granule-sized aggregrates, presumably cumulates, of olivine and augite in some of the basaltic rocks.

HIGH-PRESSURE MEGACRYSTS

The rocks in which the small ultramafic aggregates occur typically also contain abundant large separate crystals of minerals which are more likely to be products of deep-crustal or upper-mantle crystallization than of shallow crystallization. Large—to at least 1 cm—equant crystals of augite, black and nearly vitreous as seen in hand specimen and lacking conspicuous cleavage, typically occur in these rocks. So do corroded or reaction-rimmed crystals of olivine, smaller than the augites but larger than is typical in most of the other basaltic rocks. Sparse, large—to as much as 2 cm—hornblende prisms are present. A single 6-mm octahedron of dark-gray spinel was noted. These minerals resemble the high-pressure megacrysts described by Binns (1969) from compositionally similar basalts and basanites in Australia. Binns deduced that the pressure at the site of crystallization of the megacrysts was between 10 and 18 kb, indicating a depth between 35 and 65 km. The large corroded crystals of plagioclase and anorthoclase in many basaltic and trachytic rocks of the Hallett province may also be products of crystallization at depth.

DESCRIPTIONS OF ANALYZED SPECIMENS

The 34 rock specimens for which chemical analyses are reported in tables 2 and 3 are described briefly in this section. Two numbers are given for each specimen: the first is the column number of the sample in the tables, and the second, in parentheses, is the field number. The sample localities are indicated on the maps (figs. 4, 6, 14, 17) by the field numbers without the suffixed letters (which distinguish types at each locality).

Hallett Peninsula

Nos. 1–14 (table 2)

1 (213A). **Nepheline-andesine trachybasalt.** Dense medium-dark-gray rock, studded by small black crystals of hornblende and augite. Contains about 5 percent of seriate phenocrysts of olivine, pleochroic to dusky yellow; 1 percent of phenocrysts of labradorite with narrow rims of andesine; and less than 1 percent of phenocrysts of brown hornblende rimmed by opaque granules. Groundmass consists of subequal amounts of tiny (0.02 mm long) prisms of greenish clinopyroxene and of alined laths (0.05–0.6 mm long) of andesine ($\sim An_{35}$), with abundant granules (0.004–0.5 mm) of opaque minerals and abundant poikilitic anhedra of anorthoclase and nepheline. Sparse nepheline crystals are euhedral. Apatite and carbonate occur in minor amounts. Subaerial flow capping ridge west of Arneb Glacier at altitude 450 m (fig. 14).

2 (214B). **Nepheline trachybasalt.** Dense medium-dark-gray rock studded by small black phenocrysts. Seriate augite euhedra to 3 mm long are faintly pleochroic in pale olive and form 3 percent of the rock; phenocrysts of brown hornblende rimmed by opaque granules form 1 percent. Plagioclase ($\sim An_{50}$) laths, most shorter than 0.2 mm, form 10 percent of the groundmass, which consists largely of dark and extremely fine grained holocrystalline material containing very abundant 0.002-mm granules of opaque minerals, granules and tiny prisms of green clinopyroxene, and very poikilitic finely granular nepheline and alkali feldspar. This specimen is almost identical chemically to number 1 and may be from the same lava flow, but it is very different petrographically, for it contains little plagioclase, and that markedly more calcic than in the other specimen, so the granular feldspars must differ markedly. Subaerial flow capping ridge west of Arneb Glacier at altitude of about 600 m (fig. 14).

3 (212C). **Olivine-andesine trachybasalt.** Dense medium-light-gray rock. Holocrystalline and nonporphyritic. Contains about 40 percent andesine ($\sim An_{35}$) in laths 0.1–0.5 mm long, in part enclosed in ophitic plates of titaniferous(?) pale-yellowish-brown augite (about 20 percent of the rock), and in part separated by anhedra of sodic anorthoclase (refractive index $\approx$ balsam; confirmed by X-ray methods; about 20 percent of rock). Small grains of slightly altered yellowish olivine form about 5 percent of the rock, and opaque granules about 8 percent. Nepheline appears in the norm (4 percent) but was not recognized petrographically. This rock is similar in bulk composition to samples 1 and 2 and may belong to the same flow, but it is quite distinct petrographically from either of the others. Subaerial flow capping ridge west of Arneb Glacier at an altitude of about 300 m (fig. 14).

4 (212A). **Analcite-olivine trachybasalt.** Medium-gray rock that contains sparse small vesicles. Nonporphyritic, holocrystalline, fine grained. About half the rock consists of laths 0.1–0.5 mm long of plagioclase ($\sim An_{50}$), and about 15 percent consists of yellowish-gray to greenish-yellow clinopyroxene in needles and short prisms shorter than 0.03 mm. Variably iddingsitized olivine crystals smaller than 0.1 mm form 5 percent of the rock; analcite constitutes a similar amount, occurring both as a groundmass mineral and as vesicle linings. Anorthoclase anhedra constitute about 15 percent of the rock,

and opaque granules about 7 percent. Analcite, anorthoclase, and phillipsite were identified by G. M. Fairer by X-ray methods; phillipsite was not recognized optically. Pillow-clast in palagonite breccia, at altitude of about 275 m on ridge west of Arneb Glacier (fig. 14).

5 (211B–2). **Olivine-andesine trachybasalt.** Dense medium-dark-gray rock speckled by lighter spots 2–3 mm in diameter. Holocrystalline, fine grained. About 50 percent of the rock consists of plagioclase—one-third of it in seriate tabular phenocrysts to 2 mm long of labradorite ($\sim An_{60}$), the rest in 0.1-mm laths of andesine ($\sim An_{40}$). Olivine, partly altered to iddingsite, constitutes 5 percent of the rock and occurs mostly as groundmass granules but partly as microphenocrysts. About 15 percent of the rock consists of 0.005- to 0.01-mm granules and microprisms of pale-olive clinopyroxene, a like amount consists of poikilitic 0.01-mm anhedra of anorthoclase, and 10 percent consists of opaque granules and microphenocrysts. Apatite, calcite, and analcite are present in amounts of a percent or so each. Pillow(?)-lava complex in the palagonite breccia section, altitude 180 m on the ridge west of Arneb Glacier (fig. 14).

6 (247A). **Augite-sanidine-nepheline phonolite.** Massive, medium-light-gray holocrystalline rock. The texture is chaotic, with patchy distribution of masses of varying texture and mineralogy, a dominance of anhedral and poikilitic shapes, and an abundance of replacement relationships. Phenocrysts: oligoclase, about 3 percent, in tablets to 4 mm long, variably replaced by granular nepheline and zeolites; augite, about 5 percent, pleochroic in olive green, with or without dusky-yellow cores; and pseudormophs, about 3 percent, of finely granular augite and opaque minerals after brown hornblende, which remains as ragged cores in some pseudomorphs. The groundmass consists mostly of ragged-edged tablets of sanidine, typically about 1 mm long, composing about 35 percent of the rock, and anhedra of nepheline, also about 35 percent, which partly are interspersed with sanidine and partly occur in purer masses of ragged anhedra. Natrolite and analcite each composes about 5 percent of the rock, and occur in part in masses of these two minerals alone or with calcite, and in part as groundmass anhedra throughout the rock. Small ragged anhedra of augite constitute about 5 percent of the rock and are dispersed throughout it, as are small granules of opaque minerals. Interior of an intrusive megapillow, east side of Hallett Peninsula (fig. 14).

7 (247B). **Phonolite.** Light-olive-gray rock, seamed by a fine network of white to olive veinlets of analcite or calcite, or both. The rock consists largely of a fine-grained ($\sim$0.01 mm) hash of high-birefringence clay, clinopyroxene granules, zeolites, and unidentified felsic minerals. Scattered through this are several percent each of microphenocrystic laths of sanidine and euhedra of nepheline and their argillitic pseudomorphs, and a few percent of tiny needles of hornblende pseudomorphed by finely granular clinopyroxene and opaque minerals. Margin of intrusive megapillow (same mass as no. 6), east side of Hallett Peninsula (fig. 14).

8 (236B). **Olivine - clinopyroxene - anorthoclase - oligoclase trachyte.** Dense aphanitic holocrystalline medium-gray rock. Sparse phenocrysts of oligoclase as thin tablets, anorthoclase as stubby, resorbed, poikilitic crystals, variably altered olivine, and green aegerine-augite(?), which is pleochroic in pale olive and has a large +2V. Groundmass consists of laths of oligoclase, granules of green clinopyroxene, iddingsite, and opaque minerals, and very poikilitic small anhedra of anorthoclase and possibly feldspathoids. Large lava pod in palagonite breccia, altitude 280 m, west side of Hallett Peninsula (fig. 14).

9 (249E). **Hydrated trachyte tuff.** Earthy yellowish-gray rock. Consists of poorly defined clasts, mostly a few millimeters in diameter, of texturally varied trachytes, greatly altered to clay, analcite, and other minerals. Most clasts contain tiny laths of sanidine, small equants of anorthoclase, and opaque granules. The thin section contains one cluster of small clinopyroxene phenocrysts pleochroic in green. Matrix for breccia, east side of Hallett Peninsula near Cape Wheatstone (fig. 14).

10 (274–1). **Olivine basalt scoria.** Mottled grayish-red and reddish-gray finely scoriaceous rock. Seriate phenocrysts of pale-olive augite, and fewer of olivine, are set in a groundmass of laths of labradorite, granules of clinopyroxene, fewer granules of iddingsite, minute crystals of unidentified alkali minerals, and hematite-clouded glass. Cinder cone, altitude 1,700 m, east of crest of Hallett Peninsula (fig. 14).

11 (249D). **Porphyritic trachybasalt.** A rock of striking appearance: abundant black equant euhedra of augite to 1.5 cm in diameter are set in a grayish-red groundmass. The augite phenocrysts are pleochroic in pale olive and have narrow rims pleochoric in pale yellowish brown. There are sparser phenocrysts of yellowish pseudomorphs after olivine and of calcic labradorite. The groundmass is holocrystalline and consists of laths of sodic labradorite, anhedral anorthoclase, subophitic augite, pleochroic in pale yellowish brown, and granules of iddingsite and of opaque minerals. Center of steep dike about 5 m thick, intrusive into trachyte breccia; east side of Hallett Peninsula, near Cape Wheatstone (fig. 14).

12 (246C). **Trachyte.** Medium-gray microvesicular rock containing sparse euhedral phenocrysts of andesine. The dominant mineral is oligoclase, which forms seriate laths 0.02–0.5 mm long, the larger ones showing marked flow parallelism. The groundmass also contains tiny anhedra of anorthoclase(?), minute needles of greenish clinopyroxene, abundant opaque granules, irregular volumes in which hematite is concentrated, masses of highly birefringent light-brown material, and a little glass. Interior of dike, half a meter thick, cutting trachyte plug, east side of Hallett Peninsula (fig. 14).

13 (246A). **Quartz trachyte.** Dense yellowish-gray rock peppered with dark minerals. Fractures parallel to strong flow structure display bright sheen. Euhedral phenocrysts of anorthoclase make up a few percent of the rock. The groundmass is formed mostly (about 80 percent) of densely packed well-oriented laths of sanidine, typically about 0.3 mm long and having smooth side pinacoids and less regular other faces. Other minerals are ragged and interstitial and are irregularly distributed. Extremely irregular quartz constitutes about 5 percent of the rock. There are two amphiboles—a dusky-yellow nonpleochoric low-birefringence fibrous one that contains rare cores of altered clinopyroxene, and an extremely pleochroic (dark-green, yellowish-brown, nearly opaque bluish-green) high-birefringence amphibole which in part occurs as separate anhedra and in part occurs as tips and margins of anhedra of the fibrous amphibole. The dark amphibole may be a barkevikitic hornblende; the two amphiboles together make up about 5 percent of the rock. A few percent of the

TABLE 2.—*Chemical analyses and calculated components of volcanic rocks of Hallett Peninsula*

[Specimens described in text; sample localities shown on fig. 14. Samples 1, 2, 3, 4, 5, 10, 11, 13, and 14 analyzed in U.S. Geol. Survey laboratories, Denver, 1965; major oxides by Ellen S. Daniels by gravimetric methods, and 6-step semiquantitative spectrographic analyses by A. L. Sutton, Jr. Samples 6, 7, 8, 9, and 12 analyzed in U.S. Geol. Survey laboratories, Washington, D.C., 1965; major oxides by X-ray fluorescence and colorimetric methods by P. L. D. Elmore, Samuel Botts, and Lowell Artis, and 6-step semiquantitative spectrographic analyses by J. L. Harris. n.d., not determined. Looked for but not detected: Ag, As, Au, B, Bi, Cd, Eu, Ge, Hf, Hg, In, Li, Pd, Pr, Pt, Re, Sb, Sm, Sn, Ta, Te, Th, Tl, V, and W]

	Trachybasalt flows			Trachybasalt nodular lavas		Megapillows: Phonolite		Megapillows: Trachyte	Hydrated trachyte tuff	Olivine basalt scoria	Dikes		Quartz trachyte plugs	
						Interior	Margin				Trachybasalt	Trachyte		
Sample No.	1	2	3	4	5	6	7	8	9	10	11	12	13	14
Field No.	213A	214B	212C	212A	211B–2	247A	247B	236B	249E	274–1	249D	246C	246A	247C
Major oxides as analyzed, weight percent														
SiO_2	45.30	45.86	46.25	45.64	48.51	51.7	53.0	56.1	58.2	45.97	42.85	53.3	63.33	67.75
Al_2O_3	17.77	17.99	17.45	17.28	17.71	20.6	20.9	17.7	12.5	16.25	14.05	17.0	15.35	14.88
Iron:														
Fe_2O_3	4.30	4.06	6.04	8.3	4.85	2.4	3.0	5.3	3.3	9.38	10.45	8.5	5.78	3.77
FeO	6.66	7.13	6.03	3.69	6.25	2.3	.80	2.8	.14	1.73	2.25	1.0	.92	.31
(Total as FeO)	(10.5)	(10.8)	(11.5)	(11.1)	(10.6)	(4.5)	(3.5)	(7.6)	(3.1)	(10.2)	(11.7)	(8.7)	(6.1)	(3.7)
MgO	4.09	4.07	4.33	4.20	3.45	1.0	.2	1.2	.7	6.88	6.90	1.7	.16	.02
CaO	9.07	9.17	8.80	8.7	8.00	3.5	1.9	3.4	2.3	9.92	10.56	4.5	.98	1.01
Na_2O	5.26	5.37	4.41	4.0	5.07	10.0	10.2	7.0	5.1	4.19	2.55	5.5	6.57	5.80
K_2O	1.96	1.84	1.81	1.80	1.80	3.1	3.9	3.4	3.0	1.69	1.33	3.3	5.08	5.25
H_2O^+	.40	.33	.17	1.14	.27	2.9	3.9	.70	8.4	.18	1.29	1.1	.44	.29
H_2O^-	.34	.10	.15	.73	.10	.17	.28	.40	5.2	.08	1.54	.51	.38	.08
TiO_2	2.49	2.56	2.89	2.78	2.47	.72	.24	.94	.24	2.76	3.00	1.8	.40	.24
P_2O_5	1.16	1.14	1.07	1.08	1.16	.21	.02	.38	.02	.64	.47	.72	.05	.01
MnO	.24	.24	.23	.22	.24	.30	.31	.35	.13	.20	.18	.27	.16	.14
CO_2	.78	.02	.31	.22	.16	.49	.80	.15	.69	.07	2.35	.21	.23	.34
Cl	.16	.13	.09	.08	.03	n.d.	n.d.	n.d.	n.d.	.12	.10	n.d.	.07	.03
F	.13	.14	.11	.10	.09	n.d.	n.d.	n.d.	n.d.	.11	.09	n.d.	.18	.25
Sum	100.11	100.15	100.14	100.02	100.16	----	----	----	----	100.17	99.96	----	100.08	100.17
Less O	.09	.09	.07	.06	.05	----	----	----	----	.08	.06	----	.10	.11
Total	100.02	100.06	100.07	99.96	100.11	99	99	100	100	100.09	99.90	99	99.98	100.06
Minor elements, weight percent														
Ba	0.1	0.1	0.05	0.07	0.07	0.1	0.1	0.1	0.03	0.07	0.03	0.1	0.02	.003
Be	0	0	0	0	0	.0005	.0005	.0003	.0003	0	0	.0003	.0007	.0005
Ce	.02	0	0	0	.015	.05	.07	.05	.03	0	0	.03	.03	.02
Co	.002	.002	.003	.003	.002	0	0	0	0	.005	.005	.001	0	0
Cr	.002	.001	.002	.002	.0007	.0003	0	.0003	0	.07	.02	.0003	.0001	0
Cu	.003	.005	.003	.003	.002	.0007	.00015	.002	.00015	.007	.01	.0015	.0005	.0005
Ga	.003	.003	.003	.003	.003	.002	.002	.002	.0015	.003	.003	.002	.005	.005
La	.01	.01	.01	.01	.01	.03	.05	.03	.015	.007	.003	.015	.015	.01
Mo	0	0	0	0	0	.001	.0007	.001	0	.001	0	.001	0	0
Nb	.01	.01	.007	.007	.01	.007	.01	.01	.005	.01	.005	.005	.015	.015
Nd	.015	.015	.015	.015	.02	.02	.02	.02	0	.007	0	.02	.02	.015
Ni	.002	.002	.002	.002	.001	0	.02	0	.005	.015	.01	0	0	0
Pb	0	0	0	0	0	0	.0005	.0015	.0003	0	0	.0003	0	0
Sc	.001	.001	.0015	.0015	.001	0	0	0	0	.001	.002	.001	.0003	.0003
Sr	.2	.15	.15	.15	.15	.15	.1	.1	.01	.15	.1	.1	.003	0
V	.02	.02	.02	.03	.015	0	0	0	0	.03	.05	0	0	0
Y	.002	.002	.002	.003	.002	.003	.003	.003	.003	.002	.002	.003	.003	.003
Yb	.0003	.0003	.0003	.0003	.0003	.0003	.0003	.0003	.0003	.0003	.0002	.0003	.0007	.0007
Zr	.03	.03	.02	.03	.03	.02	.03	.1	.07	.03	.015	.03	.07	.07
Major oxides, recalculated to 100 percent for components listed, weight percent														
SiO_2	46.0	46.0	46.5	46.6	48.7	54.0	56.1	56.9	68.0	46.0	45.2	54.6	64.0	68.12
Al_2O_3	18.0	18.0	17.5	17.7	17.8	21.5	22.1	18.0	14.6	16.3	14.8	17.4	15.5	15.0
Fe_2O_3	4.4	4.1	6.1	8.5	4.9	2.5	3.2	5.4	3.9	9.4	11.0	8.7	5.8	3.8
FeO	6.8	7.2	6.1	3.8	6.3	2.4	.9	2.8	.16	1.7	2.4	1.0	.9	.31
MgO	4.2	4.1	4.4	4.3	3.5	1.0	.21	1.2	.8	6.9	7.3	1.7	.16	.02

CaO	9.2	9.2	8.8	8.9	8.0	3.7	2.0	3.5	2.7	9.9	11.1	4.6	1.0	1.0
Na_2O	5.3	5.4	4.4	4.1	5.1	10.4	10.8	7.1	6.0	4.2	2.7	5.6	6.6	5.8
K_2O	2.0	1.9	1.8	1.8	1.8	3.2	4.1	3.5	3.5	1.7	1.4	3.4	5.1	5.3
TiO_2	2.5	2.6	2.9	2.8	2.5	.8	.25	1.0	.28	2.8	3.2	1.8	.40	.24
P_2O_5	1.2	1.1	1.1	1.1	1.2	.22	.02	.39	.02	.6	.5	.7	.05	.01
MnO	.24	.24	.23	.22	.24	.31	.33	.36	.15	.20	.19	.28	.16	.14
Normative composition														
Salic:														
Q (SiO_2)	0	0	0	0	0	0	0	0	15.3	0	0	0	6.2	13.8
Or ($K_2O \cdot Al_2O_3 \cdot 6SiO_2$)	11.8	10.9	10.8	10.9	10.7	19.1	24.4	20.4	20.7	10.0	8.3	20.0	30.3	31.2
Ab ($Na_2O \cdot Al_2O_3 \cdot 6SiO_2$)	21.3	21.8	28.8	30.7	34.8	32.6	36.7	51.5	50.4	22.9	22.0	47.7	51.2	47.6
An ($CaO \cdot Al_2O_3 \cdot 2SiO_2$)	20.0	20.1	23.0	24.5	20.5	2.3	0	7.0	2.8	21.1	24.7	12.3	0	0
Ne ($Na_2O \cdot Al_2O_3 \cdot 2SiO_2$)	12.2	12.3	4.4	2.0	4.3	30.2	29.3	4.7	0	6.3	0	0	0	0
Hl (NaCl)	.27	.22	.15	.14	.05	0	0	0	0	.20	.17	0	.12	.05
Femic:														
Ac ($Na_2O \cdot Fe_2O_3 \cdot 4SiO_2$)	0	0	0	0	0	0	0	0	0	0	0	0	3.9	1.4
Wo ($CaO \cdot SiO_2$)	7.3	7.3	5.6	5.0	4.8	6.0	4.1	3.2	4.4	8.9	10.8	1.9	1.4	1.3
En ($MgO \cdot SiO_2$)	4.6	4.3	4.3	4.3	3.1	2.6	.5	2.8	2.0	7.7	9.6	3.6	.4	.05
Fs ($FeO \cdot SiO_2$)	2.2	2.6	.7	0	1.4	1.7	0	0	0	0	0	0	0	0
Fo ($2MgO \cdot SiO_2$)	4.1	4.1	4.6	4.5	3.9	0	0	.19	0	6.6	6.0	.5	0	0
Fa ($2FeO \cdot SiO_2$)	2.2	2.7	.8	0	1.9	0	0	0	0	0	0	0	0	0
Mt ($FeO \cdot Fe_2O_3$)	6.3	5.9	8.8	4.7	7.0	3.6	3.1	7.6	.21	0	0	0	2.4	.8
Hm (Fe_2O_3)	0	0	0	5.3	0	0	0	.17	3.7	9.4	11.0	8.7	2.9	0
Il ($FeO \cdot TiO_2$)	4.8	4.9	5.5	5.4	4.7	1.4	.5	1.8	.5	4.1	5.4	2.8	.8	2.8
Tn ($CaO \cdot TiO_2 \cdot SiO_2$)	0	0	0	0	0	0	0	0	0	0	.8	1.0	0	.5
Pf ($CaO \cdot TiO_2$)	0	0	0	0	0	0	0	0	0	1.0	0	0	0	0
Ap [$3(CaO \cdot P_2O_5) \cdot CaF_2$]	2.8	2.7	2.6	2.6	2.8	.5	.05	.9	.06	1.5	1.2	1.8	.12	.02
Fr (CaF_2)	.16	.18	.13	.11	.08	0	0	0	0	.17	.15	0	.4	.5
Σ Salic	65.6	65.4	67.0	68.2	70.3	84.1	90.4	83.4	89.1	60.5	55.1	79.9	87.8	92.7
Σ Femic	34.4	34.6	33.0	31.8	29.7	15.9	9.6	16.6	10.9	39.5	44.9	20.1	12.2	7.3
Differentiation index: (Q+Or+Ab+Ne)	45.3	45.1	43.9	43.5	49.8	81.9	90.4	76.5	86.4	39.3	30.3	67.6	87.7	92.6

TABLE 3.—*Chemical analyses and calculated components of volcanic*

[Specimens described in text; sample localities shown on figures 4, 6, 14, and 17. Samples 15, 16, 20, 22–28, and 31–34 analyzed in U.S. analyses by A. L. Sutton, Jr. Samples 17–19, 21, 29, and 30 analyzed in U.S. Geol. Survey laboratories, Washington, D.C., 1965: tative spectrographic analyses by J. L. Harris. n.d., not determined. Looked for but not detected: Ag, As, Au, B, Bi, Cd, Eu, Ge,

	Mainland					Coulman Island			
	Olivine basalt plug	Olivine basalt aa flows		Olivine basalt in palagonite	Quartz trachyte	Olivine basalt pillow lava	Olivine basalt cinder cone	Latite lens in breccia	Trachyte lava
Sample No.	15	16	17	18	19	20	21	22	23
Field No.	210B	215C	223	251C	252–3	216	217	220C	218–1
Major oxides as									
SiO_2	44.89	43.12	45.4	47.6	69.6	44.50	47.6	52.37	60.87
Al_2O_3	13.20	13.20	14.2	18.0	14.7	16.07	16.6	17.67	17.37
Iron:									
Fe_2O_3	2.40	2.87	5.7	3.3	1.8	4.89	10.4	6.19	3.21
FeO	8.26	9.09	6.5	8.3	1.5	7.94	1.5	2.50	1.62
(Total as FeO)	(10.4)	(11.7)	(11.6)	(11.3)	(3.1)	(12.4)	(10.7)	(8.1)	(4.5)
MgO	12.86	11.51	9.3	4.6	.0	5.22	4.1	2.12	.57
CaO	9.67	11.41	11.0	8.1	.62	9.07	7.3	5.44	1.06
Na_2O	3.11	2.80	2.7	4.4	6.5	4.29	4.9	5.72	7.53
K_2O	1.15	1.30	.93	1.7	4.5	1.52	1.7	2.61	4.80
H_2O^+	.79	.18	.46	1.2	.30	1.25	.60	1.29	1.11
H_2O^-	.25	.10	.34	.44	.07	.44	.40	.85	.32
TiO_2	2.31	3.45	2.2	.27	.17	3.34	2.5	1.84	.66
P_2O_5	.54	.57	.49	.95	.02	.95	1.9	.62	.11
MnO	.19	.20	.19	.21	.11	.23	.25	.27	.23
CO_2	.38	.02	.05	.08	<.05	.19	.11	.19	.19
Cl	.04	.05	n.d.	n.d.	n.d.	.13	n.d.	.15	.08
F	.07	.10	n.d.	n.d.	n.d.	.12	n.d.	.13	.15
Sum	100.11	99.97	----	----	----	100.15	----	99.96	99.88
Less O	.04	.05	----	----	----	.08	----	.08	.08
Total	100.07	99.92	99	99	100	100.07	100	99.88	99.80
Minor elements,									
Ba	.05	.07	.03	.05	.002	.07	.03	.1	.07
Be	0	0	.0001	.0001	.0007	0	.0001	0	.0007
Ce	0	0	0	.01	.07	0	0	.015	.02
Co	.005	.005	.007	.005	0	.003	.007	.001	0
Cr	.07	.07	.07	.0015	.0003	.007	.1	.0002	0
Cu	.015	.01	.007	.003	.00015	.005	.007	.001	0
Ga	.002	.002	.001	.0015	.003	.003	.001	.003	.005
La	.007	.005	0	.01	.05	.007	0	.01	.01
Mo	0	0	.0005	.0005	.001	0	.0005	0	0
Nb	.005	.007	.003	.003	.015	.01	.003	.015	.02
Nd	0	.007	.02	.015	.02	.01	.02	.02	.02
Ni	.05	.05	.05	.02	0	.003	.1	0	0
Pb	0	0	.0015	0	.003	0	0	0	0
Sc	.002	.003	.003	.001	0	.0015	.001	.0007	.0003
Sn	0	0	0	0	.0015	0	0	0	0
Sr	.1	.15	.05	.1	.0007	.15	.1	.15	.01
V	.05	.05	.02	.015	0	.03	.01	.007	0
Y	.002	.002	.002	.003	.007	.003	.003	.003	.003
Yb	.0002	.0002	.0002	.0003	.0007	.0003	.0003	.0003	.0003
Zr	.015	.015	.02	.02	.15	.03	.02	.02	.1
Major oxides, recalculated to 100 percent									
SiO_2	45.5	43.3	46.0	48.8	69.9	45.3	48.2	53.6	61.2
Al_2O_3	13.4	13.2	14.4	18.5	14.8	16.4	16.8	18.1	17.7
Fe_2O_3	2.4	2.9	5.8	3.4	1.8	5.0	10.5	6.3	3.3
FeO	8.4	9.1	6.6	8.5	1.5	8.1	1.5	2.6	1.7
MgO	13.0	11.6	9.4	4.7	0	5.3	4.2	2.2	.6
CaO	9.8	11.5	11.2	8.3	.6	9.2	7.4	5.6	1.1
Na_2O	3.2	2.8	2.7	4.5	6.5	4.4	5.0	5.9	7.7
K_2O	1.2	1.3	.9	1.7	4.5	1.6	1.7	2.7	4.9
TiO_2	2.3	3.5	2.2	.3	.17	3.4	2.5	1.9	.7
P_2O_5	.6	.6	.5	1.0	.02	1.0	1.9	.6	.11
MnO	.19	.20	.19	.22	.11	.23	.25	.28	.23
Normative									
Salic:									
Q (SiO_2)	0	0	0	0	14.0	0	0	0	0
Or ($K_2O \cdot Al_2O_3 \cdot 6SiO_2$)	6.9	7.7	5.6	10.0	26.7	9.2	10.2	15.8	28.9
Ab ($Na_2O \cdot Al_2O_3 \cdot 6SiO_2$)	14.2	6.8	21.2	28.4	50.8	24.1	42.0	47.2	58.6
An ($CaO \cdot Al_2O_3 \cdot 2SiO_2$)	19.1	19.9	24.2	25.1	0	21.0	18.5	15.8	0
Lc ($K_2O \cdot Al_2O_3 \cdot 4SiO_2$)	0	0	0	0	0	0	0	0	0
Ne ($Na_2O \cdot Al_2O_3 \cdot 2SiO_2$)	6.6	9.0	1.1	5.4	0	6.4	0	.6	2.8
Hl (NaCl)	.07	.08	0	0	0	.2	0	.3	.1
Femic:									
Ac ($Na_2O \cdot Fe_2O_3 \cdot 4SiO_2$)	0	0	0	0	3.9	0	0	0	.4
Wo ($CaO \cdot SiO_2$)	10.7	13.6	11.6	4.1	1.2	7.5	1.5	2.9	1.5
En ($MgO \cdot SiO_2$)	7.5	9.5	8.9	1.9	0	4.9	1.6	2.5	1.3
Fs ($FeO \cdot SiO_2$)	2.3	2.9	1.5	2.1	2.3	2.1	0	0	0
Fo ($2MgO \cdot SiO_2$)	17.5	13.5	10.2	6.9	0	5.8	6.1	2.0	.1
Fa ($2FeO \cdot SiO_2$)	5.8	4.7	1.9	8.2	0	2.7	0	0	0
Mt ($FeO \cdot Fe_2O_3$)	3.5	4.2	8.4	4.9	.7	7.2	0	3.7	4.1
Hm (Fe_2O_3)	0	0	0	0	0	0	10.5	3.8	.3
Il ($FeO \cdot TiO_2$)	4.4	6.6	4.2	.6	.3	6.5	3.8	3.6	1.3
Tn ($CaO \cdot TiO_2 \cdot SiO_2$)	0	0	0	0	0	0	1.4	0	0
Pf ($CaO \cdot TiO_2$)	0	0	0	0	0	0	0	0	0
Ap [$3(CaO \cdot P_2O_5 \cdot CaF_2)$]	1.3	1.4	1.2	2.4	.05	2.3	4.6	1.5	.3
Fr (CaF_2)	0.1	.2	0	0	0	.2	0	.2	.3
Σ Salic	46.8	43.5	52.0	68.9	91.5	60.9	70.6	79.8	90.4
Σ Femic	53.2	56.5	48.0	31.1	8.5	39.1	29.4	20.2	9.6
Differentiation index: (Q+Or+Ab+Lc+Ne)	27.7	23.5	27.8	43.8	91.5	39.7	52.1	63.7	90.2

rocks of Hallett Volcanic Province, other than Hallett Peninsula

Geol. Survey laboratories, Denver, 1965: major oxides by Ellen S. Daniels by gravimetric methods, and 6-step semiquantitative spectrographic major oxides by X-ray fluorescence and colorimetric methods by P. L. D. Elmore, Samuel Botts and Lowell Artis, and 6-step semiquanti- Hf, Hg, In, Li, Pd, Pr, Pt, Re, Sb, Sm, Ta, Te, Th, Tl, V, and W]

Daniell Peninsula	Adare Peninsula						Small Islands			
Olivine basalt flow	Olivine basalt flows		Olivine basalt pillows		Palog-onite	Latite dike	Basanite pillow	Olivine basalt flows		Olivine basalt scoria
24 277	25 232B	26 240B–1	27 233F	28 233D	29 233G	30 233A	31 226A	32 227B	33 225A	34 225C–2
analyzed, weight percent										
44.70	46.09	41.77	40.34	42.64	38.2	49.0	41.18	46.65	44.94	46.21
16.17	15.26	14.28	13.87	14.46	13.0	18.0	13.52	15.64	15.59	16.41
8.10	7.11	4.64	9.10	5.54	5.8	6.5	3.57	3.24	2.25	3.88
5.22	4.95	8.26	3.96	7.92	3.4	2.1	8.86	7.61	8.86	7.16
(12.5)	(11.4)	(12.4)	(12.2)	(12.9)	(8.6)	(8.0)	(12.1)	(10.5)	(10.9)	(10.7)
4.92	7.46	8.56	6.53	7.37	10.5	3.0	9.46	7.32	7.61	6.01
8.98	9.78	11.74	10.96	11.50	9.0	5.7	12.25	9.86	10.48	9.61
3.93	3.71	3.41	3.47	2.99	3.1	4.8	4.43	4.27	3.87	4.30
.75	1.57	1.39	1.02	.96	1.4	2.7	1.69	1.53	1.33	1.55
1.17	.23	.74	2.02	.99	2.4	2.0	.09	.11	.16	.34
.68	.12	.47	1.90	.51	2.5	1.8	.07	.05	.17	.27
3.67	2.71	3.73	3.61	4.01	2.5	1.8	3.47	2.81	2.98	2.90
.62	.67	.68	.70	.71	.63	.77	.99	.60	.66	.74
.19	.21	.21	.20	.20	.16	.27	.22	.21	.19	.21
.87	.10	.14	2.02	.22	7.0	.86	.02	.02	.65	.01
.07	.06	.08	.59	.05	n.d.	n.d.	.34	.10	.11	.20
.09	.09	.10	.06	.09	n.d.	n.d.	.11	.09	.09	.10
100.13	100.12	100.20	100.35	100.16	----	----	100.27	100.11	99.94	99.90
.06	.05	.06	.16	.05	----	----	.13	.06	.07	.08
100.07	100.07	100.14	100.19	100.11	100	99	100.14	100.05	99.87	99.82
weight percent										
.05	.1	.05	.03	.03	.03	.1	.07	.07	.07	.1
0	0	0	0	0	0	.0005	0	0	0	0
0	0	0	0	0	0	.05	.015	0	0	0
.005	.005	.005	.005	.005	.003	0	.005	.005	.005	.007
.005	.03	.03	.02	.02	.05	.0005	.05	.03	.03	.05
.007	.01	.01	.01	.01	.007	.0003	.01	.01	.01	.015
.002	.003	.002	.002	.002	.0015	.002	.003	.003	.003	.007
.003	.007	.007	.007	.007	0	.03	.01	.007	.007	.015
0	0	0	0	0	0	.001	0	0	.001	0
.005	.007	.007	.005	.007	.003	.01	.01	.01	.007	.015
.007	.01	.007	.007	.01	n.d.	.02	.02	.01	.01	.01
.002	.01	.01	.01	.01	.02	0	.02	.01	.02	.02
0	0	0	0	0	.0001	.0007	0	0	0	0
.002	.003	.003	.002	.003	.002	.0005	.003	.002	.002	.003
0	0	0	0	0	0	0	0	0	0	0
.15	.15	.1	.1	.1	.07	.1	.2	.15	.15	.3
.1	.03	.05	.03	.05	.015	.007	.05	.05	.05	.07
.002	.002	.002	.002	.002	.002	.003	.003	.002	.002	.005
.0003	.0003	.0002	.0002	.0002	.0002	.0003	.0003	.0003	.0003	.0007
.02	.02	.02	.01	.015	.015	.03	.02	.02	.02	.03
for components listed, weight percent										
45.9	46.2	42.3	42.7	43.3	43.6	51.8	41.1	46.7	45.4	46.6
16.6	15.3	14.5	14.7	14.7	14.8	19.0	13.5	15.7	15.8	16.5
8.3	7.1	4.7	9.6	5.6	6.6	6.9	3.6	3.2	2.3	3.9
5.4	5.0	8.4	4.2	8.1	3.9	2.2	8.9	7.6	9.0	7.2
5.1	7.5	8.7	6.9	7.5	12.0	3.2	9.5	7.3	7.7	6.1
9.2	9.8	11.9	11.6	11.7	10.2	6.0	12.2	9.9	10.6	9.7
4.0	3.7	3.5	3.7	3.0	3.5	5.1	4.4	4.3	3.9	4.3
.8	1.6	1.4	1.1	1.0	1.6	2.9	1.7	1.5	1.3	1.6
3.8	2.7	3.8	3.8	4.1	2.9	1.9	3.5	2.8	3.0	2.9
.6	.7	.7	.7	.7	.7	.8	1.0	.6	.7	.8
.20	.21	.21	.21	.20	.18	.29	.22	.21	.19	.21
composition										
0	0	0	0	0	0	0	0	0	0	0
4.5	9.3	8.3	6.4	5.8	9.4	16.9	5.2	9.0	7.9	9.2
33.6	24.2	6.5	17.3	16.8	10.0	40.3	0	19.9	15.4	23.1
25.2	20.7	20.1	22.9	23.8	19.9	20.7	13.3	19.4	21.9	21.8
0	0	0	0	0	0	0	3.7	0	0	0
0	3.7	12.0	5.0	4.6	10.8	1.4	18.9	8.4	9.1	6.5
.1	.1	.1	1.0	.1	0	0	.6	.2	.2	.3
0	0	0	0	0	0	0	0	0	0	0
6.6	9.7	14.1	12.4	12.1	11.0	1.6	16.9	10.5	10.8	8.7
5.9	8.4	10.2	10.7	9.1	9.5	1.4	11.6	7.0	6.7	5.9
0	0	2.7	0	1.8	0	0	3.9	2.7	3.5	2.2
4.6	7.2	8.0	4.6	6.7	14.2	4.6	8.4	7.9	8.7	6.5
0	0	2.3	0	1.5	0	0	3.1	3.4	5.0	2.6
7.0	8.8	6.8	3.2	8.2	4.8	2.6	5.2	4.7	3.3	5.7
3.5	1.1	0	7.5	0	3.3	5.1	0	0	0	0
7.2	5.2	7.2	7.3	7.7	5.4	3.6	6.6	5.3	5.7	5.5
0	0	0	0	0	0	0	0	0	0	0
0	0	0	0	0	0	0	0	0	0	0
1.5	1.6	1.6	1.8	1.7	1.7	1.9	2.3	1.4	1.6	1.8
.1	.1	.1	.1	.1	0	0	.1	.1	.1	.1
63.5	58.0	47.0	52.6	51.0	50.0	79.3	41.8	56.9	54.6	61.0
36.5	42.0	53.0	47.4	49.0	50.0	20.7	58.2	43.1	45.4	39.0
38.1	37.2	26.8	28.6	27.2	30.2	58.6	27.9	37.4	32.5	38.9

rock is anhedral opaque granules. Large cylindrical plug of trachyte intrusive into palagonite breccia, east side of Hallett Peninsula (fig. 14).

14 (247C). **Quartz trachyte (or quartz-poor rhyolite).** Pale-olive holocrystalline rock, speckled by lighter areas and by small dark spots. About 5 percent is of euhedral anorthoclase phenocrysts as much as 4 mm long which show no grid twinning. One percent of the rock is of mafic phenocrysts—pseudomorphs of fibrous dusky yellow amphibole after prismatic pyroxene or amphibole are irregularly transformed to very poikilitic and irregular amphibole which is pleochroic to moderate green. The very fine grained groundmass consists of subhedral laths of sanidine dispersed in a raggedly anhedral mosaic of alkali feldspar and subordinate quartz, and containing tiny shreds of moderate-green amphibole and opaque granules. Irregular small areas—the dark spots seen in hand specimen—of the groundmass have been largely replaced by opaque minerals and a little amphibole, these mafic materials being printed across the fabric of the rock and replacing quartz and anorthoclase but not albite. Sparse veinlets consist of quartz, subordinate amounts of calcite, and locally a radial-structured zeolite. Large irregular bulbous mass of trachyte, east side of Hallett Peninsula (fig. 14).

Small masses of volcanic rocks of the mainland

Nos. 15–19 (table 3)

15 (210B). **Olivine-diopside basalt.** Dense medium-dark-gray rock containing aggregates to as much as 5 mm across of greenish-yellow olivine. About 5 percent of the rock is of fragmental phenocrysts of colorless olivine, and less than 1 percent is of fragments of labradorite. The groundmass is an extremely fine grained mass of poorly shaped laths of plagioclase shorter than 0.1 mm, granules of greenish clinopyroxene about 0.01 mm in diameter, opaque granules, anhedral low-relief grains (anorthoclase?—G. M. Fairer reported the presence of this mineral from X-ray analysis), and much brownish "chlorophaeite" and "nontronite." Plug of basalt intrusive into Paleozoic granodiorite, west side of Moubray Bay (fig. 17).

16 (215C). **Olivine basalt.** Microvesicular dark-gray rock, studded by greenish-yellow olivine phenocrysts several millimeters long. These phenocrysts are variably resorbed but are unaltered, and compose about 2 percent of the rock; an additional 10 percent is of groundmass olivine granules and microphenocrysts. Seriate phenocrysts of zoned augite (cores pleochroic in light olive, rims in dusky yellow) form 1 percent of the rock and are mostly smaller than 0.5 mm. About 40 percent of the rock consists of groundmass clinopyroxene, as brownish granules smaller than 0.1 mm, and 10 percent consists of poorly shaped laths of calcic plagioclase shorter than 0.1 mm. Opaque granules about 0.005 mm in diameter are abundant. The rest of the groundmass is nearly isotropic, and its constituents were not identified optically. Small remnant of volcanic rocks near Trafalgar Glacier (fig. 4).

17 (223). **Olivine basalt.** Medium-gray rock with abundant microvesicles. A nearly opaque groundmass encloses seriate phenocrysts of olivine, nearly colorless augite, and sodic labradorite, all mostly smaller than 1 mm. Aa breccia, west of Daniell Peninsula and north of Mount Prior (fig. 14), collected by D. F. Crowder.

18 (251C). **Olivine basalt.** Dense medium-gray rock. About 20 percent of the rock consists of seriate microphenocrysts and groundmass laths of labradorite, and 2 percent consists of olivine microphenocrysts and granules. The remainder is a nearly opaque and extremely fine grained mass of opaque dust, clinopyroxene microlites, low-birefringence minerals, glass, and unidentified materials. G. M. Fairer reported X-ray recognition of anorthoclase and sanidine as well as of several of the optically identified minerals. Lens of lava in small mass of palagonite breccia, south of Tucker Glacier (fig. 4); collected by D. F. Crowder.

19 (252–3). **Quartz trachyte (or quartz-poor rhyolite).** Vesicular light-gray clinkery rock with strong flow structure. Seriate phenocrysts of anorthoclase (small −2V, weak grid twinning) and sparse microphenocrysts of green clinopyroxene (large −2V, $\rho<v$, aegerine-augite?). Groundmass consists of tiny tablets of albite, anhedra of anorthoclase(?), microlites of green clinopyroxene, opaque dust, and glass which presumably contains occult quartz and alkali feldspar. Small area of volcanic rocks capping ridge of Paleozoic rocks, near Trainer Glacier (fig. 4); collected by D. A. Coates.

Coulman Island

Nos. 20–23 (table 3)

20 (216). **Olivine basalt.** Dense aphanitic dark-gray rock. No phenocrysts. About 3 percent of the rock consists of olivine granules and prisms, smaller than 0.4 mm, variably iddingsitized; and about 20 percent consists of laths of labradorite (about An_{60}), mostly shorter than 0.1 mm. The remainder consists of pyroxene microlites and opaque dust densely clouding isotropic glass. Sparse microvesicles are lined by a radial fibrous nearly isotropic zeolite, which has negative relief and is length-slow—apophyllite? Nodular lava in palagonite breccia, north end of island (fig. 6).

21 (217). **Olivine basalt scoria.** Grayish-red cinder with a glassy skin. Ten percent of the rock consists of seriate plagioclase (about An_{50}), reaching 7 mm long but mostly shorter than 1 mm, down to 0.03-mm laths in the groundmass; 2 percent consists of partly altered colorless olivine microphenocrysts; and less than 1 percent is of clinopyroxene microphenocrysts. The remainder is a nearly opaque mass clouded darkly by opaque dust and granules and green pyroxene microgranules. Cinder cone, west flank of summit volcano (fig. 6).

22 (220C). **Latite.** Dense medium-gray aphanitic rock. Sparse phenocrysts of andesine and of pale-olive augite are set in a nearly holocrystalline but very fine-grained groundmass. The groundmass consists of 0.1-mm anhedra of alkali feldspar (anorthoclase?), which comprise perhaps 50 percent of the rock, and are crowded densely with subhedra and euhedra of the other minerals. These consist of 0.1-mm subhedral laths of calcic oligoclase, about 20 percent of the rock; minute prisms of slightly greenish clinopyroxene, about 10 percent; tiny prisms of iddingsite, presumably pseudomorphs of an iron-rich olivine, about 7 percent; 0.01-mm granules of opaque minerals, about 5 percent; nearly opaque pseudomorphs after biotite or hornblende, about 1 percent. There is a little glass, carbonate, and clay(?). Nodular lava lens in breccia, west side of island (fig. 6).

23 (218–1). **Trachyte.** Greenish-gray rock displaying bright sheen on breaks parallel to the groundmass flow structure; studded with white phenocrysts. About 10 percent of the rock consists of euhedral grid-twinned anorthoclase phenocrysts, more or less clustered, as much as 5 mm long. The groundmass is dominated by very thin laths, typically 0.3 mm long and 0.01–0.02 mm thick, of oligoclase and sanidine, in spectacularly

oriented swirled parallelism. The two groundmass feldspars are so similar in appearance and occurrence that their proportions cannot be estimated closely, but the sanidine is dominant; it has straight extinction in sections perpendicular to 010 and has entirely negative relief. The oligoclase has nearly straight extinction, albite twinning, and negative to slightly positive relief: the composition is near An_{20}. Subhedral microphenocrysts and tiny granules of clinopyroxene (aegerine-augite?—pleochroic from z'=light olive to x'=yellow green; $x \wedge c$ about 30°) make up about 4 percent of the rock; partly iddingsitized granules of greenish-yellow olivine make up about 1 percent; and microphenocrysts of opaque-rimmed brown biotite make up less than 1 percent. Interstitial analcite makes up about 5 percent of the rock, and opaque granules several percent. The optical identification of analcite and sanidine was confirmed by X-ray powder study by G. M. Fairer. North rim of Coulman caldera (fig. 6).

Daniell Peninsula

No. 24 (table 3)

24 (277). **Olivine basalt.** Massive medium-dark-gray rock. Sparse phenocrysts of labradorite and olivine, the latter now mostly iddingsite. The groundmass is dominated by seriate laths of plagioclase (about 50 percent of the rock); the larger laths, typically about 0.5 mm long, are of labradorite with narrow rims of andesine, whereas the smaller laths, typically 0.1 mm, are of andesine alone. About 5 percent of the groundmass consists of granules of iddingsite, 15 percent consists of granules and microprisms of clinopyroxene, and 10 percent consists of opaque granules. Interstitial and very poikilitic alkali feldspar (anorthoclase?) makes up about 15 percent. Veinlets of calcite cut the rock. Massive basalt lava, east side of peninsula (fig. 6).

Adare Peninsula

Nos. 25–30 (table 3)

25 (232B). **Olivine basalt.** Microvesicular dark-reddish-gray rock speckled by phenocrysts of greenish-yellow olivine, black augite, and white plagioclase. Seriate phenocrysts, augite being dominant over either olivine or plagioclase, compose about 20 percent of the rock—an unusually large amount for a basalt in this province. The augite phenocrysts are euhedral to fragmental and are dusky yellow and almost nonpleochroic; a few grains, not otherwise obviously different from the others, have vermicular reaction rims. Olivine is fresh and also includes both euhedra and fragments. Plagioclase (middle labradorite) phenocrysts are poorly shaped and include both corroded and fragmental grains; some grains display around parts of their margins narrow inclusion-clouded reaction rims, outside of which are narrow rims of uniform plagioclase more calcic than that of the rest of the crystal. The microvesicular groundmass is darkly clouded by opaque dust and granules; labradorite laths, augite euhedra, and olivine granules are recognizable, and much glass appears to be present. Lava flow, Adare Saddle (fig. 17).

26 (240B–1). **Olivine basalt.** Dense medium-dark-gray rock studded by phenocrysts that are mostly small. Ten percent of the rock consists of seriate phenocrysts of augite, weakly pleochroic in dusky yellow, as much as 8 mm in diameter; there are fewer phenocrysts of olivine and magnetite. The groundmass contains much brown glass, in which are set 0.1-mm laths of calcic plagioclase, which constitutes only about 10 percent of the rock, and more abundant granules of clinopyroxene and opaque minerals. Lava flow, crest of peninsula near north end, altitude 350 m (fig. 17).

27 (233F). **Olivine basalt.** Aphanitic medium-gray rock. Sparse microphenocrysts of olivine and augite and tiny laths of calcic plagioclase are set in a nearly opaque groundmass of opaque minerals, glass, and unidentified materials. Only a few percent of the rock consists of identifiable mineral grains. Microvesicules are filled with calcite and analcite. Chilled margin of 3-m pillow in palagonite breccia, Cape Roget (fig. 17).

28 (233D). **Olivine basalt.** Aphanitic medium-dark-gray rock. Seriate microphenocrysts of fresh colorless olivine and pale-olive augite each constitute a few percent of the rock. The groundmass is very fine grained, but holocrystalline, and consists of about 30 percent of 0.05-mm laths of calcic plagioclase, about 40 percent of 0.01-mm prisms of clinopyroxene, 10 percent of opaque granules smaller than 0.01 mm, and about 10 percent of low-birefringence low-relief material which presumably includes alkali feldspar and nepheline. The ratio of pyroxene to plagioclase is higher than is suggested by the normative composition. Interior of 1-m nodule of lava in palagonite breccia, Cape Roget (fig. 17).

29 (233G–1). **Olivine-basalt palagonite tuff.** Earthy yellowish-gray obscurely bedded rock strewn liberally with clasts to a few millimeters in diameter of medium-gray basalt. In thin section the rock is seen to consist of brown clasts of varied hydrated glassy basalts, which differ greatly in their textures and their proportions of olivine, augite, magnetite, and plagioclase. Most clasts have a yellowish-orange nearly isotropic matrix. Interstices between clasts are filled mostly with calcite, which also comprises abundant grains within many clasts. Bedded palagonite tuff, Cape Roget (fig. 17).

30 (233A). **Latite.** Aphanitic light-olive rock with abundant small flow-alined vesicles. Sparse small phenocrysts of pale-olive augite, brown amphibole, andesine, and magnetite are set in a microvesicular groundmass that displays strong trachytic flow orientation of feldspar laths. About 55 percent of the rock consists of andesine laths, typically 0.02 × 0.3 mm. Iddingsite granules, needles and granules of clinopyroxene, and opaque granules make up about 5 percent each. Interstitial material makes up about 25 percent and appears to consist of anorthoclase, analcite, calcite, and glass. Vesicles are variously empty, lined with analcite, and lined with analcite and filled with calcite. Center of dike 2.5 m wide, that cuts palagonite breccia, Cape Roget (fig. 17).

Small islands

Nos. 31–34 (table 3)

31 (226A). **Basanite.** Vesicular dark-gray rock. About 12 percent consists of fresh colorless olivine, mostly as seriate phenocrysts and microphenocrysts, but partly as groundmass granules. Pale greenish-yellow augite phenocrysts make up 3 percent of the rock, and dusky-yellow clinopyroxene prisms and granules, mostly 0.02–0.1 mm long, make up 55 percent. Opaque granules make up another 5 percent. Twenty-five percent consists of mostly clear interstitial yellow and brown glass. No feldspar or feldspathoid is present in crystalline form; the rock is named a basanite because the norm contains 23 percent nepheline plus leucite, demonstrating that the glass must be mostly of feldspathoidal composition. Rubbly lava flow, south end of Possession Island (fig. 17).

32 (227B). **Olivine basalt.** Grayish-black very vesicular rock. About 10 percent consists of olivine phenocrysts and microphenocrysts, the largest 5 mm in diameter; the mineral is unaltered, although some phenocrysts have rims of granular augite. Phenocrysts and microphenocrysts of pale-olive augite constitute 20 percent, and there are rare microphenocrysts of opaque-rimmed brown hornblende and sparse megacrysts of hornblende to 2 cm long. The groundmass consists of plagioclase laths, mostly shorter than 0.1 mm, and interstitial glass crowded and made dark by minute granules of clinopyroxene and opaque minerals. The thin section contains an autolithic(?) inclusion of olivine-augite rock. Vesicles are empty. Lava flow, McCormick Island (fig. 17).

33 (225A). **Olivine basalt.** Dark-gray vesicular rock. Augite phenocrysts constitute about 15 percent of the rock; augite is dusky yellow with or without pale-yellowish-brown rims. Colorless phenocrysts of fresh but partly resorbed olivine make up 10 percent. The groundmass consists of laths of labradorite (about 30 percent), prisms of pale-yellowish-brown clinopyroxene (about 20 percent), granules of olivine (5 percent), octahedra of magnetite (about 3 percent), plates of ilmenite (about 1 percent), and interstitial glass. Lava flow, Foyn Island (fig. 17).

34 (225C-2). **Olivine basalt.** Dark-gray scoria. Phenocrysts of olive augite and fewer phenocrysts of olivine are strewn in a microscoriaceous groundmass which appears almost opaque at low magnification. At high magnification, the groundmass is seen to contain plagioclase microlaths, pyroxene granules, alkali feldspar, glass, and abundant opaque dust and granules. Cinder from near summit of Foyn Island (fig. 17).

CHEMISTRY

Thirty-four specimens of volcanic rocks from the Hallett province were analyzed chemically (tables 2, 3). Specimens chosen represent a broad compositional spectrum of fresh, hydrated, and oxidized rocks.

MAJOR OXIDES

The chemical analyses define the volcanic province as one dominated by sodic basalts and containing subordinate felsic rocks that range from extremely sodic phonolite to relatively potassic quartz trachyte.

The highly alkaline character of most of the rocks is illustrated by figure 33. Potassium and sodium increase together in most rocks analyzed. Most of the basaltic rocks have between 3 and 5 weight-percent of Na_2O and between 1 and 2 percent of K_2O, the ratio between these oxides being typically about 2.5:1. The analyzed trachytes have between 5 and 8 percent Na_2O, and 3 and 5 percent K_2O, and a ratio of Na_2O to K_2O near 2:1. The quartz trachytes are in general the most potassic rocks sampled, having about 5 percent K_2O and 6–7 percent Na_2O, and they have the lowest ratio of sodium to potassium in the suite. The most sodic rocks are the two phonolites, each of which has more than 10 percent Na_2O, and 3–4 percent K_2O. The trachytes and quartz trachytes contain between 8 and 13 percent $Na_2O + K_2O$, the phonolites as much as 15 percent.

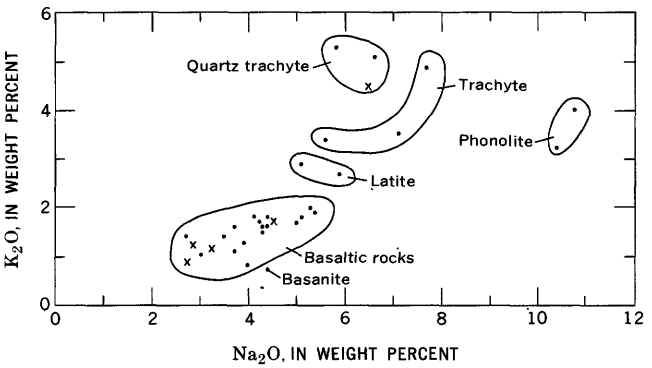

FIGURE 33.—Contents of K_2O and Na_2O in the volcanic rocks. Weight-percent amounts from analyses recalculated anhydrous, tables 2 and 3; two analyses of hydrated tuffs are omitted. Dots, offshore volcanic rocks; x's, mainland volcanic rocks.

The "differentiation index"—the sum of the normative percentages of quartz, orthoclase, albite, leucite, and nepheline (tables 2 and 3)—provides a useful measure of the gross composition of these alkaline rocks, although the genetic connotation of the term "differentiation index" is certainly erroneous in many rock suites. The major elements, of course, show a strong correlation with this index, as a correlation is forced by the calculation. The differentiation index is an expression of the amounts of silicon, sodium, and potassium in the rocks, so those elements necessarily correlate positively with it; and as magnesium, iron, and calcium are omitted from the index, they necessarily correlate negatively with it. No major-oxide variation diagram is presented here incorporating the differentiation index, because so much of the correlation is an artifice of the calculations; but the relationships with MgO and total iron are illustrated in figures 34 and 35.

Among the individual major elements, magnesium, the most refractory, provides the best single indication of the bulk composition of the rocks. Figure 34 is a magnesia-variation diagram of the analyses from the Hallett province. Most of the other oxides show nearly linear positive (FeO, TiO_2, CaO) or negative (SiO_2, Na_2O, K_2O) correlations with MgO within the range MgO=0–5. For MgO>5, correlation zones with CaO and Na_2O have gentler slopes, and correlations with SiO_2, total iron, TiO_2, and K_2O are poor.

The degree of oxidation of iron in the volcanic rocks (fig. 35) varies widely but is mostly high. From 50 to 90 percent of the iron is in the ferric state in all rocks having less than 10 percent total iron, which corresponds to the suite having a differentiation index of

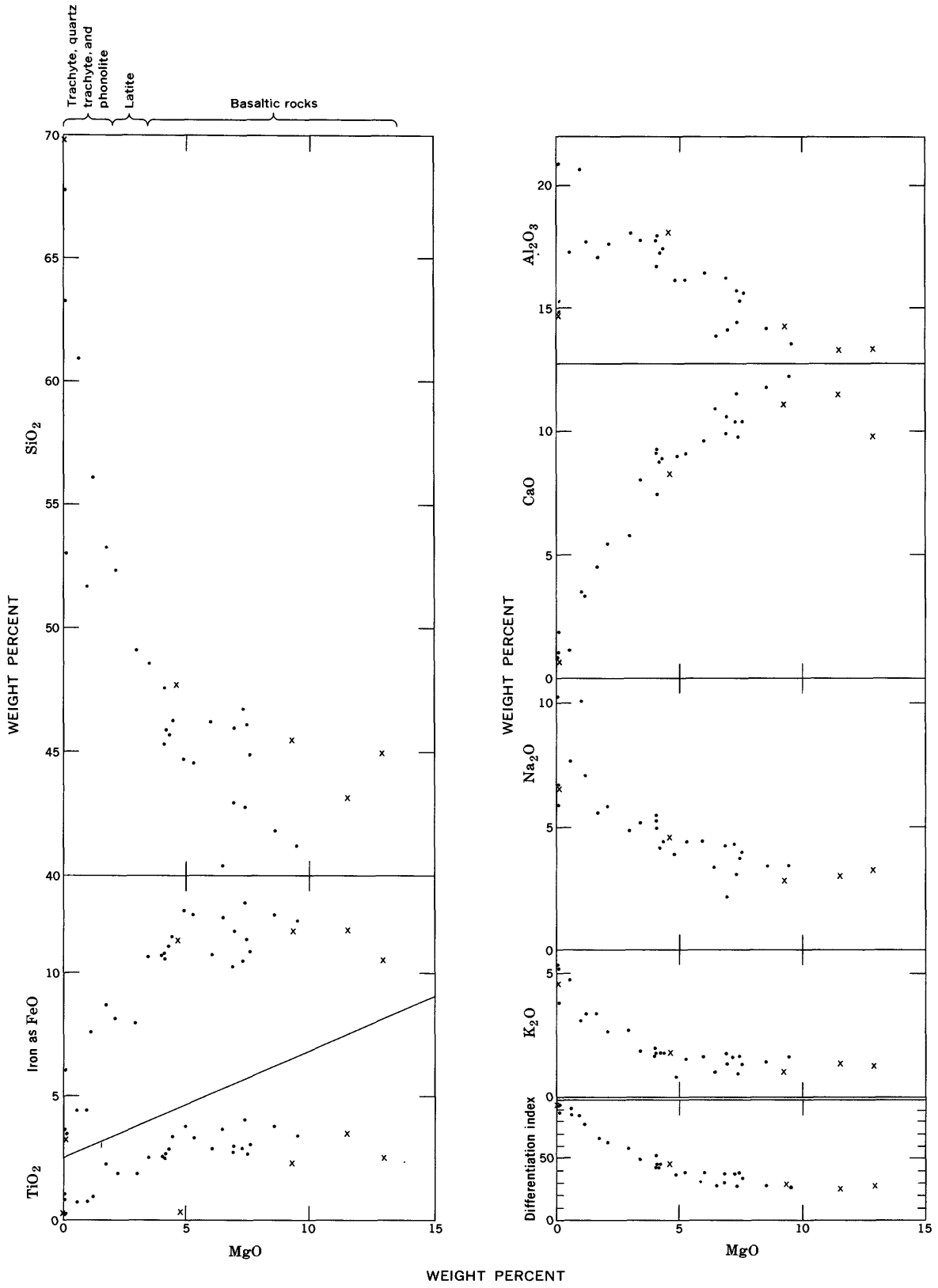

FIGURE 34.—Magnesia-variation diagram of chemical analyses of volcanic rocks of the Hallett province. Data, in weight percent, from tables 2 and 3; two analyses of hydrated tuff are not plotted. Dots, offshore volcanic rocks; x's, mainland volcanic rocks.

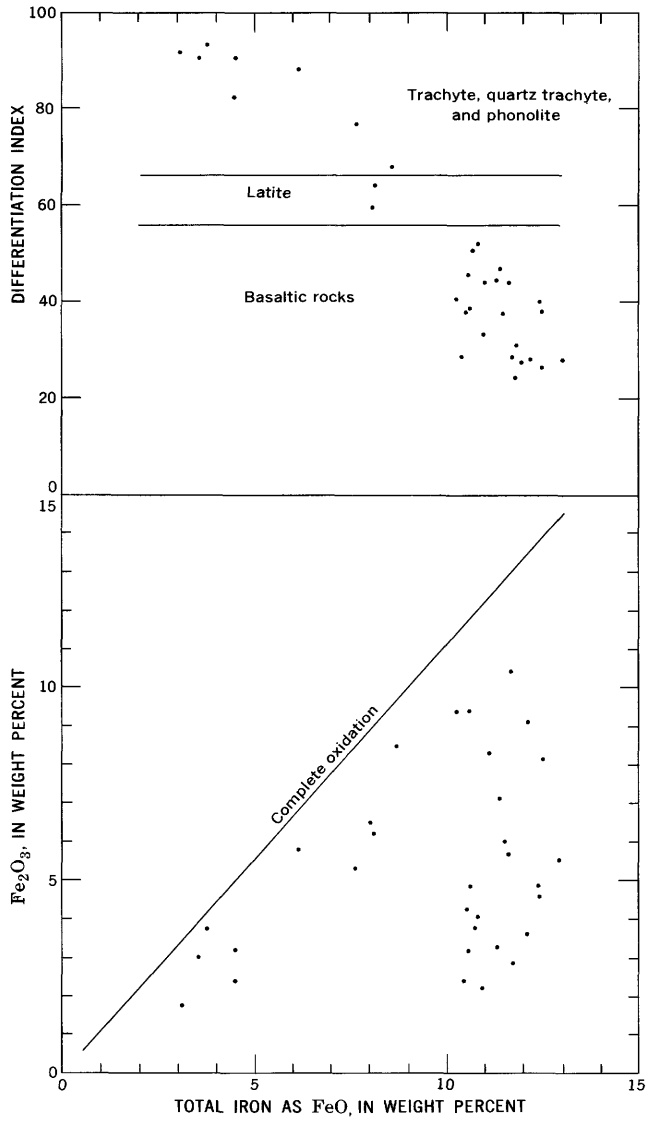

FIGURE 35.—Iron in the volcanic rocks. Differentiation index and Fe_2O_3 are plotted against total iron as FeO. Data from tables 2 and 3. Two hydrated tuffs are omitted.

more than 56. By contrast, from 20 to 85 percent of the iron is ferric in the rocks having higher (10–13 percent) total iron, but, in this group, the highly oxidized iron is in rocks that are obviously either highly differentiated or secondarily oxidized (as, red scoria).

The AFM ternary diagram (fig. 36) shows the usual symmetry of trachyte-and-basalt provinces in having a central cluster of analyses of basaltic rocks from which trachytes and other felsic rocks trend toward the alkali end of the alkali-iron join, and extremely mafic rocks trend toward the magnesia corner. The Hallett province is unusual, however, in its high proportion of alkalis even in the most mafic rocks. The contrasted trends away from the central cluster cannot

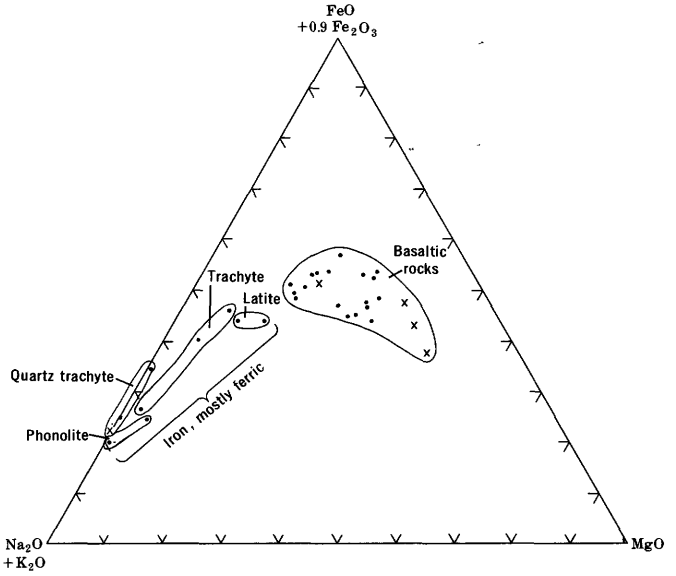

FIGURE 36.—Ternary AFM diagram of weight-percent of alkalis, magnesia, and total iron in volcanic rocks of the Hallett province. Dots, offshore volcanoes; x's, mainland rocks. Data from tables 2 and 3; two analyses of hydrated tuff are omitted.

be the complementary products of a single process, else they would fall on a single straight line. Among the models by which the actual summetry could be explained is one invoking accumulation of magnesian crystals to explain in part the composition of the most mafic rocks and separation of calcic and ferromagnesian crystals combined with addition of volatile alkalis and ferric iron to explain the least mafic rocks.

The ternary diagram of calcium, sodium, and potassium (fig. 37) shows, as does figure 33, that the ratio

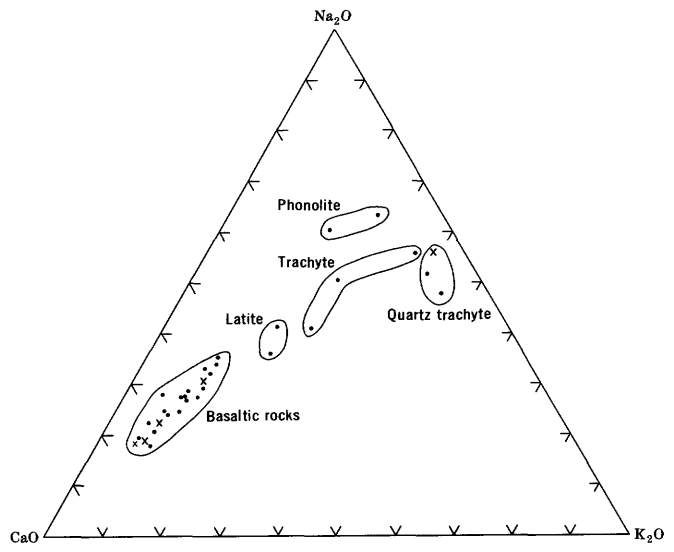

FIGURE 37.—Ternary diagram of proportions, by weight, of CaO, Na_2O, and K_2O in volcanic rocks of the Hallett province. Dots, offshore volcanoes; x's, mainland rocks. Data from tables 2 and 3; two hydrated tuffs omitted.

of potassium to sodium is nearly constant in the mafic rocks but is erratically higher in the felsic ones. Varying amounts of volatile transfer of potassium might account for the scatter in the felsic rocks. Sodium is slightly to markedly dominant by weight—hence strongly dominant in molecular proportion—over potassium in all rocks (fig. 33).

The eleven analyses of volcanic rocks of the Hallett province given by Harrington, Wood, McKellar, and Lensen (1967, p. 69–72) show variations similar to those reported here in major elements.

MINOR ELEMENTS

Minor elements also are listed in tables 2 and 3. MnO, P_2O_5, Cl, and F were determined with the major-oxide analyses, and other minor elements listed were determined by semiquantitative spectrographic methods.[2] The differentiation index is used for the abscissa against which minor-element concentrations are plotted, because most of the major oxides correlate in linear fashion with the index.

Four minor components, MnO, P_2O_5, Cl, and F, are plotted in figure 38. Phosphorus is irregularly high in rocks of low differentiation index and falls steeply in linear fashion with increasing index in high-index rocks; the extreme trachytes contain very little P_2O_5. Chlorine determinations scatter considerably but on the average are lower in the trachytes. Fluorine data, by contrast, define a linear increase through a factor of about 2 from the mafic basalts to the trachytes. The concentration of chlorine in the mafic rocks is very high (compare with data summarized by Johns and Huang, 1967). The behavior of manganese is unexpected: through most of the range of the rock suite, MnO increases with increasing index, although the lowest values of MnO are in the three quartz trachytes. Manganese thus tends to increase as both total and ferrous iron decrease (compare figs. 35 and 38), whereas in most igneous-rock assemblages manganese and ferrous iron increase together.

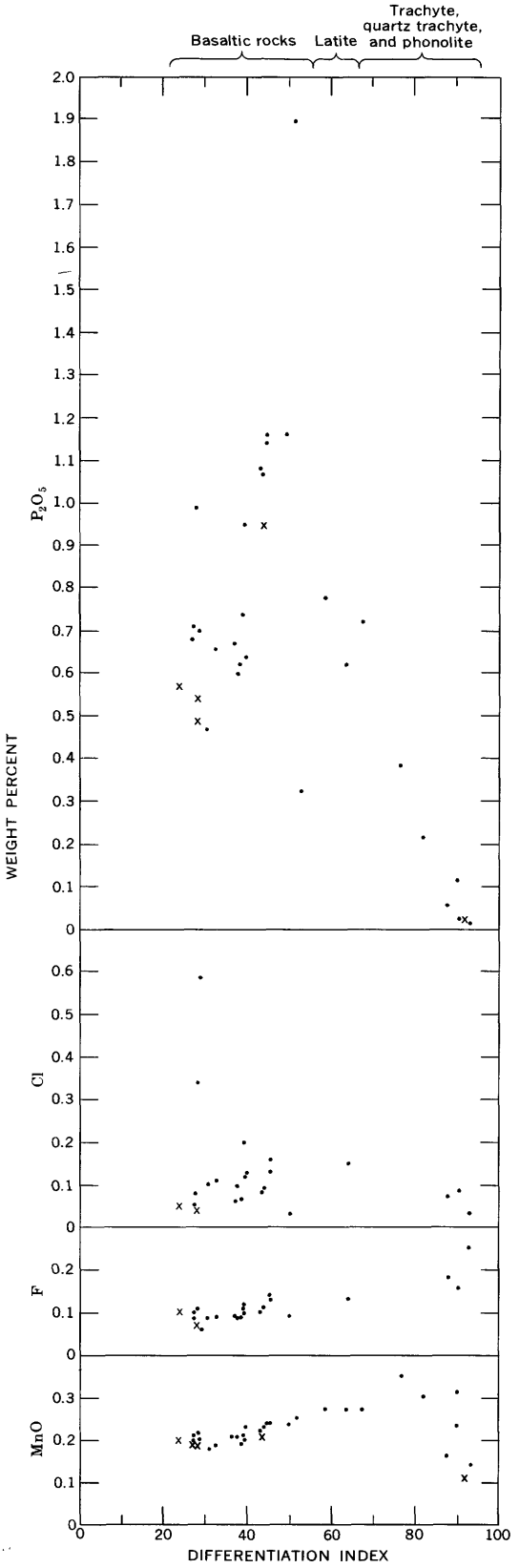

FIGURE 38.—Variation diagram of P_2O_5, Cl, F, and MnO against differentiation index for volcanic rocks of the Hallett province. Dots, offshore volcanoes; x's, mainland rocks. Data in weight percent, from tables 2 and 3. Two hydrated tuffs are omitted.

[2] The spectrographic data contain some analytical biases. The analyses made by the two analysts in different laboratories are comparable for some elements but not for others. Similar values were reported by both Sutton and Harris for Ba, Co, Cr, Nd, Ni, Y, Yb, and Zr. Sutton reported generally higher values than did Harris for Cu, Ga, Nb, Sr, and V. Harris has much more scatter than does Sutton in La determinations. Sutton detected Be and Mo in only a few samples and lead in none, whereas Harris reported those three elements in most samples. Harris reported Ce in many more samples than did Sutton, but the reverse is true of Sc. Each analyst has a bias for certain numbers; Harris is twice as likely to report a 3 (that is, 0.3, 0.03, and so forth) as a 7, and Sutton is twice as likely to report a 2 or 3 as a 5 or 15. The systematic variations in many of the minor elements are great enough to be obvious despite these small analytical biases.

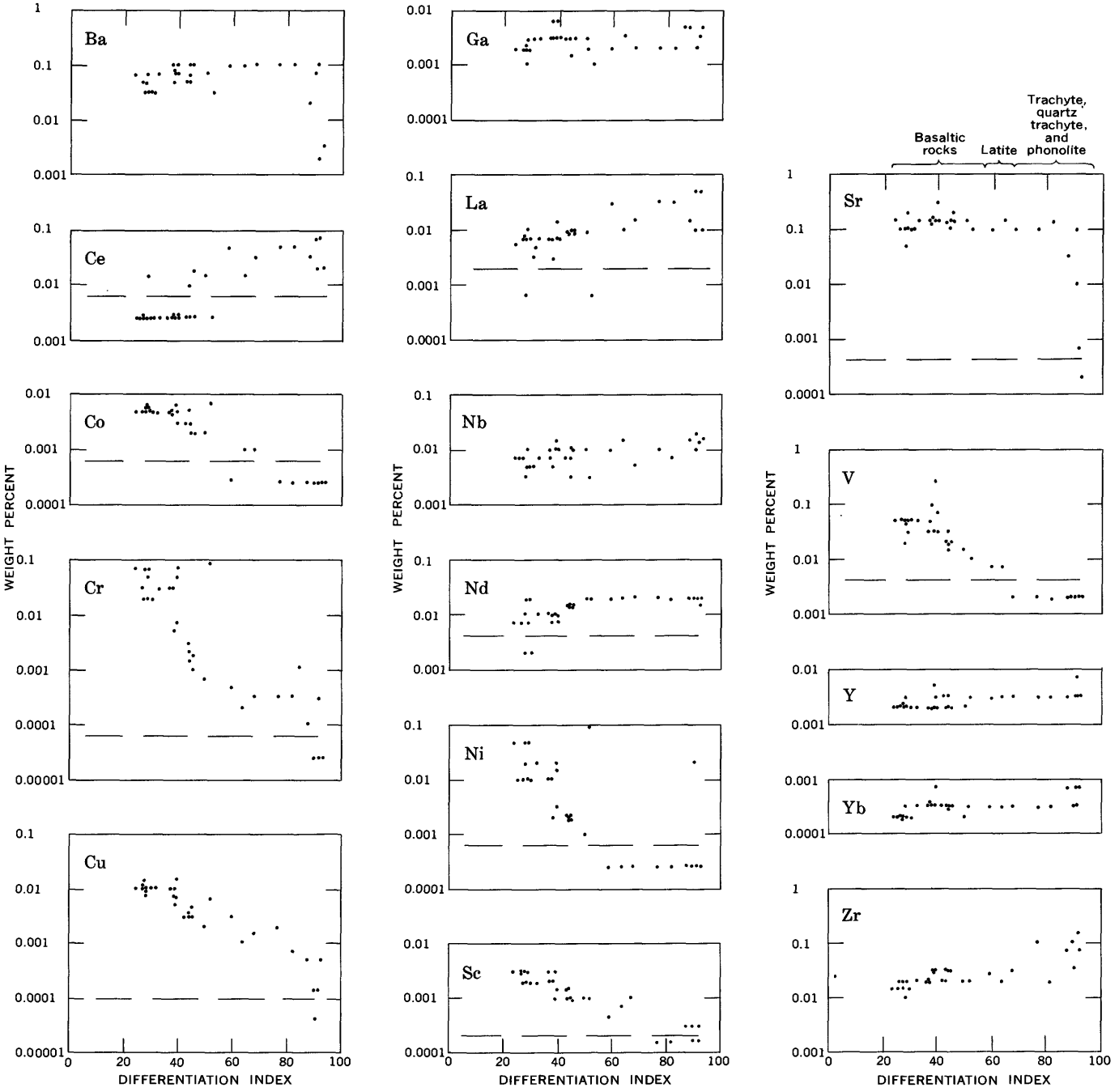

FIGURE 39.—Semilogarithmic variation diagram of minor elements, plotted against differentiation index, for volcanic rocks of the Hallett province. Dashed lines indicate threshold limits of detection by semiquantitative spectrographic analysis; less-than-threshold ("zero") determinations are plotted arbitrarily beneath these lines. Data from tables 2 and 3. Two hydrated tuffs are omitted.

Figure 39 is a variation diagram for most of the spectrographically determined minor elements. (Four elements are not plotted: lead and tin because they are reported in so few samples, and beryllium and molybdenum because only one analyst generally reported them, and in erratic amounts that do not show systematic variation with rock type.)

The metals cobalt, chromium, copper, nickel, and vanadium show the expected negative correlation with the differentiation index. These metals increase exponentially with iron and magnesium in the rocks. The abundances of chromium range through three orders of magnitude, and those of cobalt, copper, nickel, and vanadium through about two orders each.

Of the rare-earth and related metals, cerium, lanthanum, neodymium, yttrium, and ytterbium show slight to marked increase with increasing differentiation index, and so increase with silicon, potassium, and sodium in the rocks. The degree of increase with the index decreases roughly with increasing atomic weight (in order for the elements listed: La, Ce, Nd, Y, Yb), in accord with the conclusions of Haskin and Frey (1966). Scandium shows the reverse correlation, decreasing markedly with differentiation index, as anticipated from its usual association with iron and magnesium.

Barium shows a slight increase with differentiation index across most of the range but, in the highest index rocks, is very erratic, including by far the lowest values. Several of the highest-potassium rocks have very low contents of barium. (Nockolds and Allen, 1954, reported similar variation in other alkaline-basalt provinces.) Niobium increases moderately with differentiation index, and it presumably is associated with titanium, which behaves in similar fashion. Gallium (a difficult element to determine spectrographically) shows a slight but irregular increase with differentiation index, and a somewhat better correlation with aluminum content. Strontium (the worst element listed for spectrographic quantitative determination) decreases slightly with increasing differentiation index, then scatters with erratic low values in the highest-index rocks. Zirconium increases irregularly with differentiation index.

PETROLOGIC COMPARISONS

The volcanic rocks of the Hallett volcanic province are petrographically and chemically similar to those of the McMurdo Sound region of the southern Ross Sea (fig. 2, this rept.; Cole and Ewart, 1968; Harrington and others, 1967, fig. 44; Jensen, 1916; Smith, 1954; my unpub. analyses), and to the volcanic rocks of the intervening coastal region (Nathan and Schulte, 1968).

The broad patterns of major-oxide variations in the Hallett province are also similar to those found elsewhere in provinces of sodic basalts and trachytes, as in oceanic islands. Figure 40 illustrates the similarity in form of the alkali-iron-magnesium ternary variations of the Hallett volcanic rocks to those of rocks from several other basalt-and-trachyte provinces.

The similarity of the Hallett rocks to those of other basalt-and-trachyte provinces (for example, Tahiti: McBirney and Aoki, 1968) suggests that detailed petrologic study of the Antarctic suite will demonstrate the existence of two divergent petrologic series,

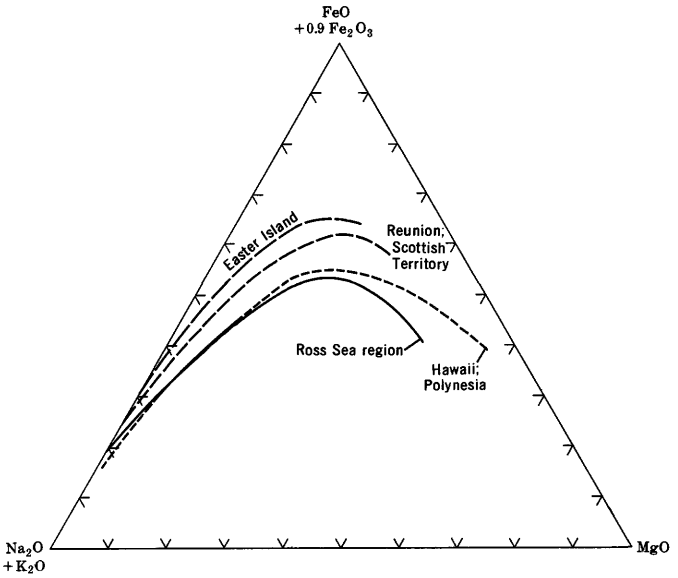

FIGURE 40.—Ternary AFM diagram of total alkalis, total iron, and magnesium for several sodic basalt-and-trachyte provinces. The Ross Sea line applies to the Hallett volcanic province (fig. 36, this rept.) and to the McMurdo Sound province (Nathan and Schulte, 1968, fig. 9). Other lines are from Nockolds and Allen (1954, figs. 16–23).

one ranging to quartz syenite, the other to phonolite, for rocks representative of these contrasted lines are present in the Hallett province.

REFERENCES CITED

Adamson, R. G., and Cavaney, R. J., 1967, Volcanic debris-layers near Mount Melbourne, northern Victoria Land, Antarctica: New Zealand Jour. Geology and Geophysics, v. 10, no. 2, p. 418–421.

Adie, R. J., 1962, The geology of Antarctica: Am. Geophys. Union Geophys. Mon. Ser., no. 7, p. 26–39.

Adie, R. J., ed., 1964, Antarctic geology: Amsterdam, North Holland Publishing Co., 758 p.

Alt, David, 1968, Pattern of post-Miocene eustatic fluctuation of sea level: Palaeogeography, Palaeoclimatology, Palaeoecology, v. 5, no. 1, p. 87–94.

Anderson, J. J., 1965, Bedrock geology of Antarctica; a summary of exploration, 1831–1962: Am. Geophys. Union Antarctic Research Ser., v. 6, p. 1–70.

Armstrong, R. L., Hamilton, Warren, and Denton, G. H., 1968, Glaciation in Taylor Valley, Antarctica, older than 2.7 million years: Science, v. 159, no. 3811, p. 187–189.

Bakayev, V. G., ed., 1966, Atlas Antarktiki: Glavnoye Upravleniye Geodezii i Kartografii MG SSSR, 225 p.

Bandy, O. L., 1968, Cycles in Neogene paleoceanography and eustatic changes: Palaeogeography, Palaeoclimatology, Palaeoecology, v. 5, no. 1, p. 63–75.

Bandy, O. L., and Wilcoxon, J. A., 1970, The Pliocene-Pleistocene boundary, Italy and California: Geol. Soc. America Bull., v. 81, no. 10, p. 2939–2947.

Behrendt, J. C., 1964, Distribution of narrow-width magnetic anomalies in Antarctica: Science, v. 144, no. 3621, p. 993–999.